

**PHOTO AND THERMO LATENT INITIATORS FOR
CATIONIC POLYMERIZATION**

**FOR THE DEGREE OF
DOCTOR OF PHILOSOPHY
IN
CHEMISTRY**

**BY
MUKESH KUMAR GUPTA**

**Dr. R. P. SINGH
(RESEARCH GUIDE)**

**POLYMER SCIENCE AND ENGINEERING DIVISION
NATIONAL CHEMICAL LABORATORY
PUNE 411 008
INDIA**

APRIL 2008

CERTIFICATE

This is to certify that the work presented in the thesis entitled “**Photo and Thermo Latent Initiators for Cationic Polymerization**” submitted by Mr. Mukesh Kumar Gupta, was carried out by the candidate at National Chemical Laboratory Pune, under my supervision. Such materials as obtained from other sources have been duly acknowledged in the thesis.

Dr. R. P. Singh

Research guide

Polymer Science and Engineering Division

National Chemical Laboratory

Pune 411 008

CANDIDATE'S DECLARATION

I hereby declare that the thesis entitled "**Photo and Thermo Latent Initiators for Cationic Polymerization**", submitted for the Degree of *Doctor of Philosophy* to the University of Pune, has been carried out by me at Polymer Science and Engineering Division, National Chemical Laboratory, Pune 411 008, India, under the supervision of **Dr. R. P. Singh**. The work is original and has not been submitted in part or full by me for any other degree or diploma to this or any other University.

Mukesh Kumar Gupta

Dedicated to MY
Parents

ACKNOWLEDGEMENT

It is a great pleasure to express my sincere thanks and a deep sense of gratitude to my supervisor Dr. R. P. Singh for his constant guidance and his valuable advises that has enabled me to complete my research work successfully. I consider myself fortunate for having a chance of working with a person like him, who is a rare blend of many unique qualities. The tremendous faith on his students sets him apart from others. I also express my sincere gratitude to Mrs. Durgesh Singh for her moral support.

I sincerely thank to Dr N. N. Joshi, OCS division, for teaching me many valuable things in organic synthesis. I am also thankful to Dr. Ganesh Pandey for his valuable suggestions and encouragement at the preliminary stage of work,

I am very much grateful to Dr. M. G. Kulkarni, Head, Polymer Science and Engineering division, for providing me access to the facilities in the division. I am very thankful to Dr D. Baskaran for valuable suggestions for my research work. Additionally, I am very thankful to all the assistance, I received from other scientists, namely, Dr. P. P. Wadgaonkar, Dr. C. Ramesh, Dr. (Mrs.) B. Garnaik, Dr. C. V. Avadhani, Dr. S. P. Vernekar, Dr A. K. Lela, Dr. T. P. Mohandas, Mr. S. K. Menon, Mrs. D. A. Dhoble and Mrs. S. Poorvi, of division is gratefully acknowledged.

I sincerely thank my seniors and Lab colleagues for their help in various capacities, co-operation and maintaining cheerful atmosphere in the laboratory. Thank you Dr. Anuj, Dr. Kartik, Dr. Anamitra, Dr. Gnaneshwar, Dr. Jitendra, Dr. Subramanayam, Dr (Mrs.) Smita, Raghu, Pradeep, Dilip, Sunil, Amit, Sarvendra, Bijendra, Rupali and Vijay. I can never forget the help from my divisional colleagues Thank you Malli, Sony madam, Mahesh bhai, Sandeep, Ravi, Dr. Munirasu, Mrs. Bapat, Dr. (Mrs) Anjana, Mrs. Nilakshi, Dhyaneshwar, Arun, Arvind, Asutosh, Vijay, Kedar, Vivek, Sachin, Dharma, Prakash, Anil, Mahadev, and all others. I also thank Mr. Mahesh, Mr. U. Dhavale, Zine and especially Mr. Silas S. Kakade for their assistance.

The kind support from the Glass blowing section (Mr. Chowdhary and group) is greatly acknowledged. I am thankful to NMR group and Dr. Rajesh Gonade (CMC) for single crystal analysis. I am also thankful to Engineering service, Store, Purchase and Administrative section for their kind support.

My special thanks go to my beloved friends Ramprakash, Bunti, Mohsin, late Puspendra, Prasant Agrawal, Jitendra, Praveenji, Ashishji, B S Yadav, Bharat Agrawal, Manoj Agrawal, Mahendra, Matadeen, Mohan Todwal, Satish, Deepak and Vinod for their individual support and encouragement during my carrier.

At this moment, I remember few of my former teachers, prof. B. L. Verma, prof. R. K. Bansal, prof. G. L. Taleshra, Mr. Gopi Ram Jogi, Mr. S. L. Todwal, Mr. Mangilal Sharma, Mr. Bansidhar Gurjar, Mr Satyapal Singh, Mr. Radhamohan, Mr. Ramesh Verma, Prof. (Mrs) Neeta Patni, and all other my teachers as they built the foundation for this achievement.

I wish to thank all my fellow colleagues in NCL, Manoj K, Khirud, Anuj, Mehraj Baag, Pradip (maity), Sushil, Ravindra, Ganesh, Prabhas, Anand (sivakar), Sashi (Bairagi), Bhargav, Nilesh, Nishant (Gupta), Kanan, Victor, Sukhenda, Nitin, Sitaram, Savita, G. sahuo, Rosy, Suman, Manasvini, Panchami, Mahima, Indu, Reeta, Atul, Sanbhag, Debasish G, Swaroop, Kishore (bhaiya), Deepak Jadav, Sunil Pandey, Puspesh, Sivanand Pai, Prashad, Lakshi, Pranjal Kalita and Barua, Amit Delori, Sailesh, Murali,, Sushim, Abhishek (Dube), Bhuvan, Sarvesh, Arsad, Sunil, Sampa, Kamendra, Atul Thakur, Akhilesh Tanower, Raghupathy, Nookaraju, Bhalchandra, Pateliya, Indresh, Rehman, sumanth, Jitendra, Anand (harbindu), Umesh, Sudharsan, Manje, and other hostel members for their cheerful company and making my NCL life very lively and enjoyable. I also am indebted to Chakarvorty and other mess workers of G J Hostel for mess facility.

Most important, it has been a difficult task to capture and express my feelings for my family members. I have no words to express my gratitude to my Parents and family members, without knowing much what I am doing exactly, just wishing me all the time with no expectations. Their patience and sacrifice were always a main source of inspiration and will remain throughout my life. Their blessings and encouragement have always made me an optimist in any unknown areas I had ventured.

Finally I thank CSIR for the Senior Research Fellowship and the Director, NCL for allowing me to carry out this work at this prestigious institute.

Mukesh Gupta
April, 2008

Contents

Abstract	i
Abbreviations	iv
List of Tables	vi
List of Figures	viii
List of Schemes	xii

Chapter 1: Introduction

1. Introduction	1
1.1 Polymers	1
1.2 Cationic Polymerization	1
1.3 Externally stimulated cationic polymerization	2
1.3.1 Photo induced cationic polymerization	2
1.3.1.1 Direct acting system	3
1.3.1.1.1 Onium salts	3
1.3.1.1.1.1 Direct photolysis	4
1.3.1.1.1.1.1 Aryldiazonium salts	4
1.3.1.1.1.1.2 Diaryliodonium salts	5
1.3.1.1.1.1.3 Sulfonium salts	6
1.3.1.1.1.1.4 Phosphonium salts	7
1.3.1.1.1.1.5 N-alkoxy pyridinium salts	8
1.3.1.1.1.1.6 Phenacylpyridinium salts	8
1.3.1.1.1.1.7 Phenacylanilinium salts	9
1.3.1.1.1.1.8 Polymer bound onium salt	9
1.3.1.2 Indirect acting photo systems	10
1.3.1.2.1 Initiation <i>via</i> charge transfer complexes	11

1.3.1.2.2	Energy transfer photosensitization	11
1.3.1.2.3	Electron transfer photosensitization	12
1.3.1.2.4	Initiation via free radical mediation	16
1.3.1.2.4.1	Oxidation of carbon centered free radical	16
1.3.1.2.4.2	Addition fragmentation reactions	17
1.3.1.3	Ferrocenium salts	19
1.3.1.4	Latent sulfonic acid	20
1.3.1.5	Photosensitive organosilanes	21
1.3.1.6	Phenol based non-salt initiator	21
1.3.2	Thermally induced cationic polymerization	22
1.3.2.1	Diaryliodonium salts	22
1.3.2.2	Sulfonium salts	23
1.3.2.3	Pyridinium salts	23
1.3.2.4	Anilinium salts	24
1.3.2.5	Pyrazinium salts	24
1.3.2.6	Hydrazinium salts	25
1.3.2.7	Woodward reagent	25
1.3.2.8	Phosphonium salts	26
1.3.2.9	Polymer bound onium salts	26
1.3.2.10	Salt free initiators	27
1.4	Perspectives and future prospects	28
1.5	References	29

Chapter 3: Thermally Induced Cationic Polymerization using Phosphonium Salts as Initiator		35
3.1	Introduction	35
3.2	Experimental	36
3.2.1	Materials	36
3.2.2	Initiator synthesis	36
3.2.2.1	Dibenzosuberene based phosphonium salts	36
3.2.2.1.1	Dibenzosuberenytriphenylphosphonium chloride (3.1a)	37
3.2.2.1.2	Dibenzosuberenytriphenylphosphonium hexafluoroantimonate (3.1b)	38
3.2.2.1.3	Dibenzosuberenytriphenylphosphonium hexafluorophosphate (3.1c)	38
3.2.2.1.4	Dibenzosuberenytriphenylphosphonium hexafluoroarsenate (3.1d)	39
3.2.2.1.5	Dibenzosuberenytriphenylphosphonium tetrafluoroborate (3.1e)	39
3.2.2.1.6	Dibenzosuberenytri- <i>n</i> -butylphosphonium hexafluoroantimonate (3.2)	40
3.2.2.1.7	Dibenzosuberenytriphenylphosphonium hexafluoroantimonite (3.3)	40
3.2.2.2	Synthesis of xanthenylphosphonium salts	41
3.2.2.2.1	Xanthenyltriphenylphosphonium chloride (3.4a)	42
3.2.2.2.2	Xanthenyltriphenylphosphonium hexafluoroantimonate (3.4b)	42
3.2.2.2.3	Xanthenyltriphenylphosphonium hexafluorophosphate (3.4c)	43
3.2.2.2.4	Xanthenyltriphenylphosphonium hexafluoroarsenate (3.4d)	44

3.2.2.2.5	Xanthenyltriphenylphosphonium tetrafluoroborate (3.4e)	44
3.2.2.2.6	Xanthenyltri- <i>n</i> -butylphosphonium hexafluoroantimonate (3.5)	44
3.2.2.3	Synthesis of 2-substituted xanthenyltriphenylphosphonium hexafluoroantimonate	45
3.2.2.3.1	2-Carboxy-4-chloro-diphenyl ether (3.6a)	46
3.2.2.3.2	2-Chloro xanthone (3.6b)	46
3.2.2.3.3	2-Chloro xanthidrol (3.6c)	47
3.2.2.3.4	2-(4-Methylphenoxy) benzoic acid (3.7a)	48
3.2.2.3.5	2-Methyl xanthone (3.7b)	49
3.2.2.3.6	2-Methyl xanthidrol (3.7c)	50
3.2.2.3.7	2-(4-Methoxyphenoxy) benzoic acid (3.8a)	50
3.2.2.3.8	2-Methoxy xanthone (3.8b)	51
3.2.2.3.9	2-Methoxy xanthidrol (3.8c)	52
3.2.2.3.10	2-Chloro xanthenyltriphenylphosphonium hexafluoroantimonate (3.6d)	53
3.2.2.3.11	2-Methyl xanthenyltriphenylphosphonium hexafluoroantimonate (3.7d)	53
3.2.2.3.12	2-Methoxy xanthenyltriphenylphosphonium hexafluoroantimonate (3.8d)	54
3.2.3	Typical polymerization procedure	55
3.2.4	Measurements	55
3.3	Results and discussion	56
3.3.1	Initiators	56
3.3.1.1	Thermal stability of phosphonium salts	61
3.3.1.2	Solubility of phosphonium salts	63
3.3.2	Dibenzosuberene based phosphonium salts as thermo-latent initiator	65
3.3.2.1	Polymerization of GPE	65
3.3.2.1.1	Effect of counter anion	65
3.3.2.1.2	Effect of phosphine moiety	68

3.3.2.1.3	Effect of double bond in dibenzosuberonyl ring	70
3.3.3	Xanthene based phosphonium salts as thermo-latent initiator	71
3.3.3.1	Polymerization of GPE	71
3.3.3.1.1	Effect of counter anion	71
3.3.3.1.2	Effect of phosphine moiety	74
3.3.3.1.3	Polymerization mechanism	76
3.3.4	Substituted xanthenyl phosphonium salts as thermo-latent initiator	77
3.3.4.1	Polymerization of GPE	77
3.3.4.2	Polymerization of CHO	80
3.4	Conclusions	81
3.5	References	82

Chapter 4: Photo chemically and thermally induced radical promoted cationic polymerization using allylic phosphonium salts as initiators

4.1	Introduction	84
4.2	Experimental	85
4.2.1	Materials	85
4.2.2	Phenyl azotriphenyl methane (PAT)	85
4.2.3	2-(bromomethyl)- N, N-dimethyl acryl amide	86
4.2.4	2-(bromomethyl)- acryloyl morpholine	87
4.2.5	2-(bromomethyl)- N, N-dimethyl acrylamide triphenyl phosphonium hexafluoroantimonate	88
4.2.6	2-(bromomethyl)- acryloyl morpholine triphenylphosphonium hexafluoroantimonate	89
4.2.7	Characterization	90
4.2.8	Polymerization procedure	90
4.3	Results and discussion	90
4.3.1	Initiator synthesis	91
4.3.2	Polymerization	91

4.3.2.1	Thermal polymerization of CHO	92
4.3.2.1.1	Polymerization in the absence of radical sources	92
4.3.2.1.2	Polymerization in the presence of radical sources	92
4.3.2.2	Photo polymerization of CHO	94
4.3.2.2.1	Polymerization in the absence of radical source	94
4.3.2.2.2	Polymerization in the presence of radical source	94
4.3.3	Polymerization mechanism	97
4.4	Conclusions	97
4.5	References	98

Chapter 5: Photo cationic polymerization using benzophenone based allyl ammonium salts as initiators

		99
5.1	Introduction	
5.2	Experimental	100
5.2.1	Materials	100
5.2.2	Synthesis of 2-(N, N-dimethylcarboxy-3-propenyl)(phenylcarbonyl-4-phenylene) dimethylammonium hexafluoroantimonate (DMPDA)	100
5.2.3	Synthesis of 2-(morpholinocarboxy-3-propenyl) (phenylcarbonyl-4-phenylene) dimethylammonium hexafluoroantimonate (MPDA)	101
5.2.4	Typical polymerization procedure	102
5.2.5	Measurements	102
5.3	Results and discussion	102
5.3.1	Initiator synthesis	102
5.3.2	Photopolymerization	103
5.3.3	Mechanism of photopolymerization	107
5.4	Conclusions	110
5.5	References	110

Chapter 6: Diselenides as novel non-salt photo initiator for photosensitized cationic polymerization of N-vinyl carbazole

6.1	Introduction	111
6.2	Experimental	111
6.2.1	Materials	111
6.2.2	Synthesis of diphenyl diselenide (DPDS)	112
6.2.3	Synthesis of dibenzyl diselenide (DBDS)	113
6.2.4	Synthesis of 1, 4-dicyanonaphthalene (DCN)	114
6.2.4.1	Synthesis of 1, 4-dibromonaphthalene (DBN)	114
6.2.4.2	Synthesis of 1, 4-dicyanonaphthalene (DCN)	115
6.2.5	Synthesis of dicyanoanthracene (DCA)	116
6.2.5.1	Synthesis of 9, 10-dibromoanthracene (DBA)	116
6.2.5.2	Synthesis of 9, 10-dicyanoanthracene (DCA)	116
6.2.6	General procedure for photo polymerization of NVC	117
6.2.7	Measurements	118
6.3	Results and discussion	118
6.3.1	Synthesis of initiator and sensitizer	118
6.3.2	Polymerization	120
6.3.2.1	Photo polymerization of NVC using DPDS as initiator	121
6.3.2.2	Photo polymerization of NVC using DBDS as initiator	122
6.3.3	Mechanism of photoreaction	124
6.4	Conclusions	125
6.5	References	125

Chapter 7: Summary and Conclusions

7.1	Summary and conclusions	127
7.2	Scope for future work	128

Photo and Thermo Latent Initiators for Cationic Polymerization

ABSTRACT

During the past three decades cationic polymerization stimulated by heat or light has received considerable attention and practically applied in variety of areas, including printing inks, adhesive, surface coating and photolithography ^[1-4]. Onium salt initiators such as sulfonium ^[5], pyridinium ^[6], ammonium ^[7], hydrazinium ^[8], and phosphonium ^[9] have been developed as potential thermally latent cationic initiators. However, allyl onium salts in conjugation with radical initiator are also found to initiate cationic polymerization. Thus, depending upon the kind of radical initiator chosen, initiation can be accelerated by heat or light ^[10]. Allylic ammonium salts based on ethyl acrylates having benzophenone moiety as sensitizer in the initiator itself has been developed as one component photosensitization system. ^[11] In photo initiated cationic polymerization, most of the onium salts absorbs below 300 nm that limits its practical applications ^[12], because medium and high-pressure mercury lamp emits most spectrum of their radiation above 300 nm. Photosensitization is the best method to overcome from this problem. Photosensitization process includes photoelectron transfer (PET) with photo-excited sensitizer ^[13,14], free radical ^[15] and charge transfers complexes. ^[16]

Based on literature studies, we found our interests in designing new thermo and photo latent initiators for cationically polymerizable monomers. These ideas have been broadly classified into the following objectives

- Designing new phosphonium salts initiators for cationic polymerization.
- Photo chemically and thermally induced radical promoted cationic polymerization using allyl phosphonium salts
- Developing an initiator having both photosensitizer and initiation moiety for photo cationic polymerization.
- Non-salt based photosensitization system for cationically polymerizable monomers.

The above objectives have been divided into the following chapters:

Chapter 1: Introduction

An overview of the literature on synthesis of initiators and their use in externally stimulated cationic polymerization.

Chapter 2: Scope and objectives of the present work

The scope and objectives of the present thesis will be described

Chapter 3: Thermally induced cationic polymerization using phosphonium salts as initiators

Different types of phosphonium salts (dibenzosuberonyl, xanthenyl) having different counter anions and phosphine moiety (SbF_6 , PF_6 , AsF_6 , BF_4) were synthesized and their initiation activity was examined in bulk polymerization of GPE from ambient to 200 °C temperature for 1 h. Effect of time on initiator activity was also studied with different counter anions at 130 °C up to 50 h. To see the effect of substituents on the initiator activity, 2-substituted (chloro, methyl, methoxy) xanthenyl phosphonium hexafluoroantimonate salts were synthesized and their initiation activity was investigated in bulk polymerization of GPE at ambient to 200 °C temperature for 1 h. To examine the effect of steric and electronic factors on initiation activity, polymerization was performed with cyclohexene oxide (CHO) monomer.

Chapter 4: Photo chemically and thermally induced radical promoted cationic polymerization using allylic phosphonium salts as initiators

N, N-dimethylacrylamide and acryloyl morpholine based phosphonium salts with hexafluoroantimonate counter anion were synthesized and their capability to initiate cationic polymerization of CHO, in combination with free radical initiator was examined. For thermally induced polymerization, reactions were performed with and without thermal free radical initiators (PAT, AIBN, BPO). Photo polymerization was also performed with and without photo free radical initiators (TDMPO, benzophenone, benzoin). Both thermal and photo radical initiator promotes the polymerization of CHO. Photo polymerization of *n*BVE, IBVE & NVC was also studied above 290 nm.

Chapter 5. Photo cationic polymerization using benzophenone based allyl ammonium salts as initiators

Photosensitive N, N-dimethylacrylamide and acryloyl morpholine based allylic ammonium hexafluoroantimonate having benzophenone moiety in the structure were synthesized and their capability to act as self-initiating addition fragmentation agent in the photo initiated cationic polymerization of cyclic (CHO) and vinyl ether (*n*BVE, IBVE) monomer was examined at $\lambda > 290$ nm. Both the initiators work as one component photosensitization system.

Chapter 6: Diselenides as non-salt photo initiator for photosensitized cationic polymerization of N-vinyl carbazole

Photo initiated cationic polymerization of N-vinyl carbazole (NVC) with diphenyldiselenide (DPDS), dibenzoyldiselenide (DBDS) as an initiator and aromatic nitriles such as dicyanonaphthalene (DCN), dicyanoanthracene (DCA) as sensitizer was studied at $\lambda > 290$ nm in CH₂Cl₂ solvent using single electron transfer reactions.

Chapter 7: Summary and Conclusion

This chapter summarizes the results of the present work and the salient conclusions.

References

1. K. Dietlker, "Chemistry & Technology of UV & EB formulation for coating, Inks, Vol III, SITA Technology Ltd., London **1991**.
2. J. V. Crivello, *J. Polym Sci. Part A: Polym Chem.* **1999**, 37, 4241.
3. Y. Yagci, I. Reetz *Prog. Polym. Sci.* **1998**, 23, 1465.
4. Y. Yagci, T. Endo, *Adv Polym Sci.* **1997**, 127, 59.
5. K. Morio, H. Murase, H. Tsuchiya. T. Endo, *J. Appl. Polym. Sci.* **1986**, 23, 5727.
6. S. B Lee, T. Takata, T. Endo, *Macromolecules* **1990**, 23, 431.
7. S. Nakano, T. Endo, *Prog. Org. Coatings* **1993**, 22, 287.
8. T. Endo, F Sanda, *Macromol Symp* **1996**, 107, 237.
9. K. Takuma, T. Takata, T. Endo, *Macromolecules* **1993**, 26, 862.
10. Y. Yagci, *Macromol Symp* **2001**, 174, 255.
11. S. Yurtery, A. Onen, Y. Yagci, *Eur Polym J* **2002**, 38, 1845.
12. J. V. Crivello, J. H. W. Lam, *J. Polym Sci. Part A: Polym Chem.* **1980**, 18, 2677.
13. Y. Yagci, I. Lukac, W. Schnabel, *Polymer* **1993**, 34, 1130.
14. M. K. Gupta, R. P. Singh, *Macromol. Symp.* **2006**, 240, 186.
15. Y. Yagci, *Macromol Symp* **1998**, 134, 177.
16. G. Hizal, Y. Yagci, W. Schnabel, *Polymer* **1996**, 37, 2821.

Abbreviations

AFA	Addition fragmentation agents
AIBN	Azoisobutyronitrile
BPO	Benzoyl peroxide
BMDMA	2-(Bromomethyl)- N, N-dimethyl acrylamide
BMAM	2-(Bromomethyl)-acryloyl morpholine
CHO	Cyclohexene oxide
DBA	Dibromo anthracene
DBN	Dibromo naphthalene
DCN	Dicyano naphthalene
DCA	Dicyano anthracene
DPDS	Diphenyl diselenide
DBDS	Dibenzyl diselenide
DABCO	1,4-Diazabicyclo [2.2.2] octane
DCM	Dichloromethane
DTBP	2,6-Di-t-butyl-4-methyl pyridine
DMPDA	2-(N,N-dimethylcarboxy-3-propenyl)(phenylcarbonyl-4-phenylene) dimethylammonium hexafluoroantimonate
DMABP	4-(Dimethylamino)benzophenone
DMTPH	2-(N, N-dimethylcarboxy-propenyl) triphenylphosponium hexafluoroantimonate
DMF	Dimethylformamide
ECH	Epichlorohydrine

GPC	Gel permeation chromatography
GPE	Glycidyl phenyl ether
IBVE	Isobutyl vinyl ether
MTPH	2-(Morpholinocarboxy-propenyl) triphenylphosponium hexafluoroantimonate
MPDA	2-(Morpholinocarboxy-3-propenyl)(phenylcarbonyl-4-phenylene) dimethylammonium hexafluoroantimonate
<i>n</i> -BVE	<i>n</i> -Butyl vinyl ether
NVC	N-Vinyl carbazole
PDI	Polydispersity index
PPA	Polyphosphoric acid
PPO	Propylene oxide
PAT	Phenyl azotriphenyl methane
TGA	Thermogravimetric analysis
THF	Tetrahydrofuran
TMDPO	2,4,6-Trimethylbenzoyl diphenylphosphonyloxide

List of Tables

Table		Page no.
1.1	UV absorption characteristics of selected diazonium salts	5
1.2	UV absorption characteristics of selected diaryliodonium salts	6
1.3	UV absorption characteristics of selected sulfonium salts	7
1.4	UV absorption characteristics of selected phosphonium salts	8
1.5	UV absorption characteristics of N-alkoxy pyridinium salts	9
1.6	Selected photo latent anilinium salts used for cationic polymerization	10
1.7	Sensitization of onium salts with various photosensitizers	13
1.8	Sensitizing dyes for photodecomposition of diaryliodonium salts	15
1.9	Reduction potential of various onium salts	17
1.10	Addition fragmentation agents used in cationic polymerization	18
1.11	One-component addition fragmentation agents used in cationic polymerization	19
1.12	Photo latent ferrocenium salts used for cationic polymerization	20
1.13	Photo latent sulfonic acids used for cationic polymerization	20
1.14	Selected organosilanes salts used for photo cationic polymerization	21
1.15	Selected thermo-latent sulfonium salts used for cationic polymerization	23
1.16	Phosphonium salt used for cationic polymerization	26
1.17	Thermo latent polymeric onium salts	27
3.1	Phosphonium salt initiators used in present study	57
3.2	Crystal data and structure refinement for 3.1b, 3.1e, 3.4b, 3.4e	58
3.3	Solubility of phosphonium salts in various solvents and epoxy monomers	64
3.4	Polymerization of GPE using dibenzosuberonylphosphonium salts (3.1b-	66

3.1e)		
3.5	Polymerization using dibenzosuberonyltri- <i>n</i> -butylphosphonium salt	69
3.6	Polymerization of GPE using dibenzosuberonyltriphenylphosphonium salt	70
3.7	Polymerization of GPE using xanthenyltriphenyl phosphonium salts	72
3.8	Polymerization of GPE using xanthenyltri- <i>n</i> -butylphosphonium salts	75
3.9	Polymerization of GPE with 2-substituted xanthenylphosphonium salts	79
3.10	Polymerization of CHO with 2-substituted xanthenylphosphonium salts	81
4.1	Thermal polymerization of CHO initiated by thermal radical sources	93
4.2	Photopolymerization of CHO with allylic phosphonium salts in presence of various radical sources at $\lambda > 290$ nm	95
4.3	Photopolymerization of other cationic monomers with DMTPH and benzoin	96
5.1	Photopolymerization of CHO using various concentrations of allylic ammonium salt in CH ₂ Cl ₂ solvent	104
5.2	Photopolymerization of IBVE using various concentrations of allylic ammonium salt in CH ₂ Cl ₂ solvent	105
5.3	Photopolymerization of <i>n</i> -BVE using various concentrations of allylic ammonium salt in CH ₂ Cl ₂ solvent	106
5.4	Photopolymerization of various monomers in the presence of DMPDA	107
6.1	Free energy estimation of photosensitization process	120
6.2	Photosensitized cationic polymerization of NVC with DPDS	121
6.3	Photosensitized cationic polymerization of NVC with DBDS	122

List of Figures

Figure		Page no.
3.1	¹ H NMR spectrum of dibenzosuberonyltriphenylphosphonium salts	38
3.2	¹ H NMR spectrum of dibenzosuberonyltri- <i>n</i> -butylphosphonium hexafluoroantimonate	40
3.3	¹ H NMR spectrum of dibenzosuberonyltriphenylphosphonium hexafluoroantimonate	41
3.4	¹ H NMR spectrum of xanthenyltriphenylphosphonium salt	43
3.5	¹ H NMR spectrum of xanthenyl-tri- <i>n</i> -butylphosphonium hexafluoroantimonate	45
3.6	¹ H NMR spectrum of 2-carboxy-4-chloro diphenyl ether	46
3.7	¹ H NMR spectrum of 2-chloro xanthone	47
3.8	¹ H NMR spectrum of 2-chloro xanthidrol	48
3.9	¹ H NMR spectrum of 2-(4-methylphenoxy) benzoic acid	49
3.10	¹ H NMR spectrum of 2-methyl xanthone	49
3.11	¹ H NMR spectrum of 2-methyl xanthidrol	50
3.12	¹ H NMR spectrum of 2-(4-methoxyphenoxy) benzoic acid	51
3.13	¹ H NMR spectrum of 2-methoxy xanthone	52
3.14	¹ H NMR spectrum of 2-methoxy xanthidrol	52
3.15	¹ H NMR spectrum of 2-chloro xanthenyltriphenylphosphonium hexafluoroantimonate	53
3.16	¹ H NMR spectrum of 2-methyl xanthenyltriphenylphosphonium hexafluoroantimonate	54
3.17	¹ H NMR spectrum of 2-methoxy xanthenyltriphenylphosphonium hexafluoroantimonate	55
3.18	Ortep diagram of dibenzosuberonyltriphenylphosphonium hexafluoroantimonate	59

3.19	Ortep diagram of dibenzosuberonyltriphenylphosphonium tetrafluoroborate	60
3.20	Ortep diagram of xanthenyltriphenylphosphonium hexafluoroantimonate	60
3.21	Ortep diagram of xanthenyltriphenylphosphonium tetrafluoroborate	61
3.22	Thermograms of dibenzosuberonyl phosphonium salts	61
3.23	Thermograms of xanthenyl phosphonium salts	62
3.24	Thermograms of 2-substituted xanthenyl phosphonium salts	62
3.25	Temp – conversion curve in GPE polymerization with 3.1b-3.1e for 1 h	67
3.26	Time – conversion curve in GPE polymerization with 3.1b-3.1e at 130 °C for 70 h	67
3.27	Temp - conversion curve in GPE polymerization with 3.1b and 3.2 for 1 h	69
3.28	Temp-conversion curve in GPE polymerization with 3.1b and 3.3 for 1 h	70
3.29	Temp-conversion curve in polymerization of GPE with 3.4b-3.4e for 1 h	73
3.30	Time - conversion curve in polymerization of GPE with 3.4b-3.4e at 135 °C	74
3.31	Effect of temperature on polymerization with 3.4b and 3.5 for 1 h	75
3.32	¹ H NMR spectrum of 9-Benzylidene-9H-xanthene	77
3.33	Temperature - conversion curve in GPE polymerization with 2-substituted xanthenyl phosphonium salts	78
4.1	¹ H NMR spectrum of phenylazotriphenyl methane	86
4.2	¹ H NMR spectrum of 2-(bromomethyl)N, N-dimethyl acrylamide	87
4.3	¹ H NMR spectrum of 2-(bromomethyl)-acryloyl morpholine	88
4.4	¹ H NMR spectrum of 2-(N, N-dimethylcarboxy-propenyl) triphenyl phosphonium hexafluoroantimonate	88
4.5	¹ H NMR spectrum of 2-(morpholinocarboxy-propenyl) triphenylphosphonium hexafluoroantimonate	89
4.6	UV absorption spectrum of phosphonium salts in CH ₂ Cl ₂ , [phosphonium salts] = 1.25 x 10 ⁻³ mol l ⁻¹	91

4.7	Temperature-conversion curve in polymerization of CHO with allylic phosphonium salts in the absence of radical sources	92
4.8	Time-conversion curve in polymerization of CHO with DMTPH in the presence of radical sources [CHO: initiator: radical source = 5 mol l ⁻¹ : 5 x 10 ⁻³ mol l ⁻¹ : 5 x 10 ⁻³ mol l ⁻¹]	93
4.9	Time-conversion curve in polymerization of CHO with MTPH in presence of radical sources [CHO: initiator: radical source = 5 mol l ⁻¹ : 5 x 10 ⁻³ mol l ⁻¹ : 5 x 10 ⁻³ mol l ⁻¹]	94
4.10	Photopolymerization of CHO with DMTPH in presence of different concentration of benzoin [5 x 10 ⁻³ and 2 x 10 ⁻² mol l ⁻¹]	96
5.1	¹ H NMR spectrum of 2-(N, N-dimethylcarboxy-3-propenyl)(phenylcarbonyl-4-phenylene) dimethylammonium hexafluoroantimonate	101
5.2	¹ H NMR spectrum of 2-(morpholinocarboxy-3-propenyl)(phenylcarbonyl-4-phenylene) dimethylammonium hexafluoroantimonate	101
5.3	UV absorption spectra of DMABP, MPDA and DMPDA	103
5.4	Photopolymerization of CHO in presence of DMPDA [CHO] = 5 mol l ⁻¹ , λ > 290 nm, 25 °C, (A) DMPDA = 5 x 10 ⁻³ mol l ⁻¹ , (B) DMPDA = 5 x 10 ⁻⁴ mol l ⁻¹ and (C) DMPDA = 5 x 10 ⁻⁵ mol l ⁻¹	104
5.5	Photopolymerization of IBVE in presence of DMPDA [CHO] = 5 mol l ⁻¹ , λ > 290 nm, 25 °C, (A) DMPDA = 5 x 10 ⁻³ mol l ⁻¹ , (B) DMPDA = 5 x 10 ⁻⁴ mol l ⁻¹ and (C) DMPDA = 5 x 10 ⁻⁵ mol l ⁻¹	105
5.6	Photopolymerization of <i>n</i> -BVE in presence of DMPDA [CHO] = 5 mol l ⁻¹ , λ > 290 nm, 25 °C, (A) DMPDA = 5 x 10 ⁻³ mol l ⁻¹ , (B) DMPDA = 5 x 10 ⁻⁴ mol l ⁻¹ and (C) DMPDA = 5 x 10 ⁻⁵ mol l ⁻¹	106
5.7	Photo fragmentation spectra of DMPDA in GC-MS analysis	109
5.8	Photo fragmentation spectra of DMPDA in GC-MS analysis	109
6.1	¹ H NMR spectrum of diphenyl diselenide	113
6.2	¹ H NMR spectrum of dibenzyl diselenide	114
6.3	¹ H NMR spectrum of 1, 4-dibromonaphthalene	115
6.4	¹ H NMR spectrum of 1, 4-dicyanonaphthalene	116
6.5	¹ H NMR spectrum of 9, 10-dibromoanthracene	117

6.6	^1H NMR spectrum of 9, 10-dicyanoanthracene	117
6.7	UV absorption spectrum of sensitizer (DCN, DCA) and monomer (NVC)	119
6.8	GPC eluograms of pNVC where, $[\text{NVC}] = 2\text{M}$ in CH_2Cl_2 . $[\text{NVC}]$: $[\text{DPDS}]$: $[\text{DCN}] = 100:1:1$	123
6.9	GPC eluograms of pNVC where, $[\text{NVC}] = 2\text{M}$ in CH_2Cl_2 . $[\text{NVC}]$: $[\text{DPDS}]$: $[\text{DCA}] = 100:1:1$	123

List of Schemes

Scheme		Page no.
1.1	Photodecomposition of onium salt	4
1.2	Cationic photopolymerization	4
1.3	Initiation via charge transfer complex	11
1.4	Photosensitization of onium salt	12
1.5	Photosensitized cationic polymerization	12
1.6	Free radical promoted cationic polymerization	16
1.7	Mechanism of addition fragmentation reaction	17
3.1	Synthesis of dibenzosuberene based phosphonium salts	37
3.2	Synthesis of xanthenyl phosphonium salts	42
3.3	Synthesis of 2-substituted xanthenyltriphenylphosphonium salts	45
3.4	Polymerization of GPE with dibenzosubererylphosphonium salts	65
3.5	Polymerization of GPE with xanthenylphosphonium salts	71
3.6	Mechanism of GPE polymerization	76
3.7	Polymerization of GPE with 2-substituted xanthenyltriphenyl phosphonium hexafluoroantimonate	78
3.8	Polymerization of CHO with 2-substituted xanthenyltriphenyl phosphonium hexafluoroantimonate	80
4.1	Synthesis of amide based allylic phosphonium salts	91
4.2	Polymerization mechanism <i>via</i> addition fragmentation pathway	97
5.1	Synthesis of benzophenone based allylic ammonium salts	102
5.2	Radical polymerization via hydrogen abstraction mechanism	107
5.3	Polymerization via radical addition fragmentation mechanism	108
5.4	Photo fragmentation of DMPDA in GC-MS analysis	108

6.1	Synthesis of diphenyl diselenide	112
6.2	Synthesis of dibenzyl diselenide	113
6.3	Synthesis of 1, 4-dicyanonaphthalene	114
6.4	Synthesis of 9, 10-dicyanoanthracene	116
6.5	Photo polymerization of NVC	120
6.6	Mechanism of photocationic polymerization of NVC	124

Chapter 1: Introduction

1. Introduction

1.1. Polymers

A polymer is a material that is composed of with large number of small repeating units or monomer, connected by covalent bond. The word polymer is derived from the Greek words πολυ, polu, "many"; and μέρος, meros, "part". The well known example of polymers are plastic, DNA and proteins. Plastic is the popular term for polymer covering a range of natural and synthetic polymer with a variety of properties and applications. In present world, they are very necessary for providing man with a range of materials ranging from soft rubber like materials to tough plastics, from silk like fibers to fibers with the tenacity of steel ^[1-4]. Only during the recent few decades, it was recognized that polymers could also be endowed with functional properties beyond the scope of traditional structural materials like wood, metals and ceramics. Polymer preparation is no longer sufficient rather the aspects of design in the synthesis of polymer are gaining increasing importance. It is possible to design a variety of polymer architectures with differing macroscopic properties with different set of monomers by tailoring the chain length distribution, monomer sequence distribution, tacticity, nature of functionality and degree of branching ^[5].

1.2. Cationic polymerization

Process in which the active end of the growing polymer molecule is a positive ion, termed as cationic polymerization. This technique is specially used for polymerization of monomers with electron donating substituents such as alkoxy, phenyl, vinyl and 1,1 – dialkyl. Cationic polymerization is usually initiated by electrophilic compounds such as Bronsted / Lewis acids, carbocations and trialkyl oxonium salts ^[6]. The two types of initiators have been developed for cationic polymerization. First, classical initiators, which initiate polymerization immediately after addition to monomer and second, externally stimulated initiators that generate active cations only after external stimulation such as heat

or light. There are many industrial monomers (such as epoxides and vinyl ether), which have applications in curing formulations where the initiation is required at particular time and temperature.

1.3. Externally stimulated cationic polymerization

In this type of polymerization, initiation is triggered by external stimulation such as light, heat, γ -irradiation etc. The selection of appropriate wavelength of light and temperature can control the initiation. Polymerization by this method yields polymer with broad molecular distribution due to the generation of initiating species continuously. These latent initiators are capable of exhibiting no activity under ambient condition but produce active species on external stimulation such as heat or photo-irradiation. The development of efficient latent cationic initiators is desirable for their inherent storage stability, handling and solubility in monomers. In last four decades, a large number of initiators based upon external stimulation have been developed [7, 8]. The externally stimulated cationic polymerization is discussed herewith respect to mode of initiation (light and heat).

1.3.1. Photo-induced cationic polymerization

Photopolymerization is defined as the reaction of monomers or macro monomer to produce polymeric structure by light induced initiation. Photo initiators are organic or organometallic compounds that can absorb light and undergo photochemical process to form the reactive intermediates, such as free radicals or cationic species. These reactive species will subsequently initiate polymerization of functional monomers. As a key component in the photo polymerization process, a good photo initiator is expected to possess the following properties:

- ❖ High absorption in particular region of absorption, which depends on the specific applications and light source.
- ❖ Good quantum yield for the formation of initiating species.
- ❖ Low cost
- ❖ Non toxic and odorless
- ❖ Ease of handling

- ❖ Good solubility in the resin system used
- ❖ Non-yellowing properties

Based on initiating species generated, photo initiators can be divided into three categories, namely anionic, radical and cationic initiators. For anionic polymerization, very limited types of photo initiators are available due to slow polymerization rate^[9, 10]. Free radical polymerization is most developed initiation system due to its high curing speed and ready commercial availability of the variety of monomers and oligomers^[11]. There are few disadvantages like oxygen inhibition and toxicity of acrylate monomers, degradation of cured films and volume change during curing process^[12, 13]. The cationic photo polymerization has advantages for these limitations and is versatile technique and may be used to polymerize important class of monomers, including epoxides and vinyl ethers. Although, these classes of monomers cannot be cured by free radical polymerization but they exhibit many desirable properties such as low volatility, good rheological properties and negligible toxicity^[14]. Furthermore, the cured polymer films associated with these monomers exhibit excellent clarity, adhesion, abrasion resistance and chemical resistance^[15, 16]. Several classes of cationic initiators have been developed but there are few major obstacles such as relatively slow curing rate of the epoxides monomers and limited choice of soluble, highly sensitive, inexpensive cationic photo initiation. The major efforts to solve these problems are summarized in recent reviews^[17, 18].

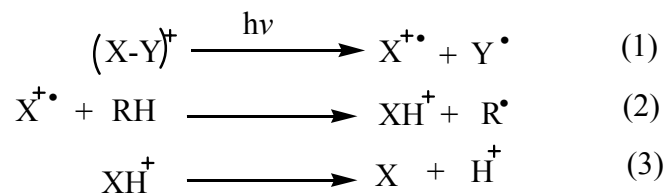
1.3.1.1. Direct acting system

1.3.1.1.1. Onium salts

Onium salts are most popular among widely used cationic photo initiators. These salts have positive charge on heteroatom and a less nucleophilic counter anion (such as SbF_6 , PF_6 , AsF_6 , BF_4 and $(\text{C}_6\text{F}_5)_4\text{B}$). Upon photolysis, these thermally and hygroscopically stable initiators undergo fragmentation irreversibly to generate active species (cation radical and Bronsted acid) and effectively initiate polymerization. These are nearly insoluble in water but readily soluble in a wide variety of common polar solvents and cationically polymerizable monomers. These compounds were found to absorb strongly in the short-wavelength (220–250 nm) UV region and function as efficient cationic photo initiators.

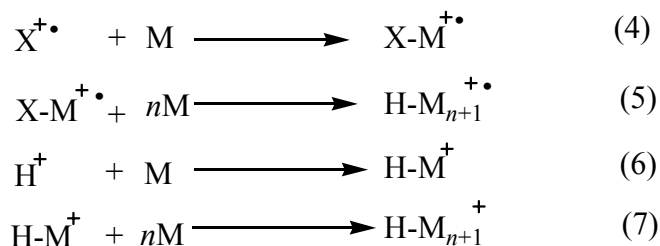
1.3.1.1.1.1. Direct photolysis

With respect to the onium salt type initiator $[(X-Y)^+ Z^-]$, cation undergoes cleavage on photo excitation as depicted in Scheme 1.1.



Scheme 1.1: Photodecomposition of onium salt

The radical cation ($X^{+\bullet}$) generated in this way may abstract hydrogen from the surrounding molecule RH. The resulting cation is unstable and undergoes dissociation into proton H^+ and stable compound X. Both initially formed radical cation and protons are the potential initiating species regarding the reaction with a polymerizable monomer (M) (Scheme 1.2).



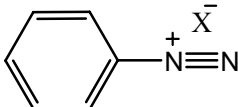
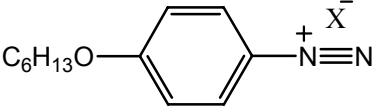
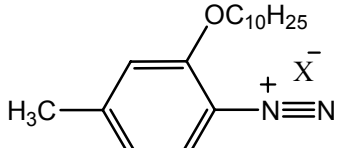
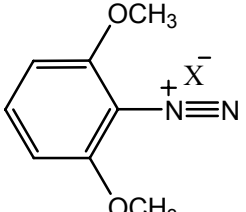
Scheme 1.2: Cationic photopolymerization

The important classes of onium salt photo initiators can be divided in the following categories.

1.3.1.1.1.1.1. Aryldiazonium salts

These are prepared by reaction of anilinium derivatives with sodium nitrite and Bronsted acid ^[19, 20]. Upon photo-irradiation, these salts undergo fragmentation and generate active species as a Bronsted acid or proton. Aryldiazonium salts show absorption characteristics below 300 nm and are good photo initiators with high quantum yield (0.3-0.6) (Table 1.1).

Table 1.1: UV absorption characteristics of selected diazonium salts

Initiator	λ_{\max} (nm)	ϵ_{\max} (l mol ⁻¹ cm ⁻¹)	Ref
	272	14,500	19
	315	24,460	20
	277 348	14,080 4,860	20
	287 377	11,850 4,050	20

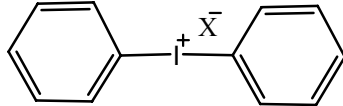
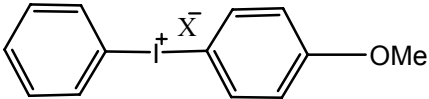
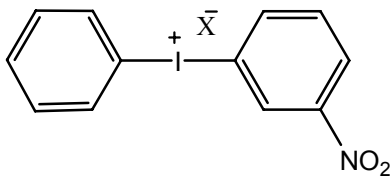
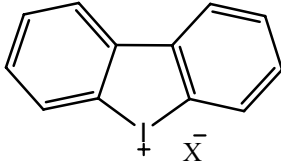
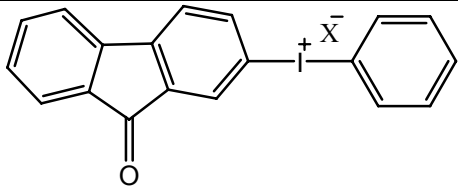
X = SbF₆/PF₆/AsF₆/BF₄/(C₆F₅)₄BF₄

The inherent thermal instability of aryldiazonium salts leads to poor latency even in the absence of light. In addition, the generation of nitrogen gas as a product of the photolysis reaction, which limits its application as cationic initiator.

1.3.1.1.1.2. Diaryliodonium salts

The preparation of iodonium salts involves the reaction of aromatic compound with potassium iodide in presence of sulfuric acid and acetic anhydride ^[21- 23]. Diaryliodonium salts are thermally stable, colorless to yellowish white crystalline compounds with quantum yields of 0.7 to 0.9, and are often soluble in polar organic solvents. Diaryliodonium salts efficiently undergo photolysis and generate aryl cations and aryl iodine radical cations as active species, which further react with solvents, monomers and impurities to give protonic acid. These have poor spectral absorption above 290 nm (Table 1.2).

Table 1.2: UV absorption characteristics of selected diaryliodonium salts

Initiator	λ_{\max} (nm)	ϵ_{\max} (l mol ⁻¹ cm ⁻¹)	Ref
	227	17,800	21
	237	18,000	21
	227	18,000	22
	264	17,300	23
	265 296 366	6,400 9,200 745	23

X = SbF₆/PF₆/AsF₆/BF₄/(C₆F₅)₄BF₄

1.3.1.1.1.3. Sulfonium salts

Triaryl and alkylaryl sulfonium salts are generally crystalline compounds, which are soluble in common organic solvents and are slightly soluble in water [24-26]. These compounds are thermally stable due to significant π - π bonding between the sulphur atom and the aromatic ring. Among these salts, alkyl aryl sulfonium salts are less thermally stable [27]. The triarylsulfonium salts display a unique combination of high thermal stability and high photosensitivity (Table 1.3). At the opposite extreme, trialkylsulfonium salts are photochemically inactive and as alkylating agents, spontaneously initiate the cationic polymerizations of certain monomers [28, 29].

The sulfonium salts bearing at least one aromatic or other resonance stabilizing chromophore may provide reasonable photosensitivity and thermal stability to the photo initiator. Indeed, phenacyl alkyl sulfonium salts [30, 31] and 4-hydroxy phenyl

dialkylsulfonium salts ^[32] are also found to display excellent photosensitivity and efficiency as cationic photo initiators.

Table 1.3: UV absorption characteristics of selected sulfonium salts

Initiator	λ_{\max} (nm)	ϵ_{\max} (l mol ⁻¹ cm ⁻¹)	Ref
	227	21,000	24
	255 280	21,700 10,100	25.
	230 300	24,330 19,500	24
	208 255 315	17,300 6,500 2,500	26
	250 280	-	30
	250 290	-	31
	255 315	6,500 2,500	32

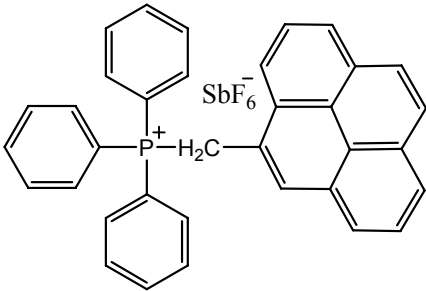
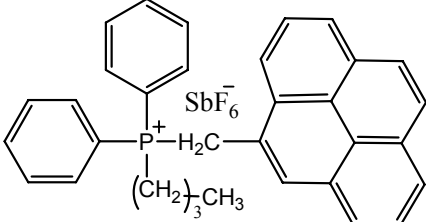
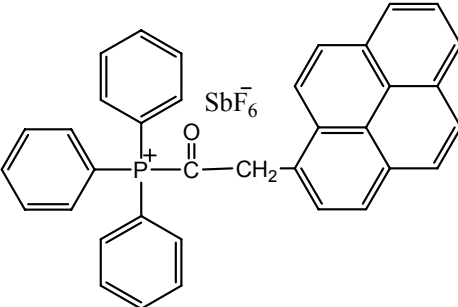
X = SbF₆/PF₆/AsF₆/BF₄/(C₆F₅)₄BF₄

1.3.1.1.1.4. Phosphonium salts

These initiators are prepared by reaction of halo methylated aromatic compounds with corresponding phosphines ^[33-37]. On photo-irradiation of these salts, the resonance

stabilized ylide and protons are formed as active species. Phenacyl phosphonium salts have also been used for cationic polymerization ^[38]. The absorption characteristics of these initiators are shown in Table 1.4.

Table 1.4: UV absorption characteristics of selected phosphonium salts

Initiator	λ_{\max} (nm)	ϵ_{\max} (l mol ⁻¹ cm ⁻¹)	Ref
	280 352	30,800 31,200	35
	280 350	38,000 40,000	35, 36
	257	32,000	37

1.3.1.1.1.5. N-alkoxy pyridinium salts

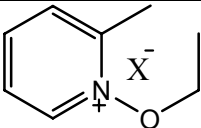
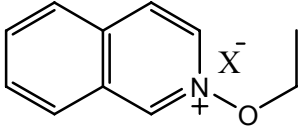
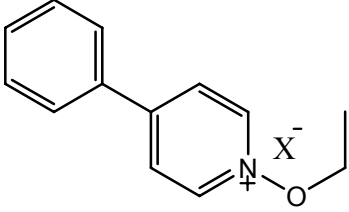
N-alkoxy pyridinium salts are prepared by a reaction of pyridine N-oxide with a triethyl oxonium salt ^[39, 40]. Quinolinium salts are also prepared in similar way ^[41]. These salts display absorption characteristics in far UV region (Table 1.5).

1.3.1.1.1.6. Phenacylpyridinium salts

The synthesis of these salts involves reaction of phenacyl chloride with corresponding pyridine derivatives ^[42-43]. The one component phenacylpyridinium salts are also

developed to extend the spectral sensitivity in long wavelength UV region ^[43]. The absorption characteristics of selected salts are shown in Table 1.6.

Table 1.5: UV absorption characteristics of N-alkoxy pyridinium salts

Initiator	λ_{\max} (nm)	ϵ_{\max} ($\text{l mol}^{-1} \text{cm}^{-1}$)	Ref
	266	5,925	39
	337	4,220	39
	310	21,440	39

X = SbF₆/PF₆/AsF₆/BF₄/(C₆F₅)₄BF₄

1.3.1.1.1.7. Phenacylanilinium salts

Phenacylanilinium salts are prepared by the reaction of phenacyl chloride with N, N-dimethyl aniline ^[44, 45]. These initiate polymerization of cyclohexene oxide, vinyl ether and N-vinyl carbazole below 300 nm (Table 1.6)

1.3.1.1.1.8. Polymer bound onium salts

Polystyrene ^[46], novolacs ^[47] based iodonium salt, aromatic poly(imide) containing triarylsulfonium salts ^[48] and pyridine N-oxide attached with poly(styrene-co-2-vinylpyridine) ^[49] as macro initiator were shown to be an efficient initiator for cationic polymerization. These photosensitive macro initiators undergo extensive chain cleavage upon UV irradiation and stimulate polymerization of epoxides.

Table 1.6: Selected photo latent anilinium salts used for cationic polymerization

Initiator	λ_{max} (nm)	Ref
	249 279 438	42
	256 395 461	42
	249 279	43
	252 442	43
	253 507	44, 45

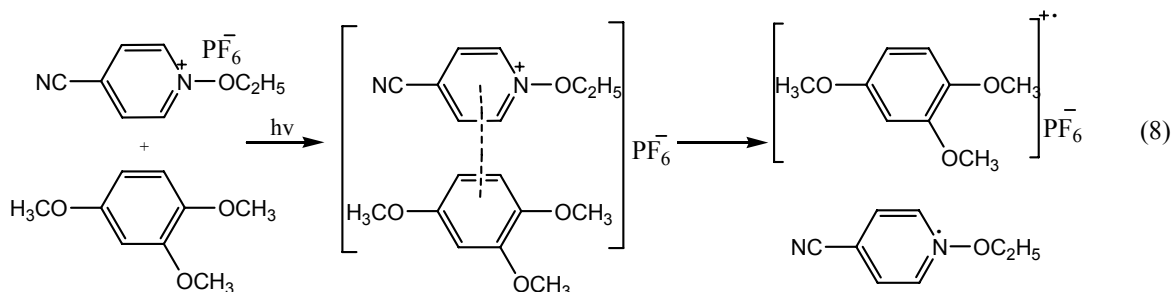
X = SbF₆/PF₆/AsF₆/BF₄/(C₆F₅)₄BF₄

1.3.1.2. Indirect acting photo systems

The majority of the onium salts absorb strongly in the wavelength range of 230-250 nm, whereas medium and high-pressure mercury lamps provide emission at 313 and 366 nm as light source. The poor absorptivity of these salts in the 300-450 nm region is great concern since, it severely limits their efficiency or light utilization in the range in which commonly available medium and high pressure mercury arc lamps provide a substantial portion of their emission. In addition, the products of photolysis also display absorption bands at or near those of the photo initiators. Thus, these products suppress further photolysis of the photo initiators due to screening effects. Chemical attachment of the chromophoric group into aromatic group of the salts is the one way to broaden the spectral sensitivity of the onium salts. However, it requires multistep synthetic procedure and the desire shift in the absorption spectrum of these salts could still not be achieved. Based on several investigations, there are some possible indirect pathways to extend the spectral sensitivity and are discussed in following sections.

1.3.1.2.1. Initiation *via* charge transfer complexes

This system involves formation of CT complex between donor and acceptor upon photoirradiation. Pyridinium salts are capable of forming ground state CT complexes with electron donors such as methyl and methoxy substituted benzene^[50]. In combination, these compounds show absorption maxima in visible region of light whereas the components are virtually transparent (Scheme 1.3).



Scheme 1.3: Initiation via charge transfer complex

For example CT complex formed between N-ethoxy-4-cyano pyridinium hexafluorophosphate and 1,2,4-trimethoxybenzene, which show an absorption maxima at 420 nm.

1.3.1.2.2. Energy transfer photosensitization

In this mechanism, the electronically excited photosensitizer (P*) interacts with ground state onium salt to promote it to its excited state. In the subsequent steps, the excited onium salts undergo fragmentation by bond cleavage in the similar way as direct photolysis. Here the function of photosensitizer is to absorb the energy of specific wavelength of light and mediates its transfer to onium salt. Pappas and Getechair^[51] have reported that the energy transfer does not occur for diaryliodonium salts and triarylsulfonium salts using photosensitizers with high triplet energies (> 70 kcal/mol) and high oxidation potential, which prevent competing energy transfer process from taking place. The phosphorescence emission from such photosensitizers is efficiently quenched in the presence of diaryliodonium and triarylsulfonium salts, thus the resulting excited state of these onium salts is unreactive towards bond cleavage. Therefore, the energy transfer does appear to occur for specific photosensitizer-salt combination. Due to inefficient energy transfer

through this process, it has little practical use in the photosensitized cationic polymerization.

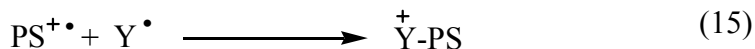
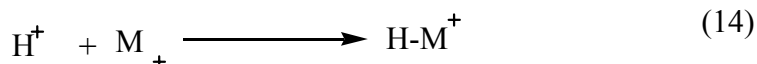
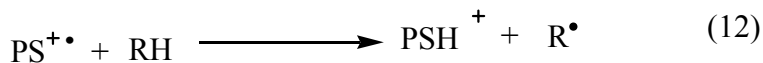
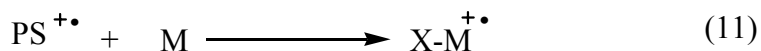
1.3.1.2.3. Electron transfer photosensitization

In this mechanism, the electron is transferred from the excited photosensitizer to onium salts with the probable involvement of an excited state complex (exciplex). In this photoredox reaction, photosensitizer is oxidized to a cation radical while the onium salt is reduced to a radical species (Scheme 1.4).



Scheme 1.4: Photosensitization of onium salt

The cation radical itself initiates the polymerization of appropriate monomers or can interact with hydrogen containing compounds in the system itself (Scheme 1.5).



Scheme 1.5: Photosensitized cationic polymerization

There are two basic requirements for the electron transfer, first the excitation energy (E^*) of the photosensitizer must be higher than difference between the net energy ($E_{\text{sen}}^{\text{ox}}$) required to oxidize the photosensitizer and the energy of onium salt ($E_{\text{onium}}^{\text{red}}$) to reduce the onium salt, second, the magnitude of the free energy (ΔG) of photosensitized energy

transfer should be negative (i.e., exothermic) by at least 10 kcal/mol (Table 1.7). The ΔG value can be determined using eq 17:

$$\Delta G = f_c(E_{1/2}^{ox} - E_{1/2}^{red}) - E(PS^*) \quad (17)$$

Table 1.7: Sensitization of onium salts with various photosensitizers

Sensitizer	Iodonium		Sulfonium		Alkoxy pyridinium	
	ΔG	Photo sens ^a	ΔG	Photo sens ^a	ΔG	Photo sens ^b
Benzophenone	-8	+	+88	-	39.8	-
Thioxanthone	-92	+	+4	-	-44.2	+
Anthracene	-193	+	-96	+	-144.4	+
Perylene	-171	+	-71	+	-121.8	+
Phenothiazine	-159	+	-63	+	-112.9	+

^a Polymerization of 3,4-epoxycyclohexylmethyl-3',4'-cyclohexene carboxylate ^[52] ^b Polymerization of cyclohexoxide ^[53]

The utilization of onium salts such as diaryliodonium as photo acid generators in photolithography and as photoinitiators for cationic photopolymerization in coating, printing ink, and adhesive applications is well known ^[54]. Moreover, many existing and future imaging methods are being designed with light sources such as lasers and light-emitting diodes (LEDs) that deliver narrow-band or monochromatic radiation in the long-wavelength UV and visible regions, in which onium salts have poorly response or completely inactive. Examples of such imaging processes include stereolithography, rapid prepress prototyping, electronic transmission and printing of images, circuit board imaging, patterning of TV screens and liquid-crystalline displays, and photopolymer printing plates. There are also several applications such as photo curable dental fillings and restoratives that make use of long wavelength ultraviolet–visible radiation to avoid skin damage. One effective method for spectrally broadening the sensitivity of onium salt photoinitiators at long wavelengths is through the use of electron-transfer photosensitization. Sensitivity for various onium salt-based cationic photo initiators have been achieved in the visible spectral region through the use of polynuclear aromatic

hydrocarbon as electron-transfer photosensitizers ^[55, 56]. Polynuclear aromatic hydrocarbons such as anthracene ^[57], pyrene ^[58], perylene ^[59], phenothiazine ^[60] and carbazole derivatives ^[61] have the requisite long-wavelength absorption characteristics and also undergo efficient photo-induced electron-transfer photosensitization with onium salt photo initiators. Although polynuclear aromatic hydrocarbons are the most efficient known examples of electron- transfer photosensitizers for onium salts but they have several serious drawbacks that limit their use. For example, they are generally expensive, toxic, and poorly soluble in most reactive monomers and polymer systems. As a result, there is a continuing unsatisfied need for the long-wavelength active photosensitizers that will circumvent the aforementioned complications.

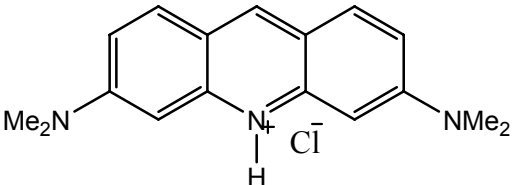
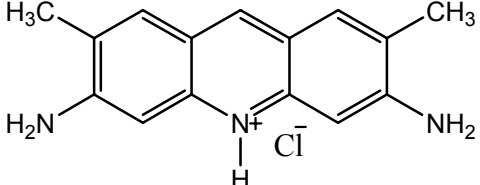
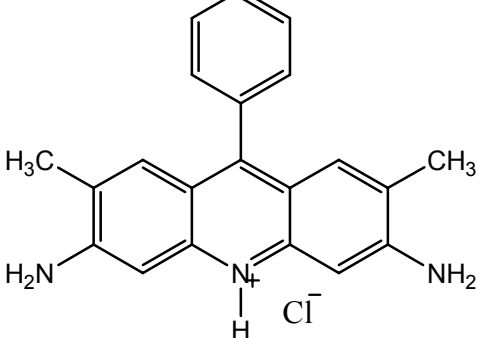
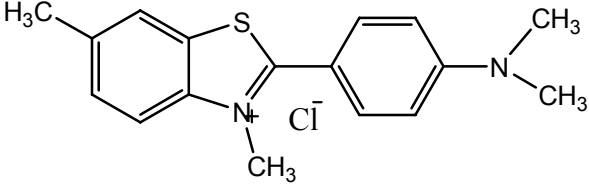
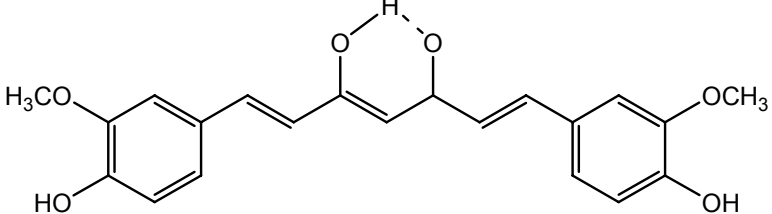
Dye sensitization is also a well-known phenomenon in organic reactions ^[62]. Several dyes have been discovered, which sensitize the photolysis of onium salts at visible wavelengths. By using the combination of a dye and an onium salt, visible light can be used for the photo initiated cationic polymerization (Table 1.8).

Necker et al ^[63] have reported a visible light system, which consists a xanthene dye, an aromatic amine and diaryliodonium salt cationic photoinitiator. The mechanism of reaction involves that the dye functions as photon acceptor and together with co-initiator (amine), produces the free radical on exposure to visible light. The iodonium salts oxidize the generated radicals into the carbocations to initiate cationic polymerization. All the three components are needed for visible light induced polymerization of epoxides.

Dyes (such as acridine (orange and yellow), benzoflavin and setoflavin T) with substituted diaryliodonium salts are used in the photosensitized cationic polymerization of epoxides in the range of 380-540 nm ^[64].

Yagci et al ^[65] have reported a ternary system consisting of an alkyl halide, dimanganese decacarbonyl $[Mn_2(CO)_{10}]$ and onium salt initiator for visible light induced cationic polymerization of cyclic ethers, bis-epoxides and vinyl ethers. The mechanism follows the free radical generation by the reaction of manganese carbonyl photoproduct with the halide group and subsequent oxidation of thus formed carbon-centered radicals to yield the reactive cations.

Table 1.8: Sensitizing dyes for photodecomposition of diaryliodonium salts

Dye	Structure	λ_{\max} , nm	Ref
Acridine Orange		539	64
Acridine Yellow		411	64
Benzoflavin		460	64
Setoflavin T		380	64
Curcumin		427	66

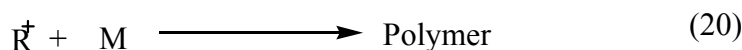
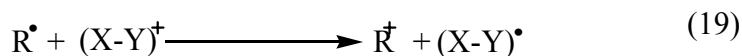
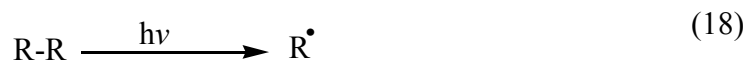
Crivello et al ^[66] have employed various derivatives of curcumin dye as efficient photosensitizer with diaryliodonium salt in the range of 340-545 nm (long wavelength UV and visible light) for cationic polymerization of vinyl, epoxy and oxetane monomers.

1.3.1.2.4. Initiation via free radical mediation

The photocationic polymerization through free radical mediation is divided in two categories, which depends on the nucleophilicity of the radical initiator.

1.3.1.2.4.1. Oxidation of carbon centered free radical

It is referred to as “free radical promoted cationic polymerization”, based on the oxidation of a free radical (high nucleophilicity) by an onium salt. This method is suitable for a variety of carbon-centered free radicals that are formed by photolysis or thermolysis of commonly used radical initiators. Many photo chemically formed radicals ^[67-72] can be oxidized by onium salts. Thus, the cation generated are used as initiating species for the cationic polymerization according to Scheme 1.6.



Scheme 1.6: Free radical promoted cationic polymerization

The possibility for the electron transfer according to reaction can be estimated with the aid of the modified Rehm-Weller equation:

$$\Delta G = f_c(E_{1/2}^{\text{ox}} - E_{1/2}^{\text{red}}) \quad (21)$$

Here $E_{1/2}^{\text{ox}}$ and $E_{1/2}^{\text{red}}$ denote the half wave potential of oxidation and reduction of the carbon centered radical and $(\text{X-Y})^+$, respectively.

The hypervalent iodine compounds, including diaryliodonium salts can also be reduced chemically employing a wide variety of chemical reducing agents ^[78]. Crivello et al have employed the ascorbate ^[79] and tin reducing agents together with diaryl iodonium salts to conduct redox initiated cationic polymerizations. Lendwith et al ^[80, 81] demonstrated that electron rich free radicals produced either by photolysis or by thermolysis are capable of

reducing iodonium salts. Yagci et al ^[82-85] have continued this work in recent years using allylic type of onium salts. The reduction potential of various onium salt is summarized in Table 1.9.

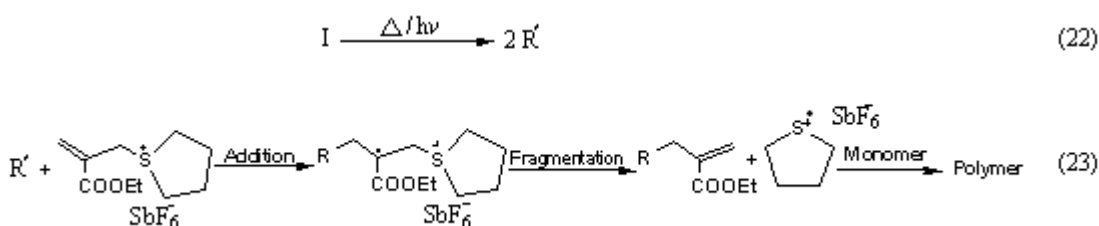
Table 1.9: Reduction potential of various onium salts

Onium Salt	$E_{1/2}^{\text{red}}$ ^a (Volts)	Ref
4-Cl-C ₆ H ₄ -N ₂ ⁺ X ⁻	0.35	73
Ph ₂ I ⁺ X ⁻	-0.2	74
Ph ₃ S ⁺ X ⁻	-1.06	75
	-0.7	76
	-0.5	74
	-0.5	77

^a) Measured vs Standard Calomel Electrode (SCE)

1.3.1.2.4.2. Addition fragmentation reactions

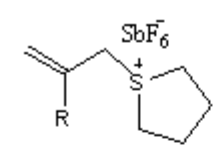
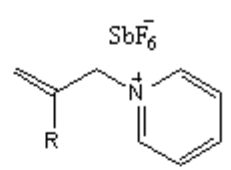
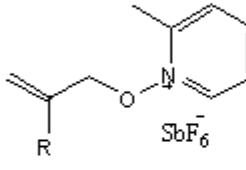
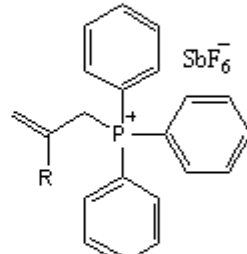
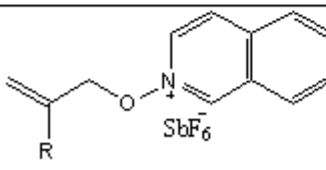
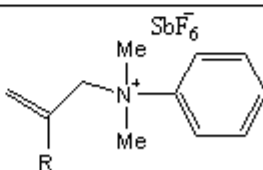
This approach involves the addition of photo chemically or thermally generated free radical (low nucleophilicity) to the allylic double bond of onium salt. The resulting intermediate radical cation undergoes fragmentation and producing another radical cation, which is capable of initiating cationic polymerization, which can be explained with S- [2-(ethoxycarbonyl) allyl] tetrahydrothiophenium ion ^[86, 87].



Scheme 1.7: Mechanism of addition fragmentation reaction

The mechanism of initiation involves, as briefly mentioned above, the addition of radical to the allylic double bond and subsequent rupture of the C-S bond. This AFA does not possess suitable chromophoric groups. An initiation by direct absorption of light can therefore, be disregarded. However, with radical photo initiators such as benzoin (irradiation at 340 nm), phosphine oxide (380 nm) and benzophenone derivatives, very fast cationic polymerization was observed (Table 1.10).

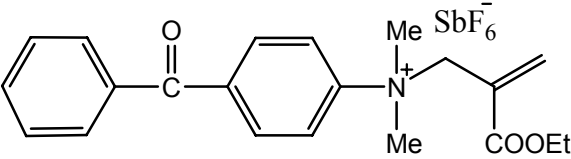
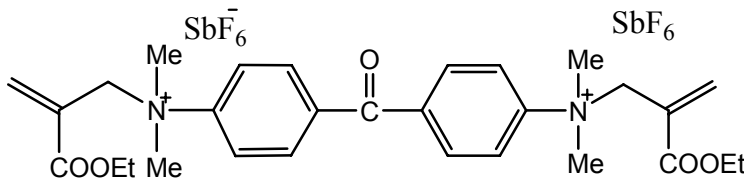
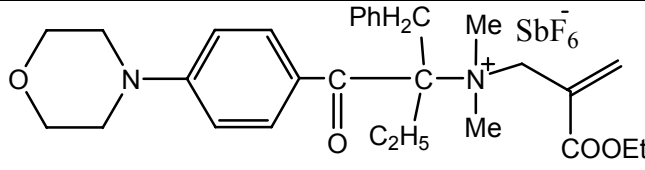
Table 1.10: Addition fragmentation agents used in cationic polymerization

Initiator	Ref	Initiator	Ref
 R = COOEt	86, 87	 R = COOEt	90
 R = H, CH3, COOEt	91, 92	 R = H, CH3, COOEt	93
 R = H, CH3	94	 R = H, CH3, COOEt	95

Moreover, as far as photo polymerization is concerned, it is extremely easy to tune a desired wavelengths range (the emission maximum of the irradiation source used) by choosing appropriate radical initiators. This system has advantage of the availability of large number of radical initiators with excellent yield and good storage stability. In addition, there is no limitation to electron donor radicals, i.e. any radical may be employed, which is capable of adding double bonds ^[88]. The other factors also determine the efficiency of the system such as light intensity, onium salt concentration and type of

radical initiator used ^[89]. Allylic salts with various substituents at the allylic moiety were shown to be highly efficient addition fragmentation agent for the initiation of cationic polymerization. In the recent years, one-component addition fragmentation agents having radical source itself in the initiator moiety are also used in photo cationic polymerization (Table 1.11).

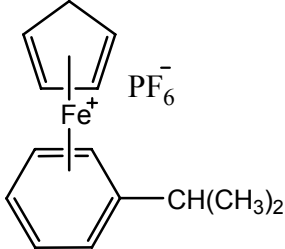
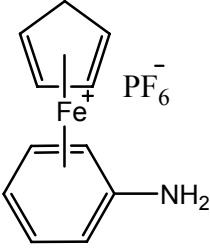
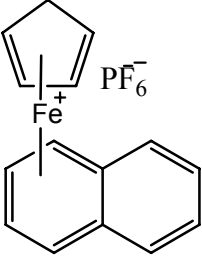
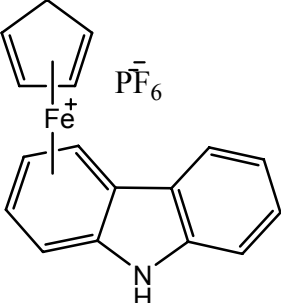
Table 1.11: One-component addition fragmentation agents used in cationic polymerization

Initiator	Ref
	96
	97
	98

1.3.1.3. Ferrocenium salts

These initiators involve easy synthesis, variability in spectral response change with the exchange of the iron arene ligands, high thermal stability and high efficiency in photo polymerization of epoxides ^[99] (Table 1.12). The mechanism of these reactions involves exchange of monomer followed by ring opening of the epoxides ^[100]. Wang et al also reported carbazole bound ferrocenium salts for cationic polymerization of epoxides ^[101]. This class of initiators has also have been utilized in the preparation of novolac epoxy resins ^[102].

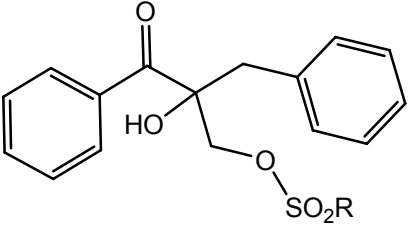
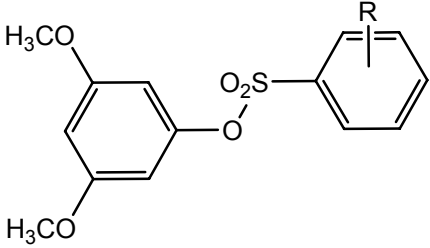
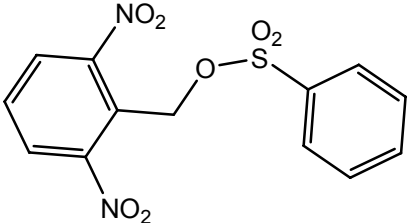
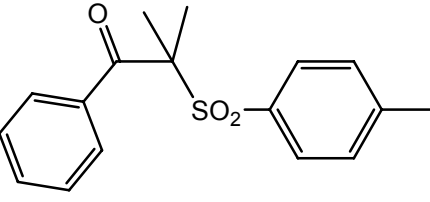
Table 1.12: Photo latent ferrocenium salts used for cationic polymerization

Initiator	Ref	Initiator	Ref
	99		100
	101		101

1.3.1.4. Latent sulfonic acid

This class of initiators includes benzoic sulphonates ^[103, 104], nitrobenzyl tosylate ^[105, 106], benzylbenzene sulphonate ^[107] and sulphonyl acetophenones ^[108, 109] (Table 1.13).

Table 1.13: Photo latent sulfonic acids used for cationic polymerization

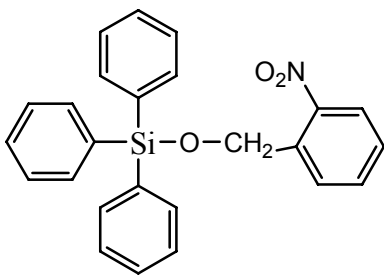
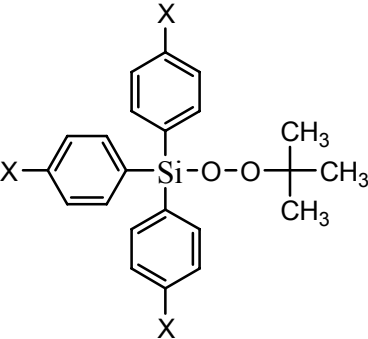
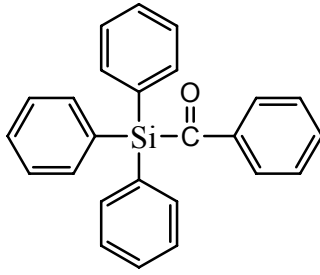
Initiator	Ref	Initiator	Ref
	103, 104		105
	105, 106		108, 109

The initiation mechanism reveals that upon photo-irradiation, sulphonic acid generates as initiating species. Initiators in this category are especially used for the polymerization of industrially important amino plast resins.

1.3.1.5. Photosensitive organosilanes

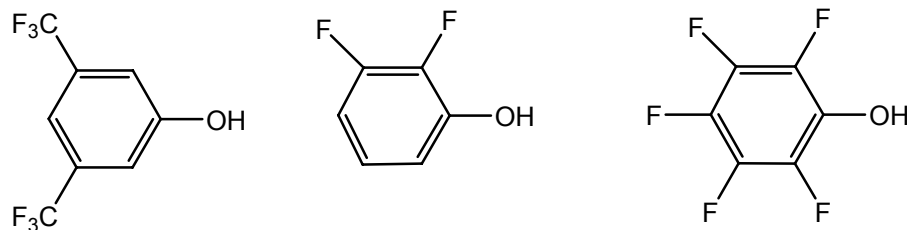
Hayase et al^[110-112] reported that the mixture of silanol and aluminium (III) complexes of β - diketones, β -ketoester or orthocarbonyl phenolate initiates cationic polymerization of cyclohexene oxide upon UV irradiation or thermal initiation (Table 1.14). The catalytic activity varies with ratio of silanol and aluminum complex and also structure of silanol compounds. The initiation mechanism involves the photo generation of silanol from the o-nitro benzyl triarylsilyl ether (ONBSi) and further combination with aluminium complex, initiates cationic polymerization of epoxides^[112].

Table 1.14: Selected organosilanes salts used for photo cationic polymerization

Initiator			
Ref	112	113	114

1.3.1.6. Phenol based non-salt initiator

These initiators having electron-withdrawing substituents in the phenolic ring are active initiators for the cationic polymerization of GPE, whereas phenols with electron donating substituents in the aromatic are failed to produce any polymer^[115]. These phenolic compounds initiate cationic polymerization under photo-excited state.



1.3.2. Thermally induced cationic polymerization

Cationic polymerization of monomer induced by thermal initiation in presence of latent cationic initiator is termed as thermally induced cationic polymerization. The properties of polymeric materials such as superior heat resistance, dimensional stability, adhesion, chemical resistance and very good mechanical properties can be tailored by having control over initiation and curing processes. One can cure coating at virtually at any temperature desired, by choosing appropriate latent thermal initiator. In case of cationic polymerization, several class of onium salts with different range of initiation temperature have been developed as efficient thermo latent cationic initiator. The onium salts with slight difference in substitution pattern found to serve as thermo as well as photo latent initiator. Beside direct thermolysis of initiator, polymerization can be initiated by indirect methods (use of free radical initiator in combination of initiator). In thermal initiation, energy is absorbed by the chemical bond whereas in photo initiation, photon energy is absorbed by suitable chromophore. Thermo-latent initiators are summarized in following categories.

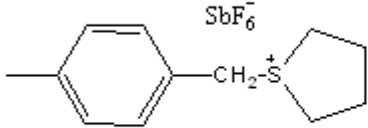
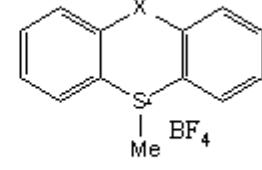
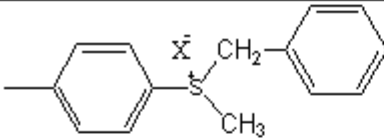
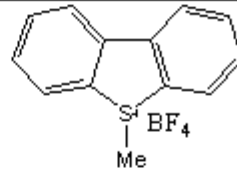
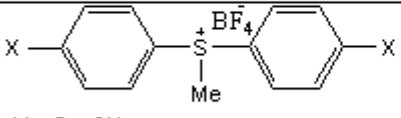
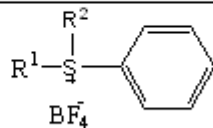
1.3.2.1. Diaryliodonium salts

Diaryliodonium salts in combination of copper catalyst (namely copper benzoate) are used as thermal initiators in cationic polymerization ^[116]. The initiation in thermal polymerization is induced by the arylation of monomer through the intermediacy of an organo copper intermediate. The reaction mechanism involves that the copper (II) undergoes reduction to copper (I) species by the use of active catalyst and in subsequent step diaryl iodonium salt is reduced by copper (I) species.

1.3.2.2. Sulfonium salts

The general preparation method involves the reaction of alkyl / benzyl halide with alky / aromatic sulfide ^[117-124]. The sulfonium salts are summarized in Table 1.15.

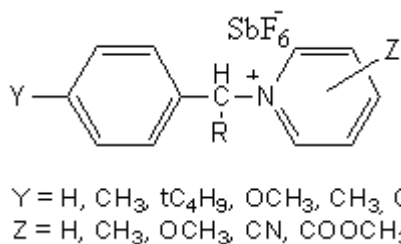
Table 1.15: Selected thermo-latent sulfonium salts used for cationic polymerization

Initiator	Ref	Initiator	Ref
	117		118, 119
	120		121
	121		121

X = SbF₆, PF₆, BF₄
X = Br, CH₃
X = O, S
R¹ = Ph, CH₃, R² = CH₃, C₃H₇

1.3.2.3. Benzyl pyridinium salts

These are prepared by the reaction of benzyl halide with substituted pyridine derivatives and used for cationic polymerization of epoxides and vinyl ether monomers. These salts show more reactivity compared to aliphatic ammonium salts.

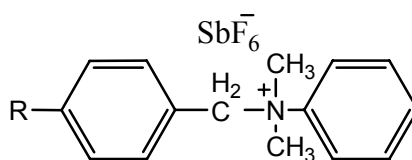


The electron withdrawing substituents at *p*-position of pyridine ring enhance the activity of the initiator ^[125]. The order of initiator activity for pyridinium ring was found to decrease as CN > H > CH₃ > N(CH₃)₂. The similar substituents at *o*-position show more activity compared to *p*-counterparts ^[126], which is determined by the combined effect of steric and

electronic factors. The activity of pyridinium salt at *p*-position of the benzene ring was found to decrease as $\text{CH}_3\text{O} > \text{Cl} > \text{t-C}_4\text{H}_9 > \text{H}$. The electron donating substituents stabilize the benzyl cation on thermal initiation ^[127]. Exceptionally, high activity for the pyridinium salt having *p*-chloro substituent on benzene ring and *p*-CN substituent on pyridine ring can be ascribed by the formation of ylide on the thermal initiation ^[126].

1.3.2.4. Benzyl anilinium salts

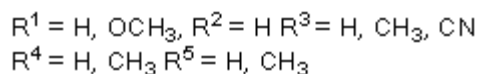
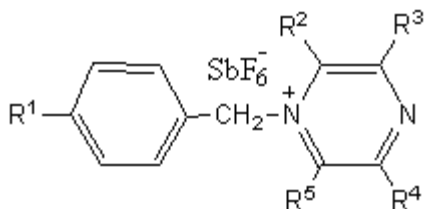
Besides pyridinium salts, benzyl anilinium salts are also found to be active initiators as described below ^[127]. Like pyridinium salts, in these salt benzyl cations are active species.



The order of reactivity with substituents at benzylic ring was found to follow the following order $\text{CH}_3\text{O} > \text{t-C}_4\text{H}_9 > \text{CH}_3 > \text{Cl}$, which can be explained by the stabilization of librated benzyl cation on thermal initiation. These initiators are more active initiators compared to the corresponding benzyl pyridinium salts. The higher activity of these salts can be ascribed due to the steric hindrance caused by the anilinium ion.

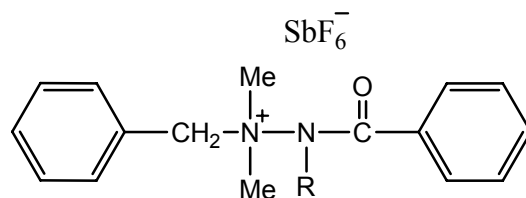
1.3.2.5. Benzyl pyrazinium salts

Benzyl pyrazinium salts based on bidentate pyrazine with electron withdrawing and donating group at the benzyl group or pyrazine ring are used as thermo-latent initiators in the cationic polymerization of GPE. The introduction of an electron-donating methyl substituent in the pyrazine ring decreased the initiator activity, while an electron-withdrawing cyano substituents in the pyrazine ring and an electron donating methoxy substituent in the benzyl group increases the initiator activity ^[128].



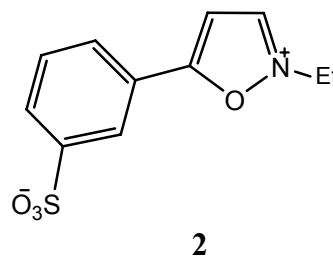
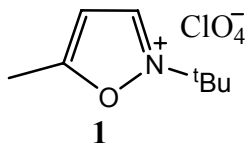
1.3.2.6. Hydrazinium salts

Hydrazinium salts are prepared by the reaction of benzoyl chloride with 1,1-dimethyl phenyl hydrazine and further anion exchange with SbF_6^- [129-131]. These salts undergo thermal decomposition to produce proton or alkyl cation as initiating species along with an imide. The activity of initiators increases with the electron withdrawing substituents on the hydrazinium salts [129].



1.3.2.7. Woodward reagent

Woodward reagent such as N-terbutyl-N-methyl-5-methylisoxazolium [Woodward's reagent L (**1**)] and N-ethyl-5-phenylisoxazolium-3⁺-sulfonate [Woodward's reagent K (**2**)] is used as the thermo-latent initiators for the cationic polymerization of GPE [132]. The order of activity was found as **1** > **2**. In particular, **1** shows relative activity at mild temperature whereas **2** acts as thermo-latent initiator in the polymerization of GPE as well as a cross-linking agent above 200 °C temperatures, which gives an insoluble polymer network in the organic solvents (CHCl_3 , THF, CH_2Cl_2 and DMSO).



1.3.2.8. Phosphonium salts

It is well known that phosphonium salts have an advantage over other onium (sulfonium, pyridinium and ammonium) salts and offers a great variety of reactivities due to their participation in d-orbital [133]. Benzylphosphonium salts have been employed as thermo-latent initiators in the temperature range of 100-200 °C in the polymerization of glycidyl phenyl ether (GPE) [133].

Table 1.16: Phosphonium salt used for cationic polymerization

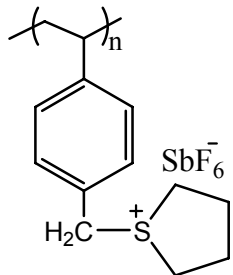
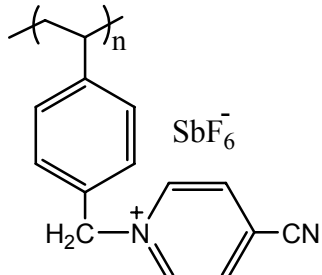
Initiator	<p>R = NO₂, Cl, H, CH₃, OCH₃</p>	<p>X = SbF₆⁻, PF₆⁻, AsF₆⁻, BF₄⁻</p>	<p>R = NO₂, H, Br, OMe R' = <i>n</i>-Bu, Ph</p>
Ref	133	134, 135	136

Endo et al have studied the initiation activity of fluorenyl phosphonium salts as an active initiator, which shows better reactivity compared to benzyl phosphonium salts [134, 135]. The initiation activity studied with 2-substituted (OMe, Me, NO₂ and H) fluorenyl phosphonium salts [136]. The order of activity was found as OCH₃ < CH₃ < H < NO₂. The order of activity is found just reverse to the other onium (benzyl pyridinium and benzyl sulfonium) salt initiators. The order of activity depends on their mode of initiation. Phosphonium salts with electron withdrawing substituents on aromatic ring are more active initiators due to facile generation of protons as active species besides formation of the phosphonium ylides.

1.3.2.9. Polymer bound onium salts

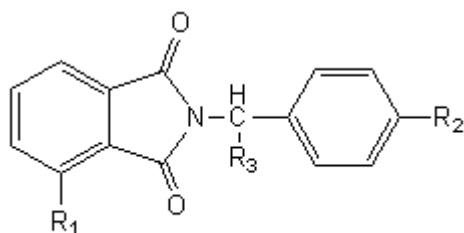
The polymeric initiators are very versatile candidates to synthesize the copolymer with vast varieties of polymer properties. These have shown good solubility in monomer as well as in organic solvents. The polymer bound sulfonium^[137] and pyridinium^[138] salts have been used to prepare graft copolymers (Table 1.17).

Table 1.17: Thermo latent polymeric onium salts

Initiator	Ref	Initiator	Ref
	137		138

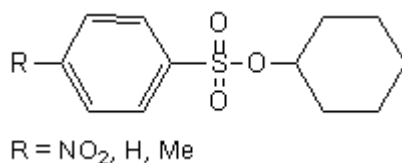
1.3.2.10. Non-salt initiators

These initiators are desirable due to non-ionic nature. These have advantage over onium salts with respect to solubility in monomer and free from inorganic impurities in the resulting polymers. The phthalamide-based initiators are found active in the polymerization of aziridines^[139]

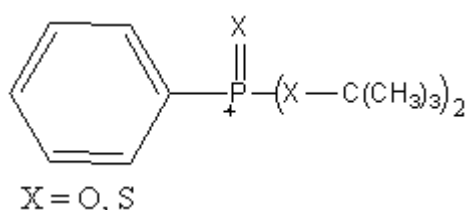


$R_1 = \text{H, NO}_2, R_2 = \text{H, OMe}, R_3 = \text{H, } i\text{-Pr, Me}$

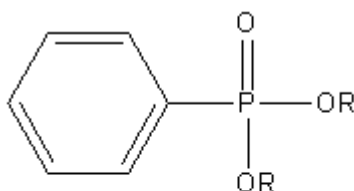
Arene sulphonate derivative are prepared by the reaction of cyclohexanol with arenesulphonyl chloride in the presence of pyridine at 0 °C. These are found to be efficient initiators for polymerization of IBVE below 100 °C.



The possible initiation species in this case might be a carbocation generated from the cleavage of C-O bond on thermal initiation. The order of initiator reactivity was found as NO₂ > H > Me. The nitro derivatives show higher activity due to stability of the resulting sulphonate anion on the initial ionization and acidity of sulphonic acid (formed by pyrolysis).



Phosphonates^[140, 141] as non-salt thermal latent initiators are used for the polymerization of isobutyl vinyl ether (IBVE), phenyl vinyl ether (PVE) and tri (ethylene glycol) divinyl ether (DVE-3).



R = CH(CH₃)Ph, C(CH₃)₃, Cyclohexyl
Phosphonate

1.4. Perspectives and future prospects

The photo and thermal cationic polymerization found to be useful in various applications such as curable epoxy can coating, ink, pressure sensitive adhesive, thermosetting resins preparation, microelectronic photo resists, volume phase holography and stereo lithography. With the increasing use of cationic polymerization in various applications, there will be need of latent cationic initiators with high quantum yield, thermal stability and solubility in specific monomer systems. Additionally, there will a need for

multifunctional monomers that can give the broad range of mechanical and physical properties of polymer to meet the demand for the various applications.

1.5. References

1. S. Mossman, *Early Plastics, Perspectives*, Leicester University Press, London, **1997**, p.1850.
2. J. L. Meikle, *American Plastic, A Cultural History* Rutgers University. Press, New Brunswick, New Jersey **1995**.
3. www.plasticsresources.com.
4. M. B. Hocking, *Science* **1991**, 251, 504.
5. J. E. Mark, *Hand Book of Polymers*, Oxford University Press **1999**.
6. C. K. Kennedy, *Carbocationic Polymerization* New York Wiley Interscience **1982**.
7. Y. Yagci, I. Reetz, *Prog. Polym. Sci.* **1998**, 23, 1465.
8. Y. Yagci, T. Endo, *Adv. Polym. Sci.* **1997**, 127, 59.
9. C. Kutal, P. A. Grutsch, D. B. Yang, *Macromolecules* **1991**, 24, 6872.
10. E. E. Wegner, A. W. Adamson, *J. Am. Chem. Soc.* **1966**, 88, 394.
11. J. G. Kloosterboer, *Adv. Polym. Sci.* **1988**, 84, 1.
12. J. G. Kloosterboer, *Adv. Polym. Sci.* **1985**, 81, 107.
13. S. P. Pappas, *UV Curing, Science and Technology*,” Vol 2, Technology Marketing Corporation, Norwalk CT, **1985**.
14. C. G. Roffey, “*Photo polymerization of Surface Coating*” Wiley, NewYork **1981**.
15. A. Reiser, “*Photo Reactive Polymer*,” Wiley New York, NY **1989**.
16. F. Lashe, H. Zweifel, *Adv. Polym. Sci.* **1986**, 78, 61.
17. J. V. Crivello, *J. Polym Sci., Part A: Polym. Chem.* **1999**, 37, 4241.
18. J. V. Crivello, *Adv. Polym. Sci.* **1984**, 1, 62.
19. G. Smets, A. Aerts, V. Erum, *Polym. J.* **1980**, 12, 539.
20. U. Müller, A. Utterodt, W. Mörke, B. Deubzer, C. Herzig, *J. Photochem. and Photobio. A: Chem.* **2001**, 140, 53.
21. F. M. Beringer, E. M. Gindler, *Iodine Abstr. Rev.* **1956**, 3, 1.
22. J. V. Crivello, J. H. W. Lam, *Polym. Symp. No.* **1976**, 56, 383.
23. J. V. Crivello, J. H. W. Lam, *Macromolecules* **1977**, 10, 1307.
24. J. P. Fouassier, D. Burr, J. V. Crivello, *J. Macromol. Chem. Pure Appl. Chem.*, **1994**, A31, 677.
25. J. V. Crivello, J. H. W. Lam, *J. Polym. Sci. Polym. Chem. Ed.* **1980**, 18, 2677.
26. J. V. Crivello, In: Dietliker, K., editor. *Chemistry and technology of UV and EB formulation for coatings, inks and paints*, Vol. 3. London: SITA Tech. **1991**, 329.
27. W. J. Hoghsed *US Patent No.* 3418289 Prior 24.12.69 to DuPont de Nemours Co.
28. V. Percec, D. Tomazos, *Polym Bull* **1987**, 18, 239.
29. V. Percec, M. Lee, *Polym Prepr* **1991**, 32, 212.
30. J. V. Crivello, J. H. W. Lam, *J. Polym. Sci Polym Chem Ed* **1979**, 17, 2877.
31. J. V. Crivello, J. H. W. Lam, *Macromolecules* **1983**, 16, 864.
32. J. V. Crivello, J. H. W. Lam, *J Polym Sci Polym Chem Ed* **1980**, 18, 1021.
33. H. Uno, T. Takata, T. Endo, *Makromol. Chem.* **1991**, 192, 655.
34. S. Gupta, L. Thijs, D. C. Neckers, *Macromolecules* **1980**, 13, 1037.
35. T. Takata, K. Takuma, T. Endo, *Makromol. Chem. Rapid Commun.* **1993**, 14, 203.
36. I. I. Abu-Abdoun, A. Ali, *Macromol. Rep.* **1993**, A30 (Suppl. 3&4), 327.

37. I. I. Abu-Abdoun, A. Ali, *Eur. Polym. J.* **1992**, 28, 73.
38. I. I. Abu-Abdoun, Aale-Ali, *Eur. Polym. J.* **1993**, 29, 1445.
39. I. I. Abu-Abdoun, A. Ali, *Eur. Polym. J.* **1992**, 28, 73.
40. Y. Yagci, A. Kornowski, W. Schnabel, *J Polym Sci. Polym. Chem.* **1992**, 30, 1987.
41. C. Reichard, *Chem. Ber.* **1966**, 99, 1769.
42. N. Yonet, N. Bicak, M. Yurtsever, Y. Yagci, *Polymer Int*, inpress.
43. Y. Nihan, N. Bicak, Y. Yagci, *Macromolecules* **2006**, 39, 2736.
44. F. Kasapoglu, A. Onen, N. Bicak, Y. Yagci, *Polymer* **2000**, 43, 25.
45. F. Kasapoglu, M. Aydin, N. Arsu, Y. Yagci, *J. Photo. Chem. Photobio. A: Chem* **2003**, 159, 151.
46. J. V. Crivello, J. L. Lee, *Polym. Bull.* **1986**, 16, 243.
47. H. S. Chao, *Eur. Pat. Appl.* No. 310882 (Prior 1.10.87) to GE.
48. J. V. Crivello, J. L. Lee, D. A. Conlon, *J. Polym. Sci. Part A: Polym. Chem.* **1987**, 25, 3293.
49. O. Karal, A. Onen, Y. Yagci, *Polymer* **1994**, 35, 4694.
50. G. Hizal, Y. Yagci, W. Schnabel, *Polymer* **1994**, 35, 2428.
51. L. R. Gatechair, S. P. Pappas, Proc. Org. Ctg. and App. Polym. Sci. Division 46, 707, Mar **1982**, Las Vegas, NV (USA).
52. B. Hazer, Y. Yagci, *Bull. Techn. Univ. Istanbul* **1984**, 37, 241.
53. Y. Yagci, I. Lukac, W. Schnabel, *Polymer* **1993**, 34, 1130.
54. J. V. Crivello, In Ring-Opening Polymerization; D. J. Brunelle, Ed.; Hanser: Munich, **1993**, p 157.
55. Crivello, J. V. In UV Curing Science and Technology; Pappas, S. P., Ed.; Technology Marketing: Stamford, CT, **1978**, p 24.
56. J. V. Crivello, F. Jiang, *Chem. Mater.* **2002**, 14, 4858.
57. J. V. Crivello, M. J. Jang, *Photochem Photobiol* **2003**, 159, 173.
58. J. V. Crivello, J. H. W. Lam, *J Polym Sci Part A: Polym Chem* **1976**, 16, 2441.
59. J. V. Crivello, J. H. W. Lam, *J Polym Sci Part A: Polym Chem* **1979**, 17, 1059.
60. E. W. Neison, T. P. Carter, A. B. Scranton, *J. Polym. Sci. Polym Chem. Ed*, **1995**, 33, 247.
61. J. V. Crivello, Y. Hua, Z. Gomurashvilli, *Macromol Chem.* **2001**, 202, 2133.
62. R. O. Kan, *Organic Photochemistry*, McGraw-Hill, New York, **1966**, p. 160.
63. Y. Bi, D. C. Neckers, *Macromolecules* **1994**, 27, 3683.
64. J. V. Crivello, J. H. W. Lam, *J. Polym. Sci. Polym Chem. Ed*, **1978**, 16, 2441.
65. Y. Yagci, Y. Hepuzer, *Macromolecules* **1999**, 32, 6367.
66. J. V. Crivello, U. Bulut, *J. Polym. Sci. Part A: Polym. Chem.* **2005**, 43, 5217.
67. Y. Yagci, W. Schnabel, *Macomol. Chem., Rapid Commun.* **1987**, 8, 209.
68. Y. Yagci, J. Borbleyand, W. Schnabel, *Eur. Polym. J.* **1989**, 25, 129.
69. N. Johnene, S. Kobayashi, Y. Yagci, W. Schnabel, *Polym. Bull.* **1993**, 30, 279.
70. A. Oken, I. E. Serhath, Y. Yagci, *Polym Bull.* **1996**, 37, 723.
71. Y. Yagci, S. Denizligil, *J. Polym. Sci., Polym Chem.* **1995**, 33, 1461.
72. Y. Yagci, I. Kminek, W. Schnabel, *Eur. Polym. J.* **1992**, 28, 387.
73. F. M. Elofson, F. F. Gadallah, *J. Org. Chem.* **1969**, 94, 854.
74. O. A. Ptitsyna, T. W. Levashova, K. P. Butkin, *Dokl Akad Nauk* **1971**, 201, 372.
75. J. Grimshaw, in: *The Chemistry of Sulfonium Groups*, C. J. M. Stirling, S. Patai, Eds., Wiley, New York **1981**.

76. A. Bottcher, K. Hasebe, G. Hizal, Y. Yagci, P. Stellberg, W. Schnabel, *Polymer* **1991**, 32, 2289.
77. Y. Yagci, W. Schnabel, *Makromol. Chem. Macromol. Symp.* **1992**, 60, 133.
78. G. A. Olah, *Halonium ions*, page 54, New York, Wiley-Interscience
79. J. V. Crivello, J. H. W. Lam, *J. Polym Sci. Polym Chem* **1981**, 19, 539.
80. A. Lendwith, *Polymer* **1978**, 19, 1217.
81. F. A. M. Abdul-Rousoul, A. Lendwith, Y. Yagci, *Polymer* **1978**, 19, 1219.
82. Y. Yagci, *Polym Commn* **1985**, 26, 7.
83. Y. Yagci A. Onen, W. Schenbel, *Macromolecules* **1991**, 24, 4620.
84. A. Onen, Y. Yagci, *J. Macromol Sci Chem.* **1990**, A27, 755.
85. Y. Bi, D. C. Necker, *Macromolecules* **1994**, 27, 3622.
86. S. Denizligil, C. McArdle, Y. Yagci, *Polymer* **1995**, 36, 3093.
87. S. Denizligil, R. Resul, C. McArdle, Y. Yagci, J-P Fousier, *Macromol. Chem. Phys.* **1996**, 197, 1233.
88. Y. Yagci, A. Onen, I. Reetz, *Macromol. Symp.* **2001**, 174, 255.
89. H. J. Timpe, A.G. Rajendran, *Eur. Polym. J.* **1991**, 27, 77.
90. V. Bicak, I. Reetz, Y. Yagci, W. Schenable, *Polym Int.* **1998**, 47, 345.
91. I. Reetz, V. Bicak, Y. Yagci, *Macromol Chem. Phys* **1997**, 198, 19.
92. I. Reetz, V. Bicak, Y. Yagci, *Polym. Int.* **1997**, 43, 27.
93. L. Atmaca, I. Kayihan, Y. Yagci, *Polymer* **2000**, 41, 6035.
94. L. Atmaca, A. Onen, Y. Yagci, *Eur. Polym. J.* **2001**, 37, 677.
95. A. Onen, Y. Yagci, *Macromolecules* **2001**, 34, 7608.
96. S. Yurtery, A. Onen, Y. Yagci, *Eur. Polym. J.* **2002**, 38, 1845.
97. A. Onen, Y. Yagci, *Polymer* **2001**, 42, 6681.
98. Y. Yagci, S. Yildirim, A. Onen, *Macomol. Chem. Phys.* **2001**, 202, 527.
99. K. Meier, H. Zweifel, *J. Imaging Sci.* **1986**, 30, 174.
100. A. Roloff, K. Meier, M. Riedicker, *Pure Appl Chem* **1986**, 9, 1267.
101. T. Wang, B. ShLi, L. X. Zhang, *Polym. Int.* **2005**, 54, 1251.
102. F. Lohse, H. Zweifel, *Adv. Polym. Sci.* **1986**, 78, 61.
103. H. Rudolph, H. J. Rosenkranz, H. G. Heine, *Appl. Polym. Synp.* **1975**, 26, 157.
104. R. Kirchmayr, W. Rutsch, *Eur. Patent Application No.* 89922 (Prior. 12.3.82).
105. F. M. Houlihan, A. Shugard, R. Gooden, F. Reichmanis, *Macromolecules* **1988**, 21, 2001.
106. F. M. Houlihan, T. N. Neeman, E. Reichmanis, J. M. Komentai, L. F. Thompson, *Polym. Mater. Sci. Eng.* **1989**, 61, 296.
107. M. G. Mikhael, A. B. Padias, H. K. Hall, *Macromolecules* **1995**, 28, 5951.
108. G. Libassi, L. Cadona, F. Broggi Radcure, 86, Conf Proc., 10th, 4/27–4/42. Assoc. Finish Processes SMF Dearborn, MI, **1986**.
109. S. P. Pappas, C. W. Lam, *J. Radiat. Cur.* **1980**, 71, 2.
110. S. Hayase, T. Ito, S. Suzuki, M. Wada, *J. Polym. Sci Polym. Chem.* **1981**, 19, 2185.
111. S. Hayase, Y. Onishi, K. Yoshikiyo, S. Suzuki, M. Wada, *J. Polym. Sci., Polym. Chem. Ed.* **1982**, 20, 3155.
112. S. Hayase, Y. Onishi, S. Suzuki, M. Wada, *Macromolecules* **1985**, 18, 1799.
113. S. Hayase, Y. Onishi, S. Suzuki, M. Wada, *Macromolecules* **1986**, 19, 968.
114. S. Hayase, T. Ito, S. Suzuki, M. Wada, *J. Polym. Sci. Polym. Chem.* **1982**, 20, 1433.
115. T. Hino, T. Endo, *Macromolecules* **2004**, 37, 1671.

116. J. V. Crivello, T. P. Lockhart, J. L. Lee, *J. Polym. Sci. Polym. Chem.* **1983**, 21, 97.
117. K. Morio, H. Murase, H. Tsuchiya, T. Endo, *J. Appl. Polym. Sci.* **1986**, 32, 5727.
118. O. Shimomura, T. Sato, *Macromolecules* **1998**, 31, 2013.
119. O. Shimomura, I. Tomita, T. Endo, *J. Polym. Sci. Polym. Chem.* **1999**, 37, 127.
120. F. Hamazu, T. Takata, T. Endo, *J. Polym. Sci. Part A Polym. Chem.* **1991**, 29, 1675.
121. O. Shimomura, I. Tomita, T. Endo, *J. Polym. Sci. Polym. Chem.* **2000**, 38, 18.
122. F. Hamazu, S. Akashi, T. Koizumi, T. Takata, T. Endo, *J Polym Sci Polym Chem* **1991**, 29, 1675.
123. O. Shimomura, I. Tomita, T. Endo, *Macromol Rapid Commun* **1998**, 19, 493.
124. O. Shimomura, I. Tomita, T. Endo, *J Polym Sci Part A Polym Chem* **1998**, 37, 217.
125. S. B. Lee, T. Takata, T. Endo, *Macromolecules* **1991**, 24, 2689.
126. S. B. Lee, T. Takata, T. Endo, *Macromolecules* **1990**, 23, 431.
127. S. Nakano, T. Endo, *J. Polym. Sci. Part A: Polym. Chem.* **1995**, 33, 505.
128. M. S. Kim, K. W. Lee, T. Endo, S. B. Lee, *Macromolecules* **2004**, 37, 5830.
129. S. B. Lee, Y. S. Park, K. W. Lee, T. Endo, *Chem Lett* **1995**, 288.
130. S. B. Lee, H. Y. Jung, K. W. Lee, *Bull Korean Chem Soc* **1996**, 17, 362.
131. M. S. Kim, S. B. Lee, K. W. Lee, T. Endo, *J. Appl. Polym. Sci.* **2005**, 95, 1439.
132. T. Hino, T. Endo, *J. Polym. Sci. Polym. Chem.* **2004**, 42, 1062.
133. K. Takuma, T. Takata, T. Endo, *Macromolecules* **1993**, 26, 862.
134. T. Toneri, F. Sanda, T. Endo, *J Polym Sci Part A Polym Chem.* **1998**, 36, 1957.
135. T. Toneri, K. Watanabe, F. Sanda, T. Endo, *Macromolecules* **1999**, 32, 1293.
136. T. Toneri, F. Sanda, T. Endo, *Macromolecules* **2001**, 34, 1518.
137. H. Uno, T. Endo, *Chem. Lett.* **1986**, 1869.
138. H. Uno, T. Takata, T. Endo, *Macromolecules* **1989**, 22, 2502.
139. T. Takata, T. Endo, Y. Z. Menciloglu, *J. Polym. Sci. Polym. Chem* **1992**, 30, 501.
140. M. S. Kim, F. Sanda, T. Endo, *Polymer* **2001**, 42, 9367.
141. M. S. Kim, F. Sanda, T. Endo, *Macromolecules* **1999**, 32, 8291.

Chapter 2: Scope and objectives of the present work

In last few decades, the importance of latent cationic initiators, which show activity by external stimulation such as heat or light, has been recognized in a number of different industrial applications such as adhesives, microelectronics, photolithography and curing of epoxy resin ^[1-2]. The development of efficient latent (photo and thermal) cationic initiators is desirable for their inherent storage stability, handling and solubility in the monomers ^[3]. Based on literature studies, we found our interest in designing new thermo and photo latent initiators for cationic polymerization. These ideas have been broadly classified into the following objectives.

1. To study the efficiency of phosphonium salts based on aromatic nucleus (such as dibenzosuberonyl, xanthenyl) having different counter anion, substituents, phosphine moiety and ring structure as thermo-latent initiator in cationic polymerization of epoxides. These initiators will be used for thermal polymerization of epoxides such as glycidyl phenyl ether (GPE) and cyclohexene oxide (CHO).
2. To examine the efficiency of amide based allyl phosphonium salts in the radical promoted cationic polymerization. The amide based allylic phosphonium salts will be used as photo and thermo-latent initiator in the presence of free radical source as addition fragmentation agent in the cationic polymerization.
3. To study the efficiency of allylic ammonium salts having an intrinsic chromophoric group for the radical generation and an allylic salt structure for the addition fragmentation agents in the photo cationic polymerization. The allylic ammonium salts based on N, N-dimethylacrylamide and acryloyl morpholine will be used for photopolymerization of cyclohexene oxide (CHO), *n*-butyl vinyl ether (*n*-BVE), isobutylvinylether (IBVE) and N-vinyl carbazole (NVC)

4. To examine the activity of non-salt based photosensitization system. The diselenides (DPDS and DBDS) will be used as non-salt initiator for photosensitized cationic polymerization of NVC.

References

1. H. F. Mark, N. G. Gaylord, N. M. Bikajes *Encyclopedia of Polymer Science and Technology*; Eds.; Interscience: New York, **1968**, 8, 303.
2. Y. Yagci, I. Reetz, *Prog Polym Sci* **1998**, 23, 1465.
3. Y. Yagci, T. Endo, *Adv Polym Sci* **1997**, 127, 59.

Chapter 3: Thermally induced cationic polymerization using phosphonium salts as initiator

3.1. Introduction

The externally stimulated initiators have gained considerable attention in applications such as curable coatings, paints, packing, fillers and adhesives, due to their control over initiation and curing process ^[1-4]. The latent cationic initiators, which exhibit no activity under ambient conditions but generate active species on external stimulation such as heating or photo-irradiation, have gained momentum over conventional anhydride and amine-based initiators ^[5-8]. Thus, development of efficient thermo-latent cationic initiators having good solubility in monomer and resistance towards air and moisture are more desirable. In last few decades, several onium salts such as diaryliodonium ^[9], benzyliodonium ^[10-13], benzylpyridinium ^[14-16], benzylammonium ^[17], hydrazinium ^[18, 19], benzylphosphonium salt ^[20] and others ^[21-25] have been developed as potential thermo-latent initiators for the cationic polymerization of glycidyl phenyl ether (GPE). It is well known that phosphonium salts have an advantage over other onium (sulfonium, pyridinium and ammonium) salts and offer a great variety of reactivities due to participation of d-orbital ^[26]. Considering these points, it was aimed to prepare thermo-latent cationic initiators based on novel phosphonium salts, which can produce stable ylides on heating which are responsible for more activity of the initiator. GPE, which is a mono functional diluent in the epoxy resins and modifier for dyes and fibers ^[27, 28], is widely used model monomers to study the efficiency of the thermo-latent initiators. Earlier, Endo et al., ^[29, 30] have employed fluorenyl phosphonium salts that exhibited the better activity than benzyl phosphonium salts ^[20]. It is assumed that aromatic nucleus (such as dibenzosuberene, xanthene) based phosphonium salts might serve as an efficient thermo-latent cationic initiators. Therefore, phosphonium salts based on these aromatic nucleuses were synthesized and their efficiency was investigated in bulk cationic polymerization of GPE. The initiator efficiency of phosphonium salts is discussed with respect to different counter anions, phosphine moiety and dibenzosuberene ring. In order to study, the effect of

substituents on initiator activity, 2-substituted (Cl, H, Me and OMe) phosphonium salts with hexafluoroantimonate counter anion were also synthesized and their initiation activity was examined in polymerization of GPE and cyclohexene oxide (CHO) monomer.

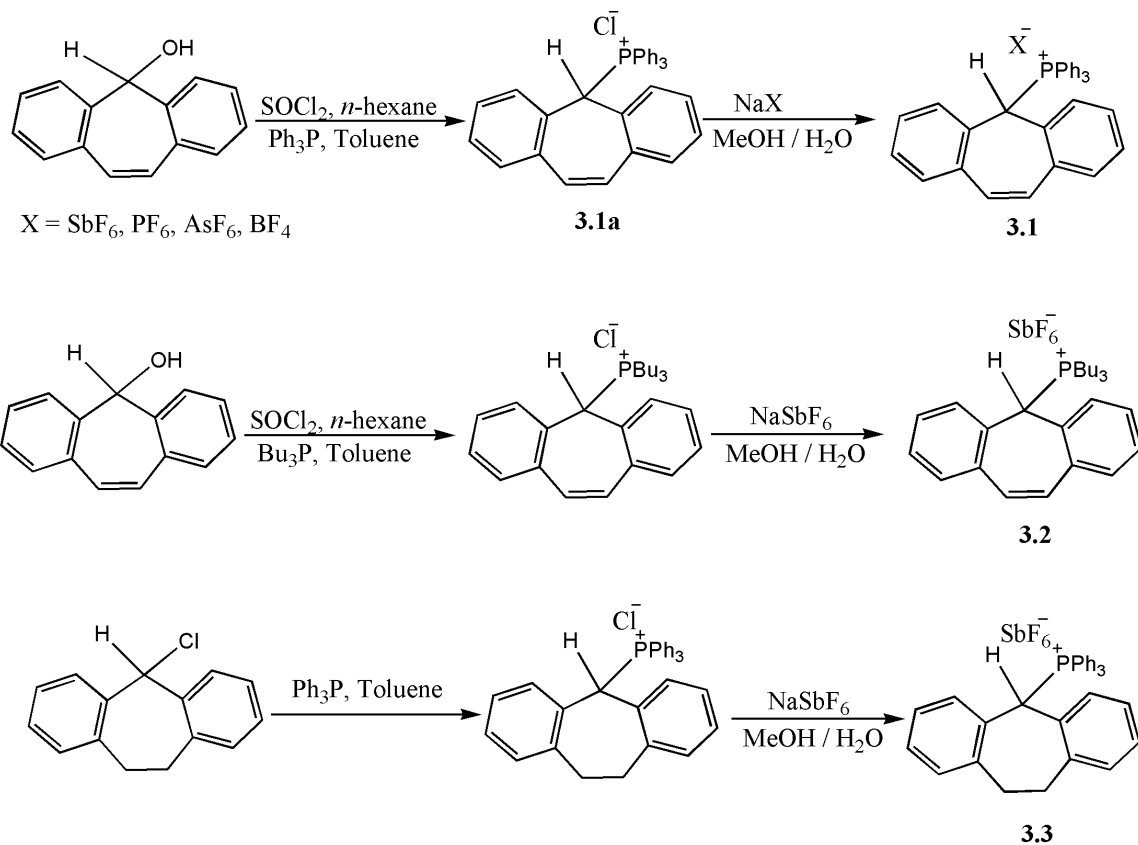
3.2. Experimental

3.2.1. Materials

Dibenzosuberanol, 5-chlorosuberane, xanthidrol, triphenylphosphine (Ph₃P), tri-*n*-butyl phosphine (Bu₃P), sodium hexafluoroantimonate (NaSbF₆), potassium hexafluorophosphate (KPF₆), sodium hexafluoroarsenate (NaAsF₆), sodium tetrafluoroborate (NaBF₄), glycidyl phenyl ether (GPE) and cyclohexene oxide (CHO) were purchased from Aldrich chemicals. The other chemicals (2-chlorobenzoic acid, 4-methoxy phenol, 4-chloro phenol, 4-methyl phenol, pyridine, Cu powder, copper (I) iodide (CuI), polyphosphoric acid (PPA), Zn dust, thionyl chloride (SOCl₂), sodium hydroxide (NaOH), hydrochloric acid (HCl), calcium chloride (CaCl₂), N, N-dimethylformamide (DMF), potassium carbonate (K₂CO₃), sodium carbonate (Na₂CO₃), tetrahydrofuran (THF), acetic acid, methanol, ethanol, *n*-hexane, toluene, diethyl ether, dichloromethane) were purchased from S. D. Fine Chemicals Ltd, Mumbai, India and used after purification whenever needed ^[31]. Monomers (GPE and CHO) and solvent (CH₂Cl₂) were dried and distilled over CaH₂ just before polymerization.

3.2.2. Initiator synthesis

3.2.2.1. Dibenzosuberene based phosphonium salts: The reaction steps used in synthesis of these phosphonium salts are given in Scheme 3.1.



Scheme 3.1: Synthesis of dibenzosuberene based phosphonium salts

3.2.2.1.1. Dibenzosuberenyiltriphenylphosphonium chloride (**3.1a**)

To the solution of dibenzosuberene-1-ol (2.08 g, 10 mmol) in *n*-hexane (20 mL), SOCl₂ (1.46 mL, 20 mmol) in *n*-hexane (10 mL) was added and refluxed for 1 h. The reaction mixture was cooled and the solvent was evaporated under vacuum. The resulting residue was dissolved in toluene (20 mL), Ph₃P (2.62 g, 10 mmol) in toluene (15 mL) was added and stirred for 1 h. The resulting precipitate was filtered, washed with toluene and dried under vacuum. Yield: 2.87 g (59 %), Elemental analysis: C₃₃H₂₆ClP (488.01 g mol⁻¹), Found: C, 81.13 %; H, 5.32 %; Calcd: C, 81.25 %; H, 5.40 %, ¹H NMR (DMSO-d₆): δ = 7.95-7.05 (m, 23 H, Ph), 6.82, 6.72 (1H, CH), 6.30 (s, 2H, CH) ppm.

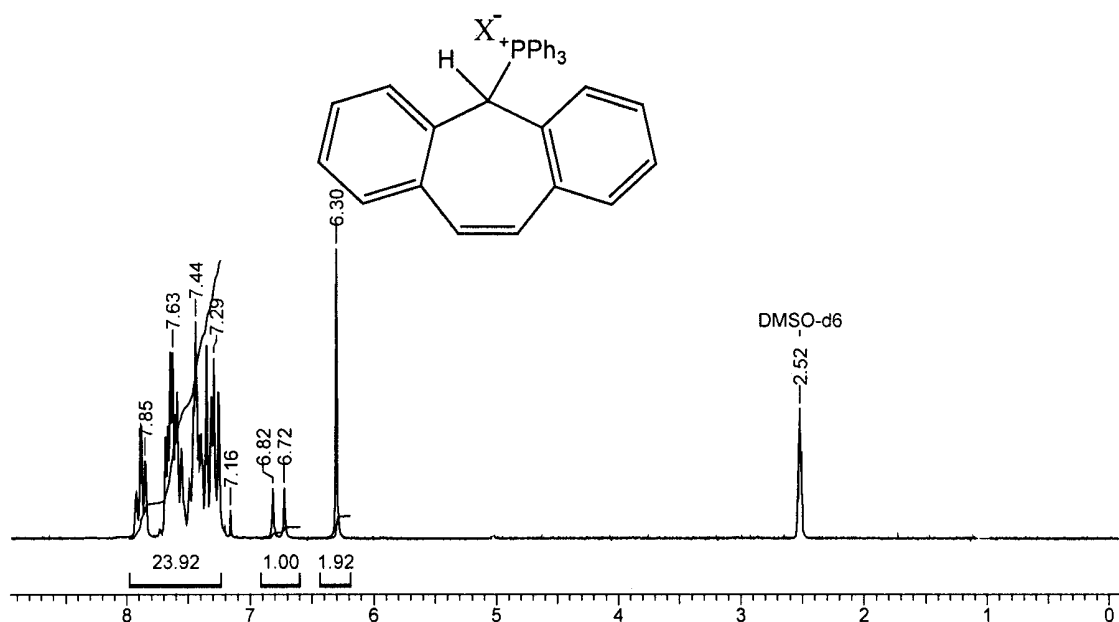


Figure 3.1: ^1H NMR spectrum of dibenzosuberonyltriphenylphosphonium salts (**3.1a-3.1e**)

3.2.2.1.2. Dibenzosuberonyltriphenylphosphonium hexafluoro antimonate (**3.1b**)

To the solution of **3.1a** (1.46 g, 3 mmol) in methanol (20 mL), was added NaSbF_6 (0.77 g, 3 mmol) in H_2O (20 mL) and stirred at ambient temperature for 30 minutes. The precipitate formed was filtered, washed with H_2O and recrystallized with ethanol- CH_2Cl_2 (8:2). Yield: 1.38 g (67 %), white crystals, mp: 268-269 °C. Elemental analysis: $\text{C}_{33}\text{H}_{26}\text{PSbF}_6$ (688.07 g mol^{-1}) Found: C, 57.73 %; H, 3.73 %; Calcd: C, 57.50 %; H, 3.80 %, FT-IR (KBr): = 3030, 1625, 1600, 1500, 1463, 1439, 1065, 743, 720, 687 cm^{-1} , ^1H NMR (DMSO- d_6): δ = 7.95-7.05 (m, 23 H, Ph), 6.82, 6.72 (1H, CH), 6.30 (s, 2H, CH) ppm, ^{13}C NMR (DMSO- d_6): δ = 136.55, 135.12, 134.66, 134.48, 132.21, 132.07, 130.83, 130.47, 129.93, 129.70, 129.48, 128.63, 117.69, 116.09, 51.25, 50.43 ppm, ^{31}P NMR (DMSO- d_6): δ = 23.29 ppm.

3.2.2.1.3. Dibenzosuberonyltriphenylphosphonium hexafluoro phosphate (**3.1c**)

This compound was prepared by reaction of **3.1a** (1.46 g, 3 mmol) with KPF_6 (0.55 g, 3 mmol) in the same manner as described for **3.1b** and recrystallized with ethanol- CH_2Cl_2 (8:2). Yield: 1.30 g (73 %), white crystals, mp: 265-266 °C, Elemental analysis: $\text{C}_{33}\text{H}_{26}\text{P}_2\text{F}_6$ (598.14 g mol^{-1}) Found: C, 66.28 %; H, 4.32 %; Calcd: C, 66.22 %; H, 4.38 %;

FT-IR (KBr): = 3030, 1625, 1600, 1500, 1463, 1439, 1065, 743, 720, 687 cm^{-1} , ^1H NMR (DMSO- d_6): δ = 7.95-7.05 (m, 23 H, Ph), 6.82, 6.72 (1H, CH), 6.30 (s, 2H, CH) ppm, ^{13}C NMR (DMSO- d_6): δ = 136.55, 135.12, 134.66, 134.48, 132.21, 132.07, 130.83, 130.47, 129.93, 129.70, 129.48, 128.63, 117.69, 116.09, 51.25, 50.43 ppm, ^{31}P NMR (DMSO- d_6): δ = 23.29 ppm.

3.2.2.1.4. Dibenzosuberonyltriphenylphosphonium hexafluoro arsenate (3.1d)

This compound was prepared by reaction of **3.1a** (1.46 g, 3 mmol) with NaAsF_6 (0.64 g, 3 mmol) in the same manner as described for **3.1b** and recrystallized with ethanol- CH_2Cl_2 (8:2). Yield: 1.04 g (54 %), white crystals, mp: 267-268 $^\circ\text{C}$, Elemental analysis: $\text{C}_{33}\text{H}_{26}\text{PAsF}_6$ (642.09 g mol^{-1}) Found: C, 61.72 %; H, 4.06 %; Calcd: C, 61.69 %; H, 4.08 %; FT-IR (KBr): = 3030, 1625, 1600, 1500, 1463, 1439, 1065, 743, 720, 687 cm^{-1} , ^1H NMR (DMSO- d_6): δ = 7.95-7.05 (m, 23 H, Ph), 6.82, 6.72 (1H, CH), 6.30 (s, 2H, CH) ppm, ^{13}C NMR (DMSO- d_6): δ = 136.55, 135.12, 134.66, 134.48, 132.21, 132.07, 130.83, 130.47, 129.93, 129.70, 129.48, 128.63, 117.69, 116.09, 51.25, 50.43 ppm, ^{31}P NMR (DMSO- d_6): δ = 23.29 ppm.

3.2.2.1.5. Dibenzosuberonyltriphenylphosphonium tetrafluoroborate (3.1e)

This compound was prepared by reaction of **3.1a** (1.46 g, 3 mmol) with NaBF_4 (0.33 g, 3 mmol) in the same manner as described for **3.1b** and recrystallized with ethanol- CH_2Cl_2 (8:2). Yield: 0.70 g (43 %), white crystals, mp: 268-269 $^\circ\text{C}$, Elemental analysis: $\text{C}_{33}\text{H}_{26}\text{BF}_4$ (540.18 g mol^{-1}) Found: C, 73.65 %; H, 4.75 %; Calcd: C, 73.35 %; H, 4.85 %. FT-IR (KBr): = 3030, 1625, 1600, 1500, 1463, 1439, 1065, 743, 720, 687 cm^{-1} , ^1H NMR (DMSO- d_6): δ = 7.95-7.05 (m, 23 H, Ph), 6.82, 6.72 (1H, CH), 6.30 (s, 2H, CH) ppm, ^{13}C NMR (DMSO- d_6): δ = 136.55, 135.12, 134.66, 134.48, 132.21, 132.07, 130.83, 130.47, 129.93, 129.70, 129.48, 128.63, 117.69, 116.09, 51.25, 50.43 ppm, ^{31}P NMR (DMSO- d_6): δ = 23.29 ppm.

3.2.2.1.6. Dibenzosuberonyltri-*n*-butylphosphonium hexafluoroantimonate (3.2)

This compound was prepared in same manner as described for **3.1a** and followed by anion exchange with NaSbF₆ in MeOH-H₂O mixture and recrystallized by ethanol-CH₂Cl₂ (8:2). Yield: 0.78 g (52 %), white crystals, mp: 212-214 °C, Elemental analysis: C₂₇H₃₈PSbF₆ (628 g mol⁻¹), Found: C, 51.46 %; H, 6.08 %; Calcd: C, 51.53 %; H, 6.04 %, FT-IR (KBr): = 3030, 2930, 2868, 1625, 1600, 1500, 1463, 1439, 1065, 743, 720, 687 cm⁻¹, ¹H NMR (DMSO-d₆): δ = 7.70-7.25 (m, 8H, Ph), 7.08 (s, 2H, CH), 5.77, 5.67 (CH, 1H), 2.05 (m, CH₂, 6H), 1.24 (m, CH₂, 6H), 1.09 (m, CH₂, 6H), 0.80 (t, CH₃, 9H) ppm, ¹³C NMR (DMSO-d₆): δ = 135.53, 131.85, 131.02, 130.48, 130.14, 129.68, 129.08, 48.11, 47.31, 23.50, 23.19, 22.62, 19.30, 18.45, 13.03 ppm, ³¹P NMR (DMSO-d₆): δ = 37.43 ppm.

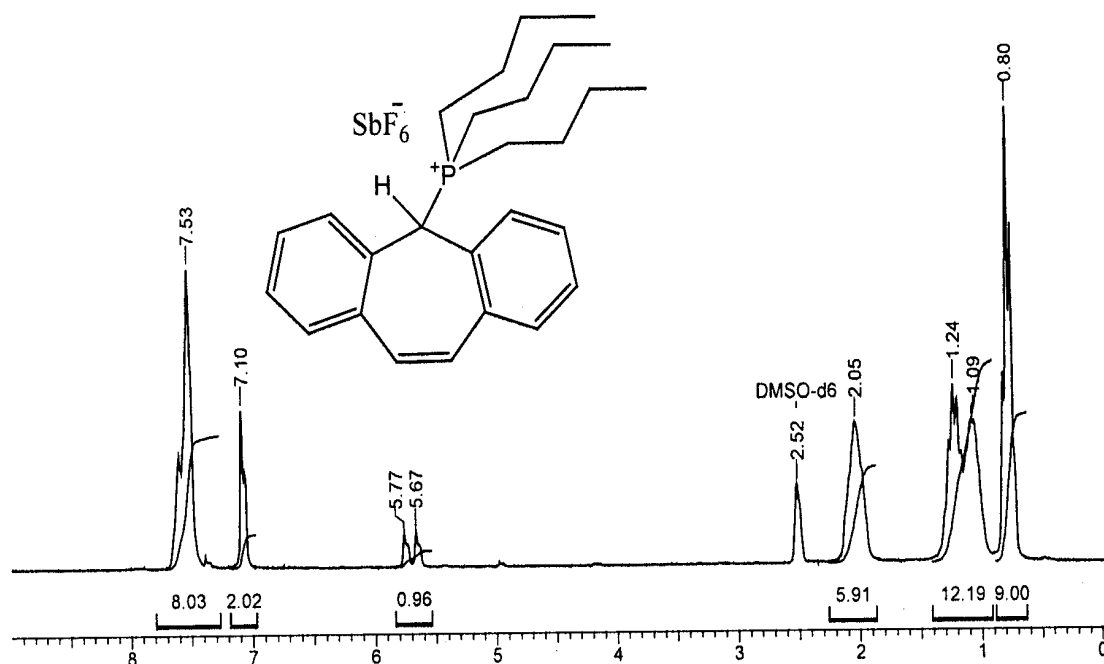


Figure 3.2: ¹H NMR spectrum of dibenzosuberonyltri-*n*-butylphosphonium hexafluoroantimonate (**3.2**)

3.2.2.1.7. Dibenzosuberonyltriphenylphosphonium hexafluoroantimonate (3.3)

To the solution of 5-chlorosuberane (10 mmol, 2.28 g) in toluene (20 mL), Ph₃P (10 mmol, 2.62 g) in toluene (15 mL) was added at ambient temperature and allowed to stir for 30 minutes. The resulted white precipitate was filtered, washed with toluene and its counter

anion was exchanged with NaSbF₆ as described for **3.1b** and recrystallized with ethanol-CH₂Cl₂ (8:2). Yield: 2.87 g (72 %), white crystals, mp: 248-251 °C, Elemental analysis Cal for C₃₃H₂₈PSbF₆: C, 57.50 %; H, 4.18 %; Found: C, 57.22 %; H, 4.22 %; FT-IR (KBr): 3030, 2930, 2868, 1625, 1600, 1500, 1463, 1439, 1065, 743, 720, 687 cm⁻¹, ¹H NMR (DMSO-d₆) δ = 7.95-7.06 (m, 23 H, Ph), 6.69, 6.58 (CH, 1H), 2.75 (s, CH₂, 4H) ppm, ¹³C NMR (DMSO-d₆): δ = 141.78, 135.29, 134.64, 132.65, 131.34, 130.22, 129.98, 126.76, 52.88, 52.18, 36.06 ppm.

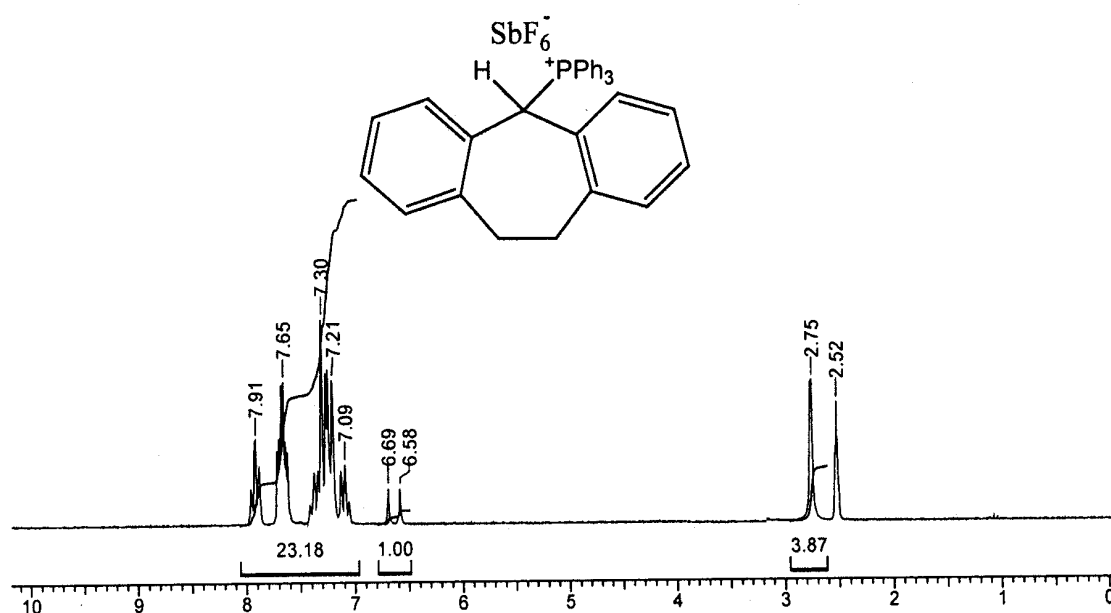
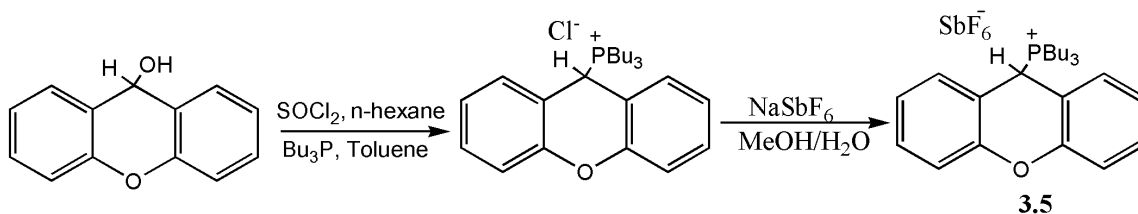
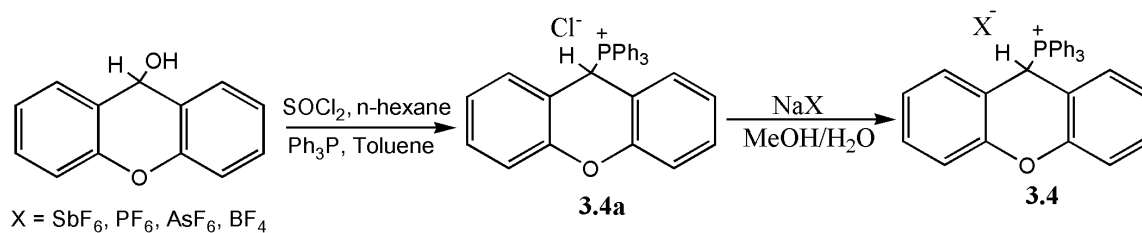


Figure 3.3: ¹H NMR spectrum of dibenzosuberyltriphenylphosphonium hexafluoroantimonate (**3.3**)

3.2.2.2. Synthesis of xanthenylphosphonium salts The reaction steps used in synthesis of phosphonium salts are given in Scheme 3.2



Scheme 3.2: Synthesis of xanthylenephosphonium salts

3.2.2.2.1. Xanthylenetriphenylphosphonium chloride (3.4a)

To the magnetically stirring suspension of xanthanol (1.96 g, 10 mmol) in *n*-hexane (20 mL), was added drop-wise a solution of SOCl₂ (1.46 mL, 20 mmol) in *n*-hexane (10 mL) at ambient temperature. After complete addition, reaction mixture was allowed to reflux for 30 minute till the solution becomes clear. This solution was cooled up to ambient temperature and evaporated under vacuum. The residue was dissolved in toluene (30 mL), Ph₃P (2.62 g, 10 mmol) in toluene (15 mL) was added drop-wise and instantaneous white precipitate formation was observed. After 1 h stirring, the reaction mixture was filtered, washed with toluene and recrystallized from ethanol-CH₂Cl₂ (8:2). Yield: 2.24 g (47 %), Elemental analysis: C₃₁H₂₄ClOP (478.05 g mol⁻¹) Calcd. C, 77.82; H, 5.01. Found: C, 77.86; H, 4.98, ¹H NMR (DMSO-d₆): δ = 7.97-7.09 (m, 23 H, Ph), 7.04 (1H, CH) ppm.

3.2.2.2.2. Xanthylenetriphenylphosphonium hexafluoroantimonate (3.4b)

To a solution of **3.4a** (1.43 g, 3 mmol) in methanol, a solution of NaSbF₆ (0.77 g, 3 mmol) in deionised water was added and stirred at ambient temperature for 30 minutes. The resulted white precipitate was filtered, washed with plenty of water and recrystallized with ethanol-CH₂Cl₂ (8:2). Yield: 1.57 g (77 %), mp: 248-249 °C, Elemental analysis: C₃₁H₂₄OPSbF₆ (678.05 g mol⁻¹) Calcd. C, 54.82; H, 3.56. Found: C, 54.82; H, 3.60. FT-IR

(KBr): 3030, 1625, 1600, 1500, 1463, 1439, 1065, 743, 720, 687 cm^{-1} , ^1H NMR (DMSO- d_6): $\delta = 7.97\text{-}7.09$ (m, 23H, Ph), 7.04 (1H, CH) ppm, ^{13}C NMR (DMSO- d_6): $\delta = 153.84$, 135.35, 134.46, 130.95, 130.52, 130.10, 129.86, 124.27, 117.12, 116.43, 114.82, 113.60, 39.76, 38.88 ppm, ^{31}P NMR (DMSO- d_6): $\delta = 21.42$ ppm.

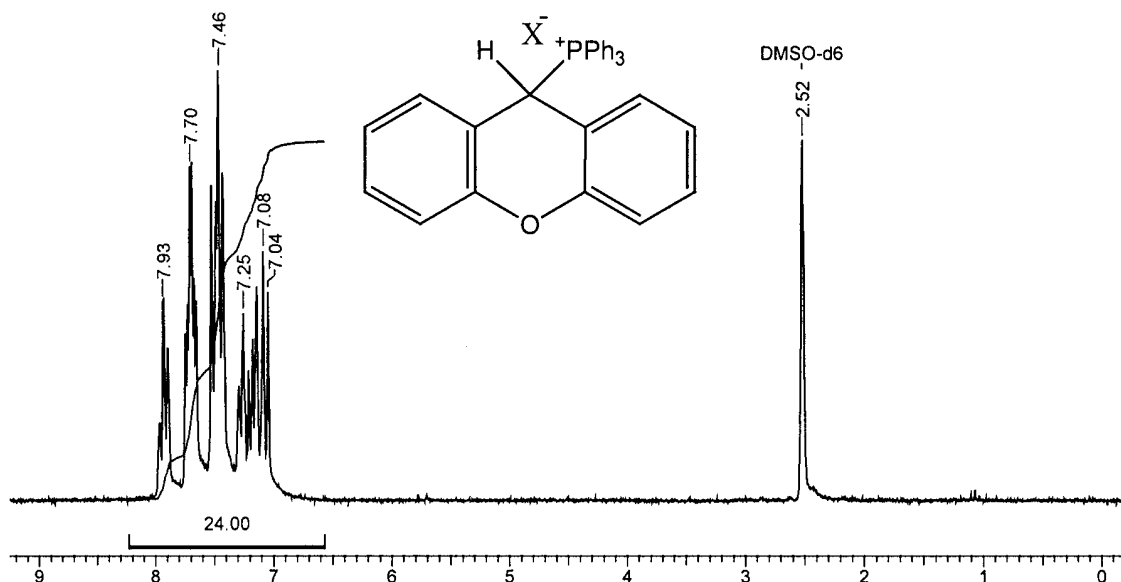


Figure 3.4: ^1H NMR spectrum of xanthenyltriphenylphosphonium salt (**3.4a-3.4e**)

3.2.2.2.3. Xanthenyltriphenylphosphonium hexafluorophosphate (**3.4c**)

This compound was prepared by reaction of **3.4a** (1.43 g, 3 mmol) with KPF_6 (0.55 g, 3 mmol) in the same manner as described for **3.4b** and recrystallized with ethanol- CH_2Cl_2 (8:2). Yield: 1.11 g (63 %), mp: 246-247 $^\circ\text{C}$, Elemental analysis: $\text{C}_{31}\text{H}_{24}\text{OP}_2\text{F}_6$ (588.12 g mol^{-1}) Calcd. C, 63.27; H, 4.11. Found: C, 63.38; H, 4.09. FT-IR (KBr): 3030, 1625, 1600, 1500, 1463, 1439, 1065, 743, 720, 687 cm^{-1} , ^1H NMR (DMSO- d_6): $\delta = 7.97\text{-}7.09$ (m, 23H, Ph), 7.04 (1H, CH) ppm, ^{13}C NMR (DMSO- d_6): $\delta = 153.95$, 135.34, 134.65, 131.02, 130.51, 130.09, 129.86, 124.33, 117.19, 116.42, 114.82, 113.61, 37.91, 38.88 ppm, ^{31}P NMR (DMSO- d_6): $\delta = 21.41$ ppm.

3.2.2.2.4. Xanthenyltriphenylphosphonium hexafluoroarsenate (3.4d)

This compound was prepared by reaction of **3.4a** (1.43 g, 3 mmol) with NaAsF₆ (0.64 g, 3 mmol) in the same manner as described for **3.4b** and recrystallized with ethanol-CH₂Cl₂ (8:2). Yield: 1.31 g (69 %), mp: 251-252 °C. Elemental analysis: Cal for: C₃₁H₂₄OPAsF₆ (632.07 g mol⁻¹) Calcd. C, 58.88; H, 3.83. Found: C, 58.80; H, 3.83. IR (KBr): 3030, 1625, 1600, 1500, 1463, 1439, 1065, 743, 720, 687 cm⁻¹, ¹H NMR (DMSO-d₆): δ = 7.97-7.09 (m, 23H, Ph), 7.04 (1H, CH) ppm, ¹³C NMR (DMSO-d₆): δ = 153.95, 135.34, 134.65, 131.02, 130.50, 130.09, 129.85, 124.27, 117.13, 116.42, 114.82, 113.61, 39.72, 38.89 ppm, ³¹P NMR (DMSO-d₆): δ = 21.41 ppm.

3.2.2.2.5. Xanthenyltriphenylphosphonium tetrafluoroborate (3.4e)

This compound was prepared by reaction of **3.4a** (1.43 g, 3 mmol) with NaBF₄ (0.33 g, 3 mmol) in the same manner as described for **3.4b**. Yield: 0.67 g (42 %), mp: 248-250 °C, Elemental analysis: C₃₁H₂₄OPBF₄ (530.16 g mol⁻¹) Calcd. C, 70.21; H, 4.56. Found: C, 70.16; H, 4.57. IR (KBr): 3030, 1625, 1600, 1500, 1463, 1439, 1065, 743, 720, 687 cm⁻¹, ¹H NMR (DMSO-d₆): δ = 7.97-7.09 (m, 23 H, Ph), 7.04 (1H, CH) ppm, ¹³C NMR (DMSO-d₆): δ = 153.94, 135.31, 134.65, 130.96, 130.52, 130.11, 124.28, 117.19, 116.43, 114.83, 113.70, 39.70, 38.86 ppm, ³¹P NMR (DMSO-d₆): δ = 21.42 ppm.

3.2.2.2.6. Xanthenyltri-*n*-butylphosphonium hexafluoroantimonate (3.5)

This compound was synthesized in the same manner as described for **3.4b** and recrystallized with ethanol-CH₂Cl₂ (8:2). Yield: 1.30 g (65 %), mp: 216 °C, Elemental analysis: C₂₅H₃₆OPSbF₆ (665.39 g mol⁻¹) Calcd. C, 48.54; H, 5.81 Found: C, 48.46; H, 5.75. IR (KBr): 3030, 2930, 2868, 1625, 1600, 1500, 1463, 1439, 1065, 743, 720, 687 cm⁻¹, ¹H NMR (DMSO-d₆): δ = 7.60-7.25 (m, 8H, Ph), 5.69, 5.62 (d, CH, 1H), 2.08 (m, CH₂, 6H), 1.29 (m, CH₂, 12H), 0.86 (t, CH₃, 9H) ppm, ¹³C NMR (DMSO-d₆): δ = 153.06, 130.65, 129.57, 124.94, 117.30, 115.38, 34.87, 34.03, 23.53, 23.23, 22.45, 16.68, 15.82, 13.06 ppm, ³¹P NMR (DMSO-d₆): 37.08 ppm.

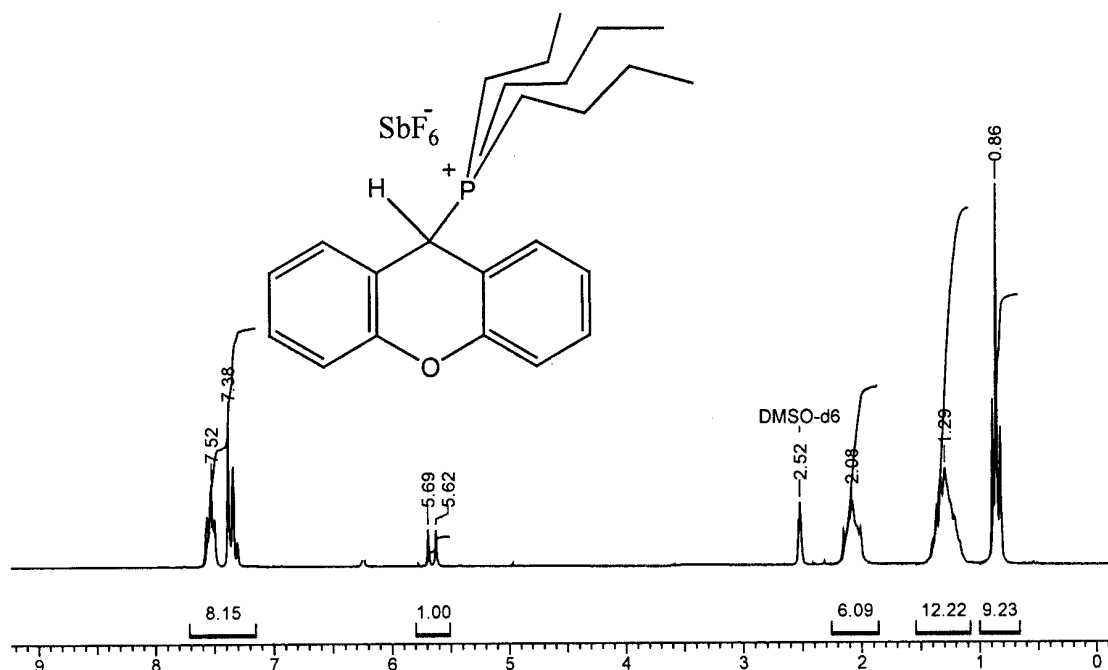
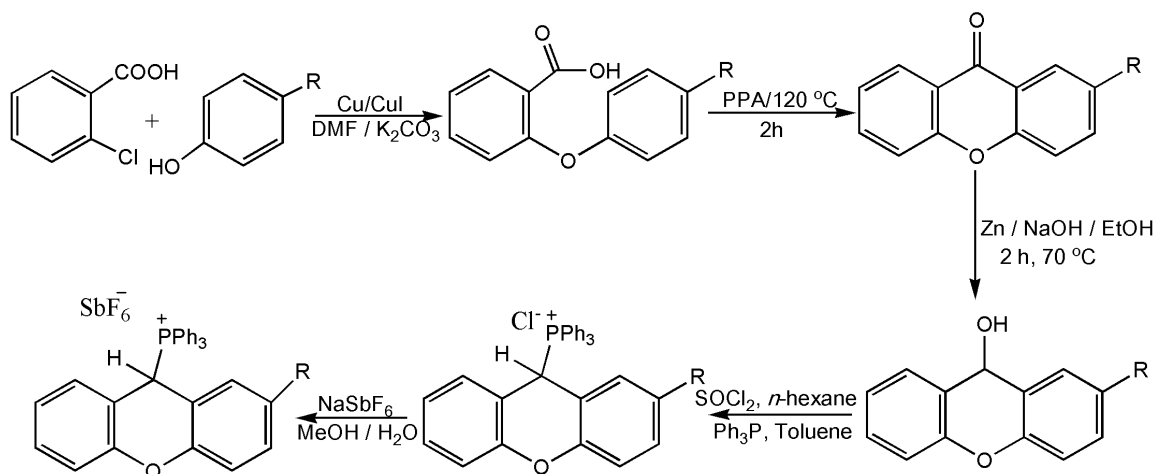


Figure 3.5: ^1H NMR spectrum of xanthenyl-tri-*n*-butylphosphonium hexafluoroantimonate (3.5)

3.2.2.3. Synthesis of 2-substituted xanthenyltriphenylphosphonium hexafluoroantimonate

The reaction steps used in synthesis of 2-substituted (Cl, H, Me and OMe) xanthenyltriphenylphosphonium salts are summarized in Scheme 3.3



R = Cl (3.6d), H(3.4b), Me(3.7d), OMe(3.8d)

Scheme 3.3: Synthesis of 2-substituted xanthenyltriphenylphosphonium salts

3.2.2.3.1. 2-Carboxy-4-chloro-diphenyl ether (3.6a) ^[32]

A mixture of 2-chlorobenzoic acid (12.52 g, 80 mmol), 4-chlorophenol (20.56 g, 160 mmol), K₂CO₃ anhydrous (22.10 g, 160 mmol), pyridine (3.2 g, 40 mmol), Cu powder (0.5 g) and cuprous iodide (0.5 g) in 50 mL water was allowed to reflux for 2 h. The mixture was basified with Na₂CO₃ solution and extracted with diethyl ether. The aqueous solution was acidified with HCl and appeared precipitate was filtered off and dissolved in NaOH. This basic solution was filtered and acidified with acetic acid, which was washed with H₂O and recrystallized with ethanol. Yield: 11 g (58 %), mp: 115 °C. white crystals, Elemental analysis: C₁₃H₉ClO₃ (248.66 g mol⁻¹) Calcd. C, 62.79; H, 3.65. Found: C, 62.65; H, 3.62, IR (KBr): 3391, 3066, 2932, 2500, 1760, 1618, 1586, 1474, 1240, 1106, 878., 755 cm⁻¹, ¹H NMR (CDCl₃): δ = 10.7-10.3 (b, -COOH), 8.5-6.6 (m, 8H, Ph) ppm.

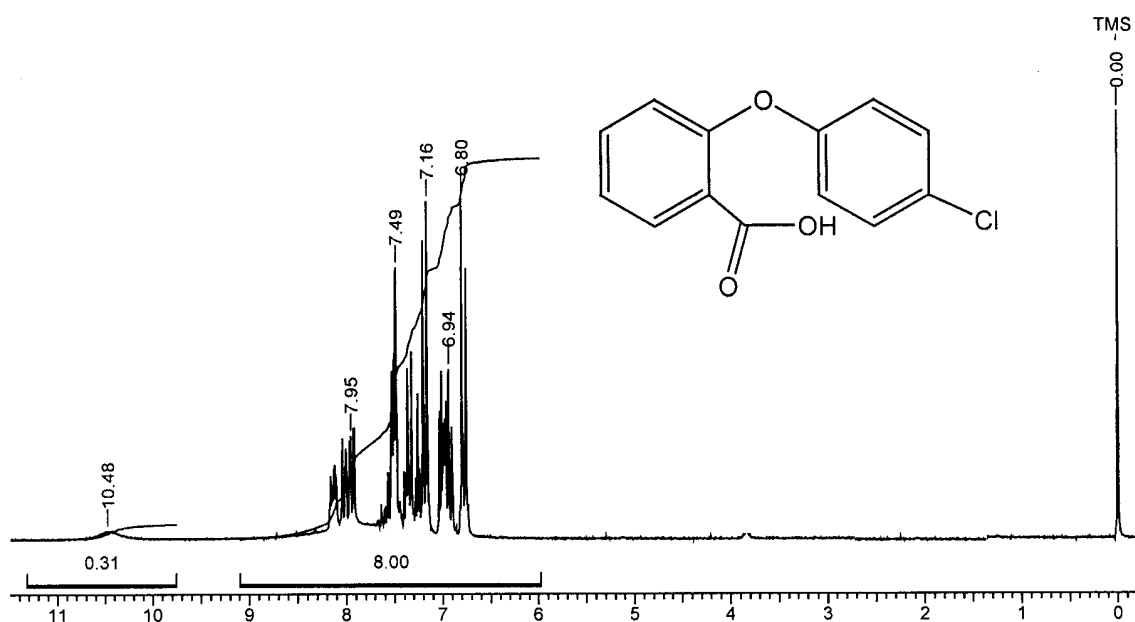


Figure 3.6: ¹H NMR spectrum of 2-carboxy-4-chloro diphenyl ether (3.6a)

3.2.2.3.2. 2-Chloro xanthone (3.6b) ^[32]

A mixture of **3.6a** (5.57 g, 20 mmol) and PPA was heated on oil bath at 120 °C for 2 h. The reaction mixture was cooled to ambient temperature and poured in ice-cold water. The resulting precipitate was filtered and treated with 0.1 M NaOH solution. The precipitate was washed with plenty of water and recrystallized with 95 % ethanol. Yield: 4.24 g (82 %), mp: 170 °C, white crystals, Elemental analysis: C₁₃H₇ClO₂ (230.65 g mol⁻¹) Calcd. C,

60.70; H, 3.06. Found: C, 60.67; H, 3.01, IR (KBr): 3391, 3066, 2932, 1618, 1586, 1474, 1240, 1106, 997, 878, 831, 755 cm^{-1} , ^1H NMR (CDCl_3): δ = 8.2-8.4 (m, 2H, Ph), 7.8-7.6 (m, 2H, Ph), 7.56-7.4 (m, 3H, Ph) ppm.

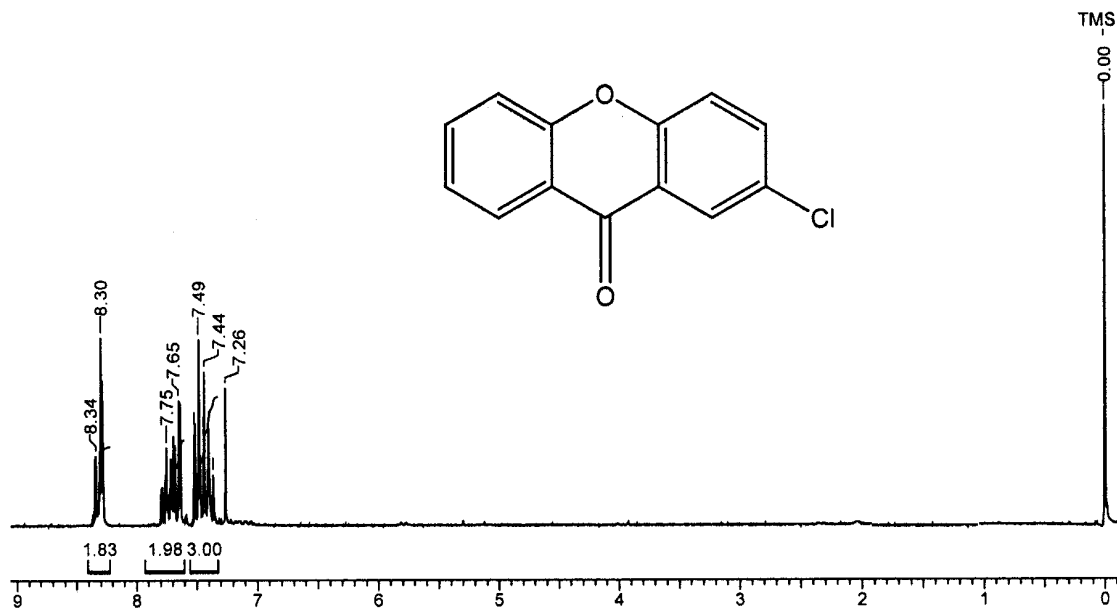


Figure 3.7: ^1H NMR spectrum of 2-chloro xanthone (3.6b)

3.2.2.3.3. 2-Chloro xanthinol (3.6c)

To the suspension of **3.6b** (2.26 g, 10 mmol) with NaOH (2.4 g, 60 mmol) in ethanol, Zn (0.96 g, 15 mmol) dust was added at 70 $^\circ\text{C}$ and stirred for 2 h. The reaction mixture was cooled and poured in ice-cold water. The resulting white precipitate was filtered and dried under vacuum. Yield: 2.06 g (89 %), Elemental analysis: $\text{C}_{13}\text{H}_9\text{ClO}_2$ (232.08 g mol^{-1}), Calcd. C, 67.11; H, 3.90 Found: C, 67.03; H, 3.87, ^1H NMR (CDCl_3): δ = 8.0-6.7 (m, 7H, Ph), 5.76 (d, 1H, CH), 2.21 (s, 1H, OH) ppm.

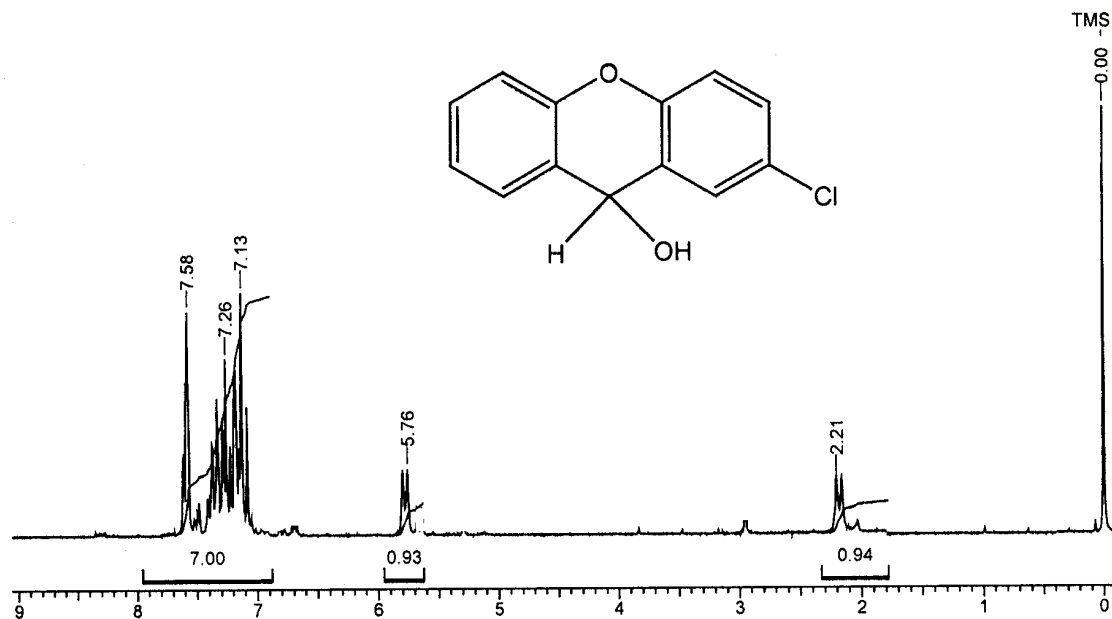


Figure 3.8: ¹H NMR spectrum of 2-chloro xanthidol (**3.6c**)

3.2.2.3.4. 2-(4-Methylphenoxy) benzoic acid (**3.7a**)^[33]

2-chlorobenzoic acid (15.7 g, 100 mmol), K₂CO₃ (14.0 g, 100 mmol), CuI (0.1 g) and copper bronze (0.1 g) was mixed in mortar by means of a pastel. After addition of 4-methyl phenol (21.8 g, 200 mmol), the reaction mixture was heated in 500 mL round bottomed flask equipped with a reflux condenser and CaCl₂ drying tube to 200 °C for 3 h. The reaction mixture was cooled to ambient temperature and 200 mL of aqueous Na₂CO₃ was added to this reaction mixture. To remove the excess of copper bronze, the reaction mixture was filtered and extracted with diethyl ether (3 x 50 mL). The aqueous phase was acidified with 10 M HCl. The precipitate was filtered, washed with water and recrystallized with ethanol. Yield: 10.6 g (47 %), mp: 124-126 °C. Elemental analysis: C₁₄H₁₂O₃ (228.24 g mol⁻¹) Calcd. C, 73.67; H, 5.30. Found: C, 73.56; H, 5.23. ¹H NMR (CDCl₃): δ = 8.40-6.80 (m, 8H, Ph), 2.37 (s, 3H, CH₃) ppm.

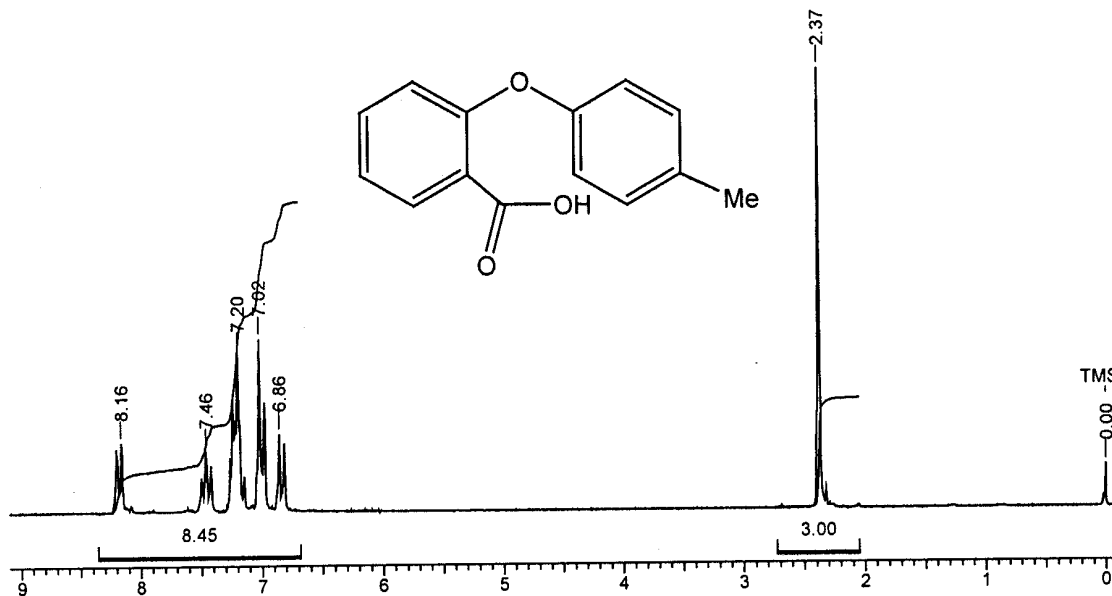


Figure 3.9: ¹H NMR spectrum of 2-(4-methylphenoxy) benzoic acid (**3.7a**)

3.2.2.3.5. 2-Methyl xanthone (**3.7b**)^[33]

The compound **3.7a** (10 g, 44 mmol) was heated with polyphosphoric acid (PPA) (50 g) at 100 °C for 2 h. The mixture was cooled to ambient temperature and poured in ice-cold water. The appeared precipitate was filtered, washed with water and recrystallized with 95 % ethanol.

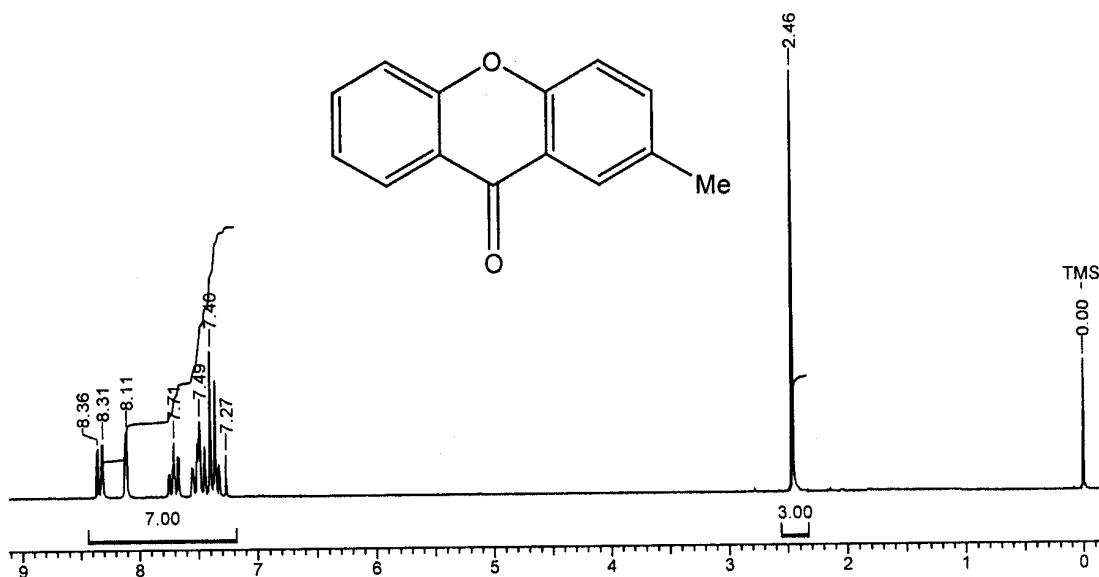


Figure 3.10: ¹H NMR spectrum of 2-methyl xanthone (**3.7b**)

Yield: 6.8 g (74 %), mp: 121-122 °C, Elemental analysis: C₁₄H₁₀O₂ (210.23 g mol⁻¹) Calcd. C, 79.98; H, 4.79. Found: C, 79.82; H, 4.71, IR (KBr): 3065, 2955, 2857, 1586, 1500, 1460, 1257, 1234, 1106, 1031, 997, 835, 755 cm⁻¹, ¹H NMR (CDCl₃): δ = 8.40-7.20 (m, 7H, Ph), 2.46 (s, 3H, CH₃) ppm.

3.2.2.3.6. 2-Methyl xanthidol (3.7c)

This compound was synthesized in the same manner as described for **3.6c**. Yield: 2.01 g (85 %), Elemental analysis: C₁₄H₁₂O₂ (212.08 g mol⁻¹), Calcd. C, 79.22; H, 5.70 Found: C, 79.13; H, 5.74, ¹H NMR (CDCl₃): δ = 8.50-7.20 (m, 7H, Ph), 5.8 (d, 1H, CH), 2.46 (s, 3H, CH₃) ppm.

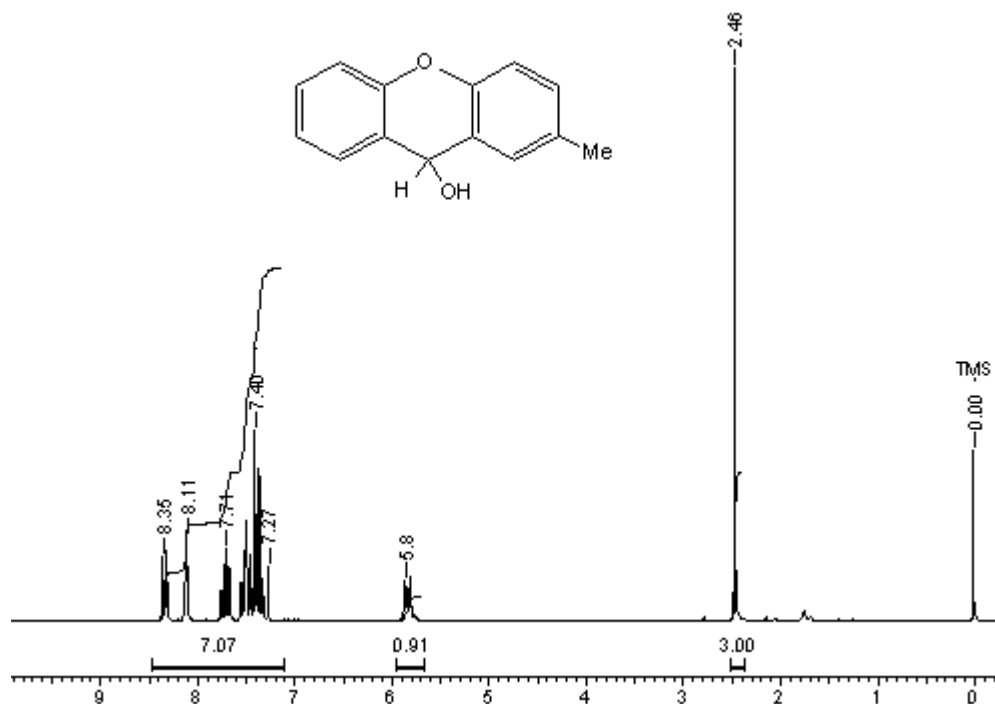


Figure 3.11: ¹H NMR spectrum of 2-methyl xanthidol (**3.7c**)

3.2.2.3.7. 2-(4-Methoxyphenoxy) benzoic acid (**3.8a**)^[33]

A suspension of 4-methoxyphenol (12.3 g, 100 mmol), 2-chlorobenzoic acid (6.15 g, 50 mmol), K₂CO₃ (21 g, 150 mmol), copper powder (0.5 g, 7.8 mmol), in DMF was refluxed for 24 h. The reaction mixture was cooled to ambient temperature and water (200 mL) was added to the reaction mixture. The brown residue was removed by filtration and green

filtrate was acidified with HCl to PH 1 to give a white precipitate. The white solid was washed with water and dried at ambient temperature and recrystallized with 50 % ethanol. Yield: 11 g (46 %), white crystals, mp: 144 °C, Elemental analysis: C₁₄H₁₂O₄ (244.24 g mol⁻¹), Calcd. C, 68.85; H, 4.95. Found: C, 68.370; H, 4.85. IR (KBr): 3065, 2998, 2917, 2834, 2500, 1760, 1618, 1585, 1500, 1480, 1460, 1440, 1323, 1260, 838, 724 cm⁻¹, ¹H NMR (CDCl₃): δ = 8.40-6.60 (m, 8H, Ph), 3.83 (s, 3H, OCH₃) ppm.

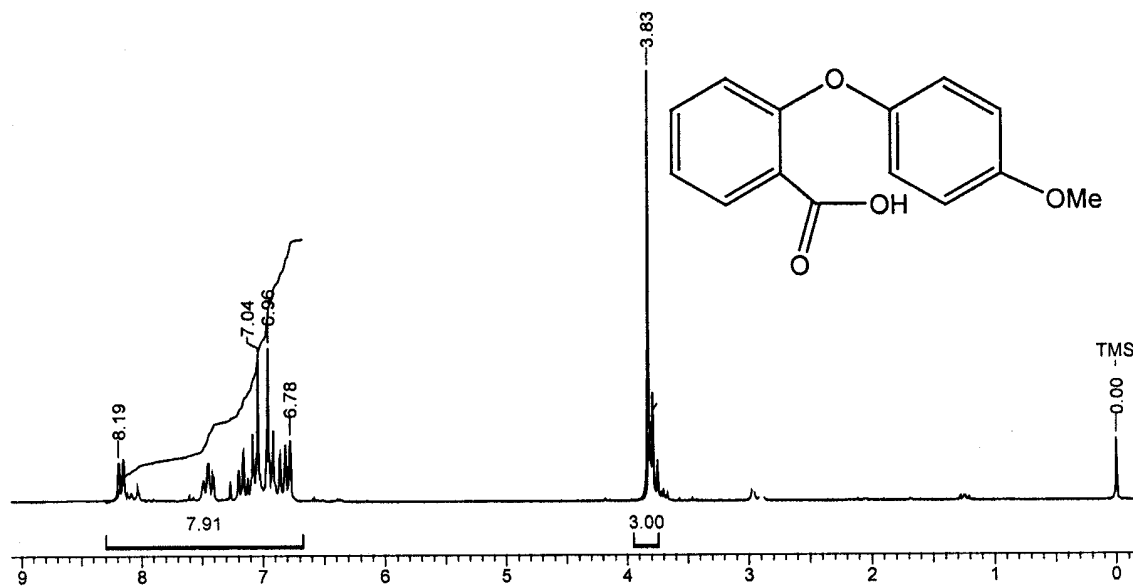


Figure 3.12: ¹H NMR spectrum of 2-(4-methoxyphenoxy) benzoic acid (**3.8a**)

3.2.2.3.8. 2-Methoxy xanthone (**3.8b**)^[33]

The compound **3.8a** (3.04 g, 13.1 mmol) was added to PPA (50 mL) at 120 °C for 2 h. The reaction mixture was cooled to ambient temperature and poured in ice-cold water. The resulting precipitate was filtered and extracted with CH₂Cl₂ (3 x 100 mL) and washed with H₂O (5 x 150 mL). The organic layer was dried over Na₂SO₄ and the solvent was evaporated under vacuum. The crude solid was recrystallized with ethanol. Yield: 3.40 g (80 %), white needles, mp: 127 °C, Elemental analysis: C₁₄H₁₀O₃ (226.23 g mol⁻¹) Calcd. C, 74.33; H, 4.46. Found: C, 74.25; H, 4.48, IR (KBr): 3065, 2998, 2917, 2834, 1618, 1585, 1500, 1480, 1460, 1440, 1323, 1260, 838, 724 cm⁻¹, ¹H NMR (CDCl₃): δ = 8.40-7.20 (m, 7H, Ph), 3.93 (s, 3H, OCH₃) ppm.

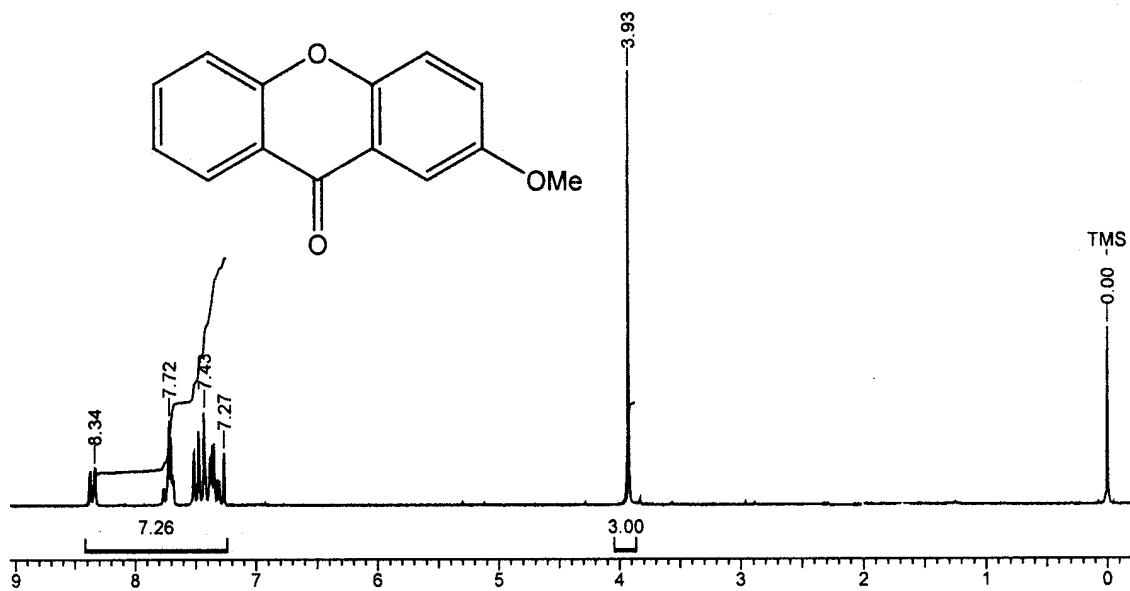


Figure 3.13: ¹H NMR spectrum of 2-methoxy xanthone (3.8b)

3.2.2.3.9. 2-Methoxy xanthinol (3.8c)

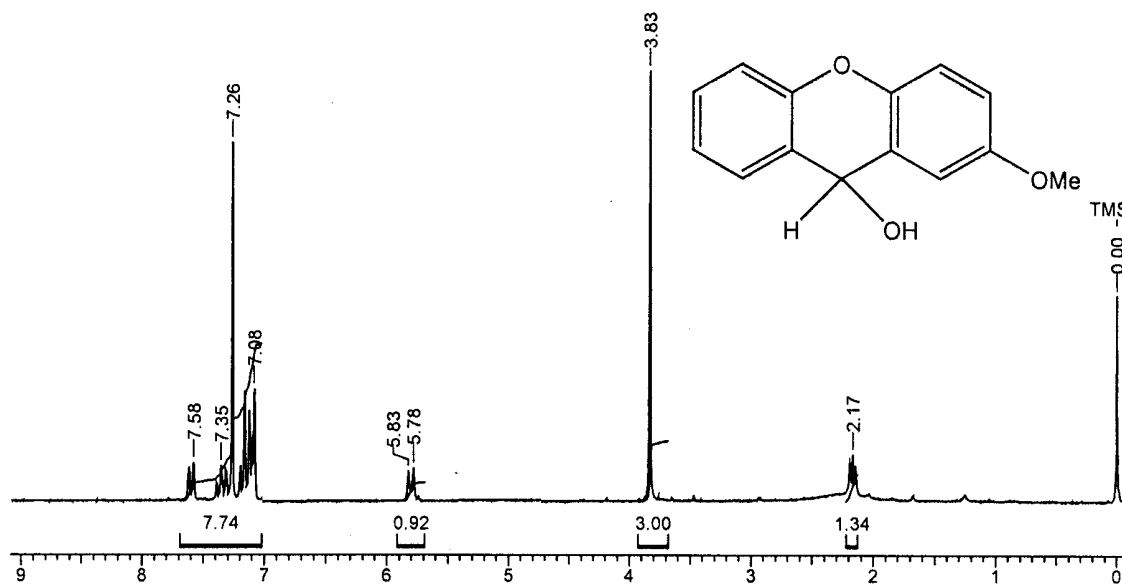


Figure 3.14: ¹H NMR spectrum of 2-methoxy xanthinol (3.8c)

This compound was synthesized in the same manner as described for **3.6c**. Yield: 2.5 g (90 %), Elemental analysis: C₁₄H₁₂O₃ (228.08 g mol⁻¹) Calcd. C, 73.67; H, 5.30 Found: C,

73.63; H, 5.38. ^1H NMR (CDCl_3): $\delta = 7.8\text{--}7.0$ (m, 7H, Ph), 5.83, 5.78 (d, 1H, CH), 3.83 (s, 3H, OCH_3), 2.17 (s, 1H, OH) ppm.

3.2.2.3.10. 2-Chloro xanthenyltriphenylphosphonium hexafluoroantimonate (3.6d)

This compound was synthesized using **3.6c** in the same manner as described for **3.4b**.

Yield: 1.6 g (75 %), white crystals, Elemental analysis: $\text{C}_{32}\text{H}_{23}\text{ClOPSbF}_6$ ($714.01 \text{ g mol}^{-1}$)
Calcd. C, 52.17; H, 3.25. Found: C, 52.17; H, 3.18. FT-IR (KBr): 3030, 1625, 1600, 1500, 1463, 1439, 1065, 743, 720, 687 cm^{-1} , ^1H NMR (200 MHz, DMSO-d_6): $\delta = 7.98\text{--}7.09$ (m, 22 H, Ph), 7.05 (s, 1 H, CH) ppm, ^{13}C NMR (200 MHz, DMSO-d_6): $\delta = 153.61, 152.66, 135.42, 134.54, 131.55, 130.11, 129.88, 127.55, 124.55, 118.65, 117.24, 116.30, 115.56, 114.69, 113.26, 39.41, 38.57$ ppm, ^{31}P NMR (200 MHz, DMSO-d_6): 21.72, 25.67 ppm.

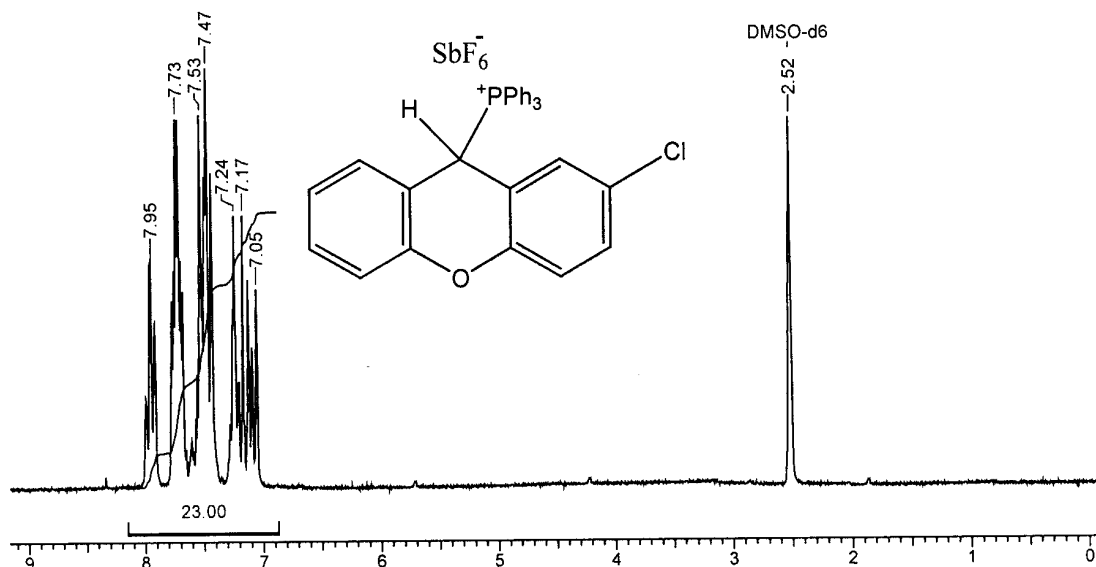


Figure 3.15: ^1H NMR spectrum of 2-chloro xanthenyltriphenylphosphonium hexafluoroantimonate (**3.6d**)

3.2.2.3.11. 2-Methyl xanthenyltriphenylphosphonium hexafluoroantimonate (3.7d)

This compound was synthesized using **3.7c** in the same manner as described for **3.4b**.

Yield: 1.32 g (65 %), white crystals, Elemental analysis: $\text{C}_{33}\text{H}_{26}\text{OPSbF}_6$ ($692.07 \text{ g mol}^{-1}$)
Calcd. C, 55.44; H, 3.78. Found: C, 55.38; H, 3.75. FT-IR (KBr): 3030, 1625, 1600, 1500, 1463, 1439, 1065, 743, 720, 687 cm^{-1} , ^1H NMR (200 MHz, DMSO-d_6): $\delta = 7.98\text{--}7.09$ (m,

22 H, Ph), 6.94 (d, 1H, CH), 2.14 (s, 3H, CH₃) ppm, ¹³C NMR (200 MHz, DMSO-d₆): δ = 154.13, 151.84, 135.25, 134.75, 133.02, 131.18, 129.97, 128.86, 124.02, 116.66, 115.07, 113.71, 39.76, 38.95, 20.07 ppm, ³¹P NMR (200 MHz, DMSO-d₆): 21.14, 25.88 ppm.

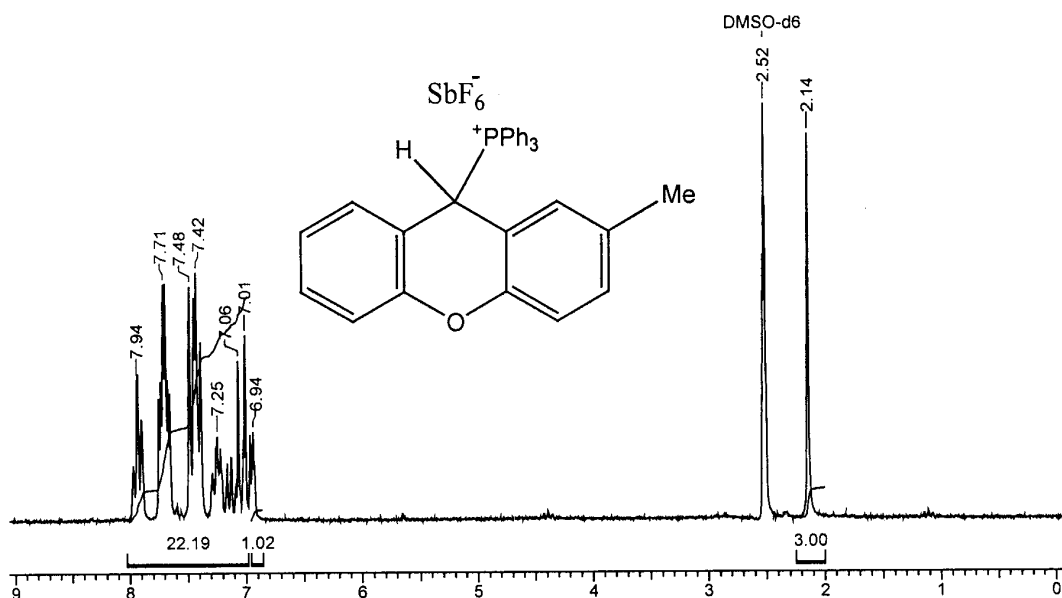


Figure 3.16: ¹H NMR spectrum of 2-methyl xanthenyltriphenylphosphonium hexafluoroantimonate (**3.7d**)

3.2.2.3.12. 2-Methoxy xanthenyltriphenylphosphonium hexafluoroantimonate (**3.8d**)

This compound was synthesized using **3.8c** in the same manner as described for **3.4b**. Yield: 1.2 g (59 %), white crystals, Elemental analysis: C₃₃H₂₆O₂PSbF₆ (708.06 g mol⁻¹) Calcd. C, 54.19; H, 3.69 Found: C, 54.19; H, 3.75. FT-IR (KBr): 3030, 1625, 1600, 1500, 1463, 1439, 1065, 743, 720, 687 cm⁻¹, ¹H NMR (200 MHz, DMSO-d₆): δ = 7.98-7.09 (m, 22 H, Ph), 6.72 (s, 1H, CH), 3.79 (s, 3H, OCH₃) ppm, ¹³C NMR (200 MHz, DMSO-d₆): δ = 155.11, 154.28, 147.75, 135.24, 134.72, 134.54, 131.55, 130.80, 120.02, 129.78, 128.86, 123.87, 117.00, 114.58, 55.38, 40.00, 39.18 ppm, ³¹P NMR (200 MHz, DMSO-d₆): 20.99, 25.67 ppm.

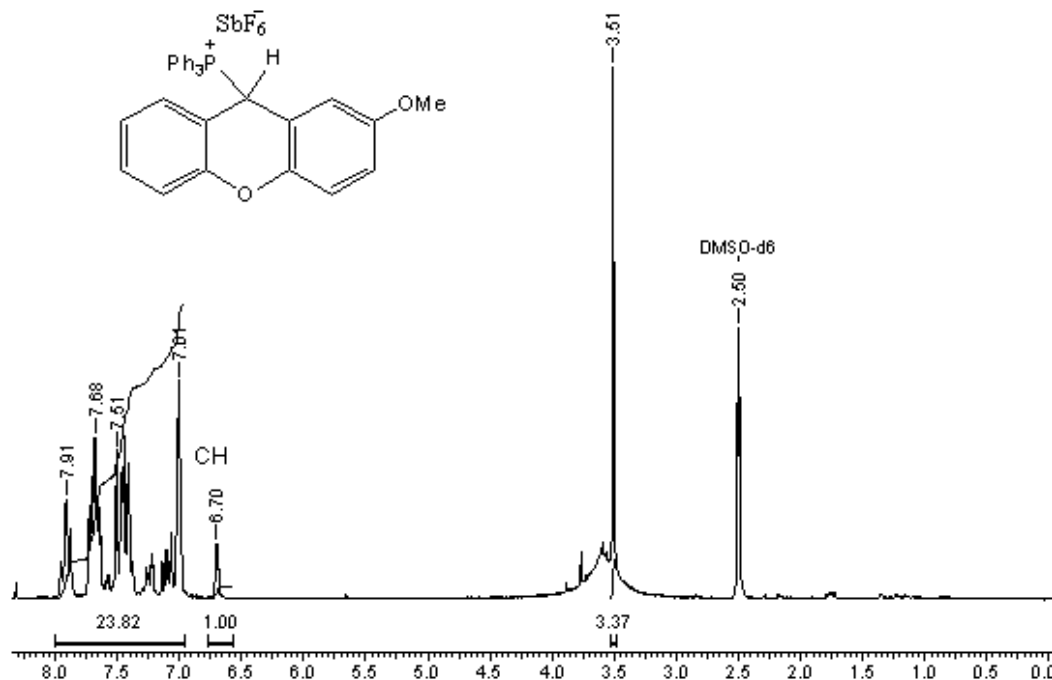


Figure 3.17: ^1H NMR spectrum of 2-methoxy xanthenyltriphenylphosphonium hexafluoroantimonate (**3.8d**)

3.2.3. Typical polymerization procedure

A mixture of monomer (5 mmol) and initiator (0.05 mmol) was placed in a flame dried ampoule equipped with three way stopcock connected to manifold and degassed for 30 minutes with three freeze-pump-thaw cycles and sealed off. The ampoule was immersed in an oil bath at the required temperature. After reaction for set time, reaction mixture was cooled in liquid nitrogen bath. The monomer conversion was determined by ^1H NMR spectroscopy from crude polymerization mixture ^[34]. The polymerization mixture was dissolved in CH_2Cl_2 and precipitated with methanol. The polymer was separated from the supernatant by decantation and dried under vacuum. The molecular weight of polymer was determined by gel permeation chromatography (GPC). The obtained polymer was identified to be poly(GPE). ^1H NMR (CDCl_3): δ 7.99-7.65 (m, 5H, $-\text{C}_6\text{H}_5$), 4.80-3.25 (m, 5H, $-\text{OCH}_2\text{CH}(\text{CH}_2\text{Ph})-$) ppm, IR (neat): 3036, 2930, 2876, 1599, 1495, 1244, 1132, 1044, 754, 661 cm^{-1} .

3.2.4. Measurements

The single-crystal diffraction data were collected on a Brüker AXS Smart Apex CCD diffractometer at 133(2) K. The X-ray generator was operated at 50 kV and 30 mA using

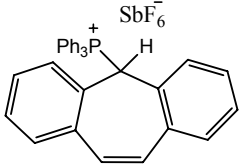
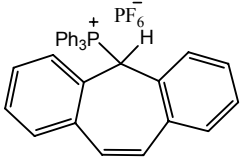
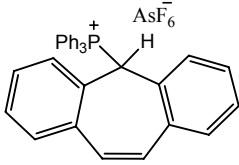
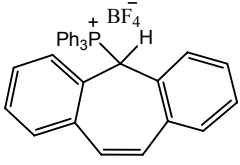
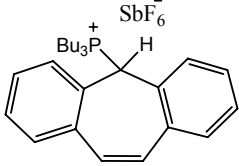
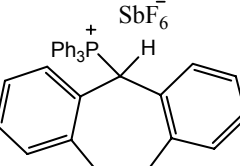
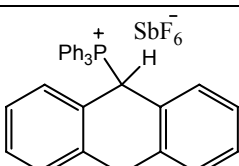
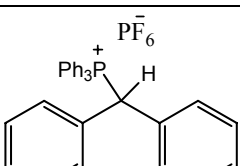
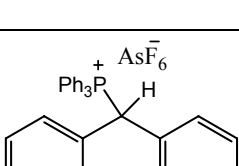
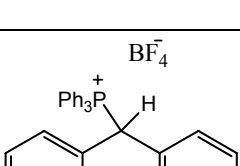
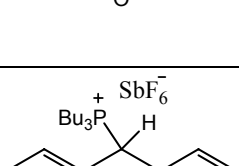
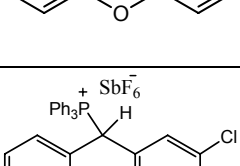
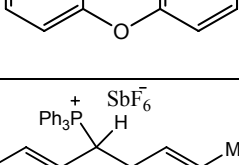
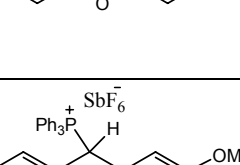
graphite-monochromatized (Mo K_{α} , = 0.71073Å) radiation. Data were collected with ω scan width of 0.3° and with three different settings of φ (0°, 90°, 180°) keeping the sample-to-detector distance fixed at 6.145 cm and the detector position (2θ) fixed at -28°. The X-ray data collection was monitored by SMART program (Bruker, 2003) [35]. All the data were corrected for Lorentzian, polarization and absorption effects using SAINT and SADABS programs (Bruker, 2003). SHELX-97 was used for structure solution and full matrix least-squares refinement on F^2 [36]. Hydrogen atoms were located from a difference Fourier map and their positional coordinates and isotropic thermal parameters were refined. ORTEPs and geometrical parameters were obtained using SHELXTL program [35]. Molecular weight was measured by gel permeation chromatography (GPC) in THF as eluent (flow rate: 1 mL/min) on a setup consisting of a pump and six Ultra Styragel column (50 to 10⁵ Å porosities) and detection was carried out with the aid of UV-100 and RI-150 detectors. Molecular weight (M_n) and polydispersities (M_w/M_n) were determined using a calibration curve obtained by polystyrene standards. NMR (¹H, ¹³C and ³¹P) spectra were recorded on a Bruker 200 MHz instrument with CDCl₃ and DMSO-d₆ (for initiators) as solvent and tetramethylsilane as internal standard. IR spectra were recorded on a Perkin-Elmer model 683 grating IR spectrometer. Elemental analysis was performed on a Thermo Finnigan Flash EA-1112 Microanalyser instrument. Thermal stability was analyzed using Perkin-Elmer TGA-7, by heating the initiators from 50 – 900 °C with a heating rate of 10 °C/min under nitrogen atmosphere with a flow rate of 20 mL/min.

3.3. Results and discussion

3.3.1. Initiators

Phosphonium salts were synthesized as described in the experimental section (Scheme 3.1, 3.2 and 3.3) and characterized by NMR (¹H, ¹³C & ³¹P), IR and elemental analysis. All the initiators are white crystalline salts and shows good stability toward air and moisture at ambient temperature (Table 3.1).

Table 3.1: Phosphonium salt initiators used in present study

Initiator	Abbreviation	Initiator	Abbreviations
	3.1b		3.1c
	3.1d		3.1e
	3.2		3.3
	3.4b		3.4c
	3.4d		3.4e
	3.5		3.6d
	3.7d		3.8d

It has been found that the counter anion does not have any effect on the δ value of methine proton in ^1H NMR spectra of initiators. Figure 3.18-3.21 shows the molecular structure of **3.1b**, **3.1e**, **3.4b** and **3.4e** obtained by single crystal XRD. The inter-atomic distance between the dibenzosuberonyl methine proton and carbon (C_1) of **3.1b** and **3.1e** was found 0.78 and 0.95 Å, respectively. The interatomic distance for **3.4b** and **3.4e** was found 0.88 and 0.83 Å, respectively.

The crystal data and structure refinement for **3.1b**, **3.1e**, **3.4b** and **3.4e** is shown in Table 3.2.

Table 3.2: Crystal data and structure refinement for **3.1b**, **3.1e**, **3.4b**, **3.4e**

Properties	3.1b	3.1e	3.4b	3.4e
Empirical formula	$\text{C}_{34}\text{H}_{28}\text{F}_6\text{PSb}$	$\text{C}_{33}\text{H}_{26}\text{BF}_4\text{P}$	$\text{C}_{31}\text{H}_{24}\text{OPSbF}_6$	$\text{C}_{31}\text{H}_{24}\text{BF}_4\text{OP}$
Formula weight	774.18	540.32	690.09	530.28
Temperature (K)	133(2)	133(2) K	133(2) K	297(2)
Wavelength (Å)	0.71073	0.71073	0.71073	0.71073
Crystal system, space group	Monoclinic, C2/c	Monoclinic, P 21/n	Monoclinic, C2/c	Monoclinic, P 21/n
Unit cell dimensions	a = 19.982(8) Å $\alpha = 90^\circ$. b = 17.452(7) Å $\beta = 93.489(7)^\circ$ c = 18.233(8) Å $\gamma = 90^\circ$.	a = 11.1201(11) Å $\alpha = 90^\circ$. b = 13.6036(14) Å $\beta = 103.726(2)^\circ$ c = 17.7576(18) Å gamma = 90° .	a = 21.701(2) Å, b = 16.3564(16) Å, c = 17.3135(16), $\alpha = 90^\circ$, $\beta = 97.218(2)^\circ$, $\gamma = 90^\circ$	a = 11.819(3) Å $\alpha = 90^\circ$. b = 15.415(4) Å $\beta = 90.579(3)^\circ$. c = 13.990(3) Å $\gamma = 90^\circ$
Volume	6347(5) Å ³	2609.5(5) Å ³	6096.6(10) Å ³	2548.6(10) Å ³
Z, Calculated density	8, 1.620 Mg/m ³	4, 1.375 Mg/m ³	8, 1.503 Mg/m ³	4, 1.382Mg/m ³
Absorption coefficient	1.148 mm ⁻¹	0.156 mm ⁻¹	1.038	0.161 mm ⁻¹
F(000)	3088	1120	2744	1096
Crystal size	0.55 x 0.35 x 0.27 mm	0.32 x 0.18 x 0.13 mm	0.47 x 0.16 x 0.14 mm	0.51 x 0.41 x 0.31 mm
Theta range for data collection	1.55 to 25.00°	1.97 to 25.00 °	1.56 to 25.00 °	1.97 to 25.00°.
Limiting indices	-23<=h<=23, -20<=k<=20, -21<=l<=21	-13<=h<=13, -16<=k<=16, -21<=l<=21	-16<=h<=25, -18<=k<=19, -20<=l<=20	-14<=h<=14, -18<=k<=18, -16<=l<=16

Reflections collected / unique	29328 / 5587 [R(int) = 0.0248]	18609 / 4592 [R(int) = 0.0306]	15824 / 5351 [R(int) = 0.0241]	10551 / 2836 [R(int) = 0.0305]
Completeness to theta =	25.00 100.0 %	25.00 100.0 %	25.00 99.8 %	25.00 63.2 %
Absorption correction	Semi-empirical from equivalents	Semi-empirical from equivalents	Semi-empirical from equivalents	Semi-empirical from equivalents
Max. and min. transmission	0.7492 and 0.5725	0.9795 and 0.9517	0.8627 and 0.6383	0.9517 and 0.9216
Refinement method	Full-matrix least-squares on F ²	Full-matrix least-squares on F ²	Full-matrix least-squares on F ²	Full-matrix least-squares on F ²
Data / restraints / parameters	5587 / 0 / 521	4592 / 0 / 456	5351 / 14 / 369	2836 / 0 / 448
Goodness-of-fit on F ²	1.061	1.060	1.054	1.059
Final R indices [I>2sigma(I)]	R1 = 0.0476, wR2 = 0.1303	R1 = 0.0463, wR2 = 0.1073	R1 = 0.0805, wR2 = 0.2531	R1 = 0.0597, wR2 = 0.1720
R indices (all data)	R1 = 0.0507, wR2 = 0.1337	R1 = 0.0534, wR2 = 0.1119	R1 = 0.0974, wR2 = 0.2731	R1 = 0.0664, wR2 = 0.1777
Largest diff. peak and hole	1.208 and -1.491 e. Å ⁻³	0.616 and -0.308 e. Å ⁻³	1.076 and -0.919 e. Å ⁻³	0.264 and -0.409 e. Å ⁻³

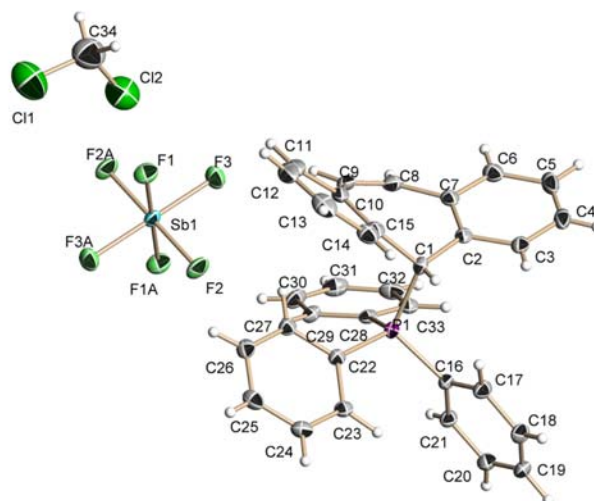


Figure 3.18: Ortep diagram of dibenzosuberonyltriphenylphosphonium hexafluoroantimonate (**3.1b**)

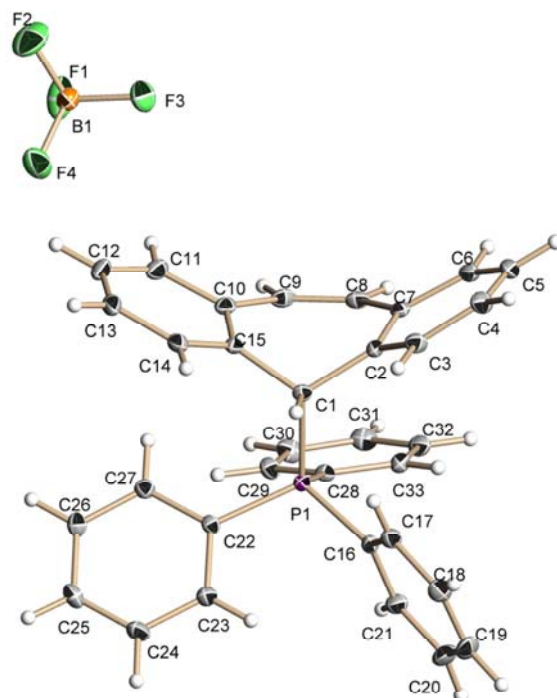


Figure 3.19: Ortep diagram of dibenzosuberonyltriphenylphosphonium tetrafluoroborate (**3.1e**)

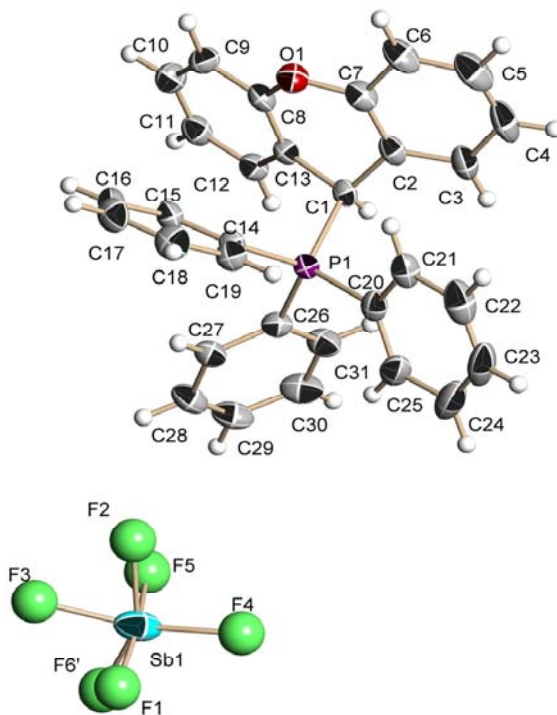


Figure 3.20: Ortep diagram of xanthenyltriphenylphosphonium hexafluoroantimonate (**3.4b**)

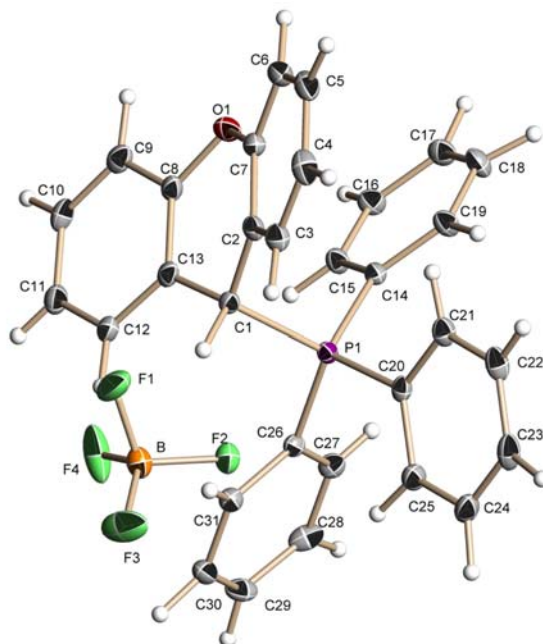


Figure 3.21: Ortep diagram of xanthenyltriphenylphosphonium tetrafluoroborate (**3.4e**)

3.3.1.1. Thermal stability of phosphonium salts

Figure 3.22 shows TGA thermograms of dibenzosuberonyl phosphonium salts under nitrogen atmosphere. It can be seen that these salts are stable up to 225 °C above which onset degradation temperature were observed.

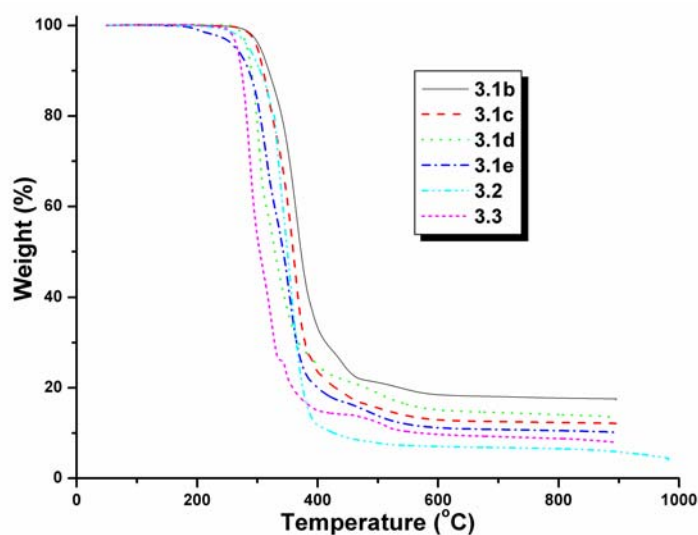


Figure 3.22: Thermograms of dibenzosuberonyl phosphonium salts

The maximum decomposition temperatures (T_d) were observed above 300 °C. Among all the salts, **3.2** has shown the lower thermal stability, which can be attributed to the presence of aliphatic (*n*-butyl) phosphine moiety.

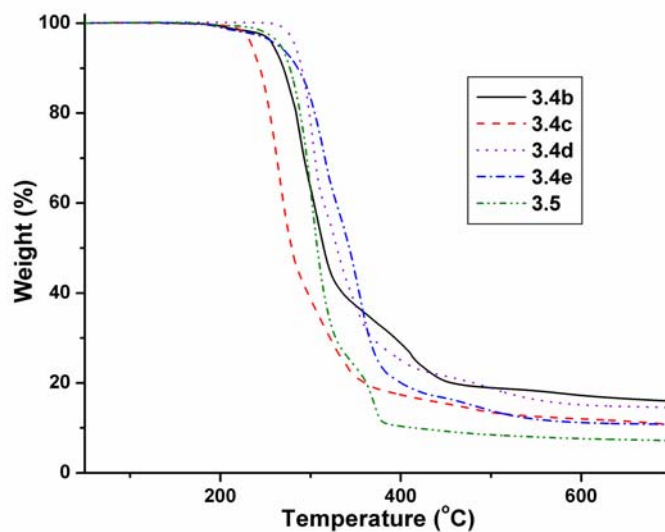


Figure 3.23: Thermograms of xanthenyl phosphonium salts

Figure 3.23 shows thermo gravimetric analysis of xanthenyl phosphonium salts having different counter anion and phosphine moiety.

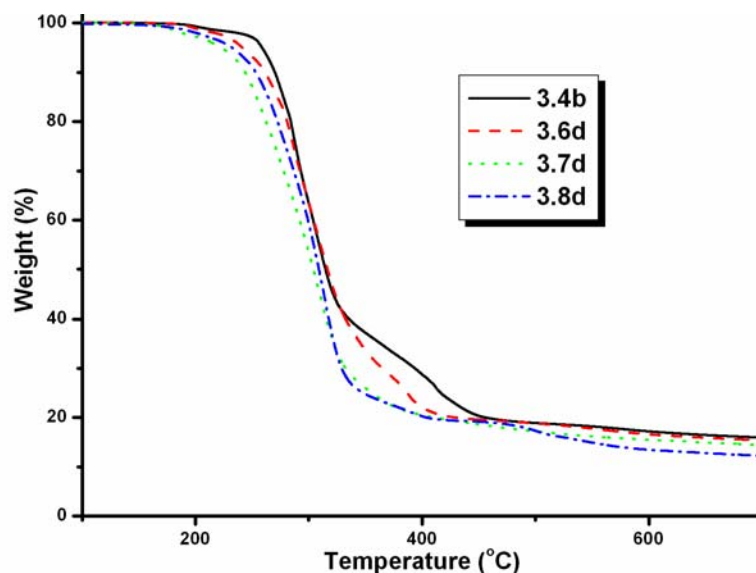


Figure 3.24: Thermograms of 2-substituted xanthenyl phosphonium salts

Figure 3.24 shows TGA thermograms of all the 2-substituted xanthenyl phosphonium salts under nitrogen atmosphere. The prepared initiators were found to be thermally stable up to

200 °C above which their onset degradation temperatures were also observed. It indicates that substituents have no significant effect on the thermal stability of phosphonium salts.

Therefore, all these phosphonium salt initiators can be used up to 200 °C. The above thermal properties might suggest the potential relevance of phosphonium salts as latent thermal cationic initiators in curing applications.

3.3.1.2. Solubility of phosphonium salts

The solubility of an initiator has an important role in the polymerization and curing of epoxy monomers. Table 3.3 shows the solubility of prepared salts in various organic solvent and epoxy monomers at ambient temperature. These salts are fairly soluble in the solvents such as acetone (CH_3COCH_3), dimethylsulfoxide (DMSO), N, N-dimethylformamide (DMF) and acetonitrile (CH_3CN), while partially soluble in chloroform (CHCl_3) and methanol (MeOH). All initiators were insoluble in less-polar solvents such as toluene (PhCH_3) and diethyl ether ($\text{C}_2\text{H}_5\text{OC}_2\text{H}_5$). Among the salts examined, **3.2** and **3.5** show better solubility in tetrahydrofuran (THF) and chloroform in comparison of other phosphonium salts. This enhanced solubility can be attributed to presence of three *n*-butyl groups. The solubility of these initiators was also examined in epoxy monomers such as GPE, CHO, propylene oxide (PPO) and epichlorohydrine (ECH). The prepared initiators have shown better solubility in GPE, ECH and PPO whereas; they are sparingly soluble in CHO. It can also be observed that the counter anion has no significant effect on the solubility of the initiators in monomers and solvents. However, the presence of aliphatic groups in phosphine moiety enhances the solubility. These solubility characteristics might indicate the use of phosphonium salts as latent cationic initiator in curing applications.

Table 3.3: Solubility of phosphonium salts in various solvents and epoxy monomers^a

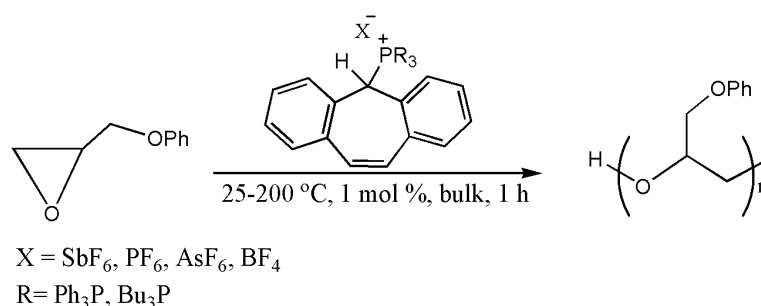
Initiator	Organic Solvents									Epoxy Monomers			
	PhCH ₃	Et ₂ O	CHCl ₃	THF	CH ₃ COCH ₃	MeOH	DMSO	DMF	CH ₃ CN	GPE	CHO	ECH	PPO
3.1b	-	-	+	++	+++	+	+++	+++	+++	+++	+	+++	+++
3.1c	-	-	+	++	+++	+	+++	+++	+++	+++	+	+++	+++
3.1d	-	-	+	++	+++	+	+++	+++	+++	+++	+	+++	+++
3.1e	-	-	+	++	+++	+	+++	+++	+++	+++	+	+++	+++
3.2	-	-	+++	+++	+++	++	+++	+++	+++	+++	+	+++	+++
3.3	-	-	+	++	+++	++	+++	+++	+++	+++	+	+++	+++
3.4b	-	-	+	++	+++	+	+++	+++	+++	+++	+	+++	+++
3.4c	-	-	+	++	+++	+	+++	+++	+++	+++	+	+++	+++
3.4d	-	-	+	++	+++	+	+++	+++	+++	+++	+	+++	+++
3.4e	-	-	+	++	+++	+	+++	+++	+++	+++	+	+++	+++
3.5	-	-	+++	+++	+++	++	+++	+++	+++	+++	+	+++	+++
3.6d	-	-	+	++	+++	+	+++	+++	+++	+++	+	+++	+++
3.7d	-	-	+	++	+++	+	+++	+++	+++	+++	+	+++	+++
3.8d	-	-	+	++	+++	+	+++	+++	+++	+++	+	+++	+++

a) Conditions: Phosphonium salts (0.1 mmol) in various solvents and monomers at ambient temperature (+++ = soluble in 0.3 mL of solvent, ++ = soluble in 0.5 mL of solvent, + = partially soluble in 1.0 mL solvent, - = insoluble), PPO = propylene oxide, ECH = epichlorohydrine.

3.3.2. Dibenzosuberene based phosphonium salts as thermo-latent initiator in cationic polymerization

3.3.2.1. Polymerization of GPE

The bulk polymerization of GPE was carried out with 1 mol % of initiator (**3.1b-3.1e**, **3.2**, **3.3**) in 25-200 °C temperature range for 1 h (Scheme 3.4).



Scheme 3.4: Polymerization of GPE with dibenzosuberenylyphosphonium salts

The conversion of GPE was determined by ¹H NMR spectrum of crude polymerization mixture. The monomer with any of initiators was not consumed at ambient temperature, even after 3 weeks. Above corresponding threshold initiation temperature (>100 °C) only, the monomer conversion was generally observed, indicating the thermal latency of prepared initiators. In general, with all the initiators the molecular weight (M_n) was found to be about 2000-3800 (polydispersity: 1.1 to 1.6) by GPC (Table 3.4, 3.5 and 3.6).

3.3.2.1.1. Effect of counter anion

The effect of counter anions on initiator activity was rationalized by monitoring monomer conversion as a function of reaction temperature and time. Figure 3.25, shows the temperature vs. conversion curve. It can be seen that with increasing temperature, the conversion % increases (Table 3.4). The polymerization of GPE with **3.1b**, **3.1c**, **3.1d** and **3.1e** proceeds above 100, 120, 120 and 100 °C temperature, respectively to afford polymer with molecular weight (M_n) of 2000-3800.

Table 3.4: Polymerization of GPE using dibenzosuberonylphosphonium salts (**3.1**)^a

Initiator	Temperature (°C)	Conversion^b (%)	M_n^c	M_w/M_n
	100	0		
3.1b	110	11	2500	1.3
	120	32	2900	1.4
	130	71	3200	1.4
	140	85	3100	1.4
	150	93	3800	1.4
	160	100	3800	1.5
	3.1c	120	0	
130		7	2100	1.2
140		15	2300	1.2
160		22	2400	1.1
180		28	2400	1.3
200		27	2500	1.3
3.1d		120	0	
	130	2	2000	1.2
	140	7	2200	1.2
	160	18	2400	1.1
	180	22	2300	1.3
	200	22	2400	1.3
3.1e	100	0		
	110	15	2200	1.2
	120	22	2300	1.1
	130	27	2300	1.2
	140	32	2200	1.2
	160	34	2600	1.2
	180	35	2500	1.3
	200	34	2500	1.3

^aConditions; initiator 1 mol % vs. GPE for 1 h. ^bDetermined by ¹H NMR,^cDetermined by GPC based on polystyrene standards.

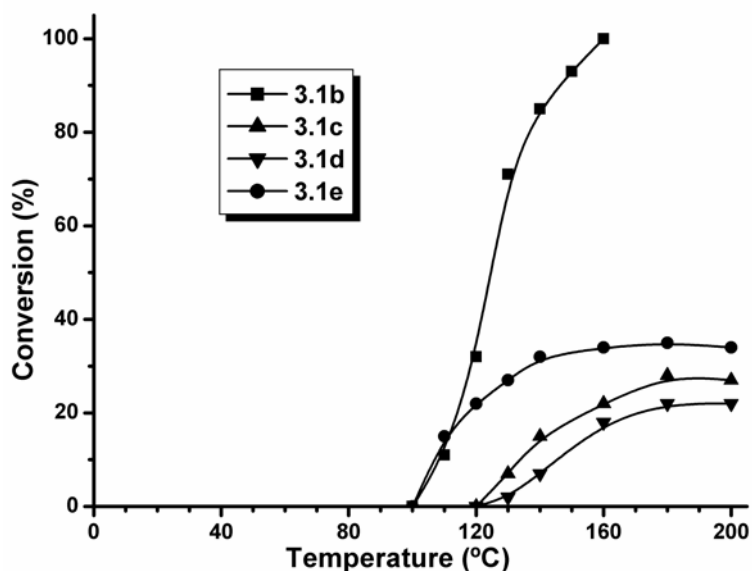


Figure 3.25: Temp – conversion curve in GPE polymerization with **3.1b-3.1e** for 1 h

The polymerization at 130 °C, with **3.1b**, **3.1c**, **3.1d** and **3.1e**, GPE attains 71, 7, 2 and 27 % conversion, respectively. A quantitative conversion was observed at 160 °C with **3.1b**, whereas, **3.1c**, **3.1d** and **3.1e** attain 27, 22 and 34 %, respectively, even at 200 °C. This suggests the overall initiator activity order as **3.1b** > **3.1e** > **3.1c** > **3.1d**. The effect of reaction time was examined by performing polymerization at 130 °C for 70 h.

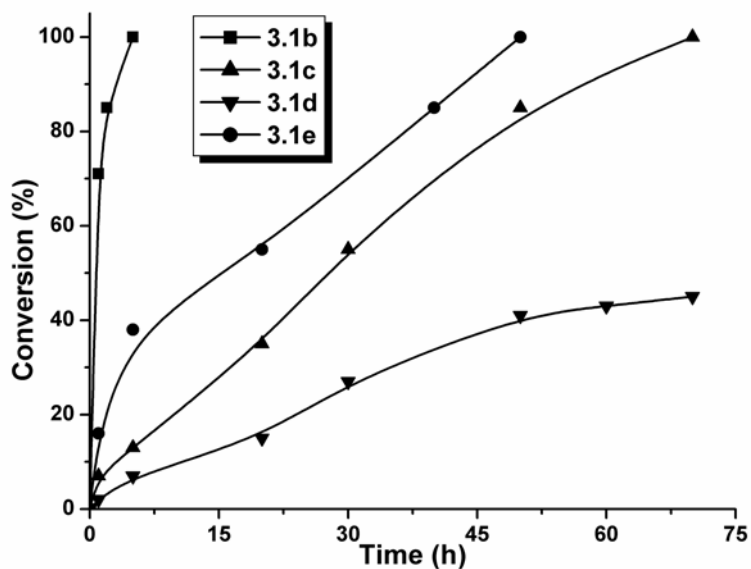


Figure 3.26: Time – conversion curve in GPE polymerization with **3.1b-3.1e** at 130 °C for 70 h.

Figure 3.26, shows an increase in conversion (%) with time. It also suggests that with increasing time, the order of activity, in terms of rate of conversion to be as **3.1b** > **3.1e** > **3.1c** > **3.1d**. The order of activity should be **3.1b** > **3.1c** > **3.1d** > **3.1e** as based on the nucleophilicity of counter anion²⁹. The higher activity of **3.1e** over **3.1c** and **3.1d** can be explained by considering two factors. (i) The higher acidity of dibenzosuberonyl methine proton, which can be attributed to comparatively longer inter-atomic distance between the methine proton and carbon of **3.1e** (0.95 Å) than **3.1b** (0.78 Å). The more inter atomic distance is correlated to higher acidity of methine proton. (ii) The nucleophilicity of counter anion, which depends upon inter-ionic distance between oxonium cation and counter anion. The longer distances denote the less nucleophilicity of counter anion, hence more activity of the initiator. According to Endo et al^[29], the increasing order of nucleophilicity of counter anion is as $\text{SbF}_6^- < \text{PF}_6^- < \text{AsF}_6^- < \text{BF}_4^-$. Thus, **3.1e** should show lower activity. In present study the initiator **3.1e**, have a counter anion with largest nucleophilicity and its methine proton with highest acidity. The above-mentioned both factors compensate with each other, which might be motive for its higher activity of **3.1e** over **3.1c** and **3.1d**. Moreover, this behavior also can be supported by the fact that GPE undergoes 15 % and 11 % conversion with **3.1e** and **3.1b**, respectively, whereas no conversion with **3.1c** and **3.1d** at 110 °C (Figure 3.25).

3.3.2.1.2. Effect of phosphine moiety

To understand the effect of phosphine moiety on initiator activity, polymerization of GPE was carried out with 1 mol % of **3.1b** (Ph_3P) and **3.2** (Bu_3P) from 25-170 °C for 1 h (Table 3.5). The temperature–conversion curve is shown in Figure 3.27, which shows that polymerization starts with **3.1b** and **3.2** above 100 and 130 °C, respectively to afford the polymer with molecular weight (M_n) of 2600-3100 (Table 3.5). At particular temperature 140 °C, with **3.1b** and **3.2**, the conversion was about 85 % and 18 %, respectively.

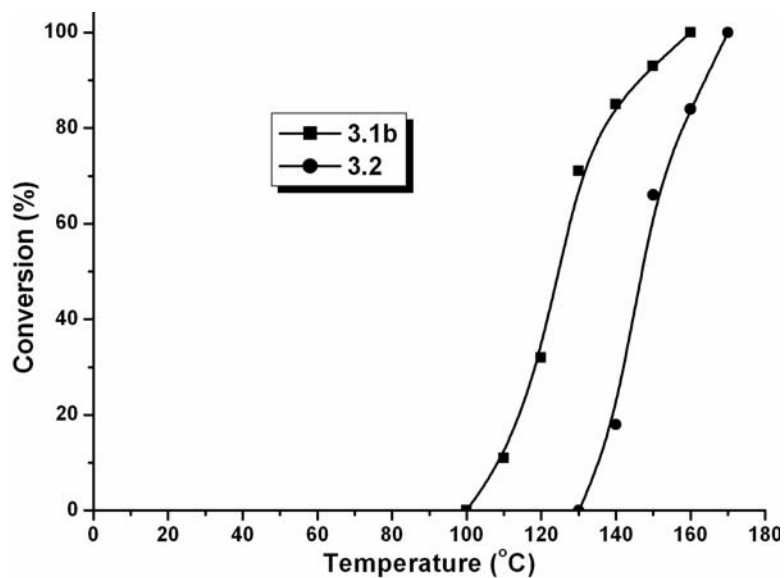
Table 3.5: Polymerization using dibenzosuberonyltri-*n*-butylphosphonium salt (**3.2**)^a

Initiator	Temperature (°C)	Conversion ^b (%)	M _n ^c	M _w /M _n
3.2	130	0		
	140	18	2600	1.4
	150	66	3000	1.5
	160	84	2900	1.5
	170	100	3100	1.6

^aConditions; initiator 1 mol % vs. GPE for 1 h. ^b Determined by ¹H NMR.

^cDetermined by GPC based on polystyrene standards.

With increasing temperature, the conversion with **3.1b** and **3.2** proceeds and attains the maximum conversion (100%) at 160 and 170 °C, respectively. The higher activity of **3.1b** compared to **3.2** may be attributed to the formation of more stable ylide with first one, which may be explained by extended conjugation of three phenyl rings of Ph₃P with dibenzosuberene ring as compare to *n*-butyl groups [37, 38].

**Figure 3.27:** Temp - conversion curve in GPE polymerization with **3.1b** and **3.2** for 1 h

Moreover, the higher activity can be supported by δ value of suberenyl methine proton of **3.1b** (at 6.83 ppm) in comparison to **3.2** (at 5.75 ppm) in ¹H NMR spectrum. The higher

shift in δ value of methine proton can be correlated with higher acidity, which is related to the initiator activity [26].

3.3.2.1.3. Effect of double bond in dibenzosuberonyl ring

To examine the effect of double bond (extended conjugation) in the dibenzosuberonyl ring on initiator activity, polymerization was performed with **3.3** and compared with **3.1b** (Table 3.6).

Table 3.6: Polymerization of GPE using dibenzosuberonyltriphenylphosphonium salt (**3.3**)^a

Initiator	Temperature (°C)	Conversion ^b (%)	M_n^c	M_w/M_n
3.3	110	0		
	120	15	2500	1.3
	130	47	3000	1.4
	140	75	3400	1.4
	150	88	3800	1.5
	160	100	3700	1.5

^aConditions; initiator 1 mol % vs GPE for 1 h. ^bDetermined by ¹H NMR.

^cDetermined by GPC based on polystyrene standards.

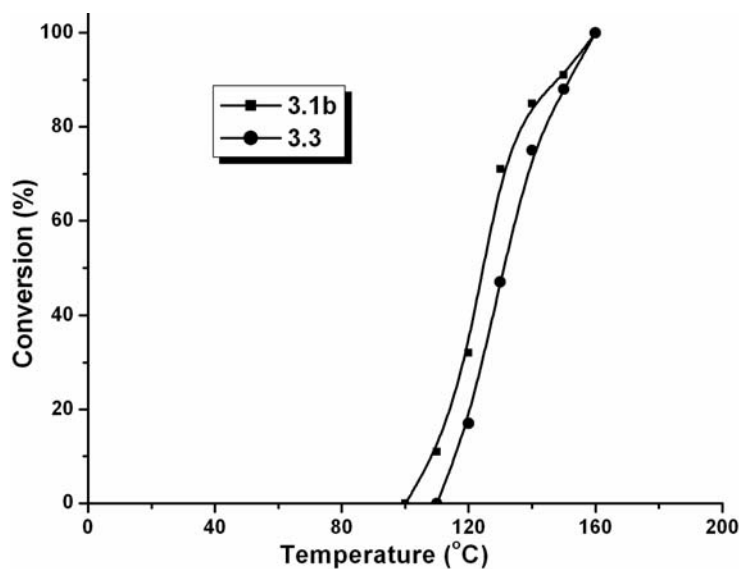


Figure 3.28: Temp-conversion curve in GPE polymerization with **3.1b** and **3.3** for 1 h

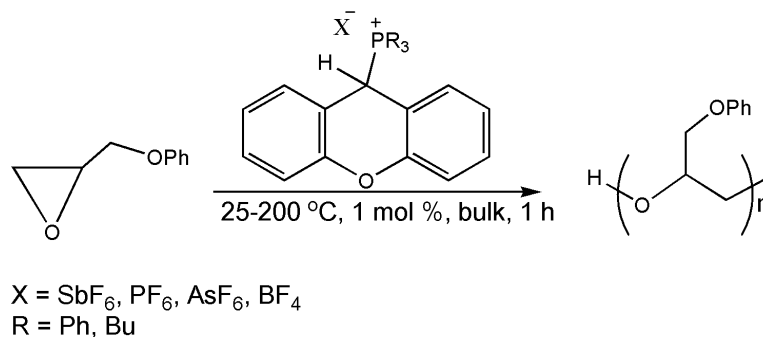
Figure 3.28 shows the temperature – conversion curve. It also suggests that the polymerization starts only above 110 °C. At 120 °C, with **3.1b** and **3.3**, the conversion was about 32 % and 15 %, respectively indicating the higher activity of **3.1b** in low temperature region. With both initiators, 100 % conversion was observed at 160 °C. In comparison of **3.3**, the higher initiator activity of **3.1b** in low temperature region could be ascribed by the stability of resulting ylide with more extended conjugation. The δ value of methine proton in ^1H NMR spectrum, also confirms the higher acidity of **3.1b** (6.83 ppm) compared to **3.3** (6.67 ppm).

3.3.3. Thermally induced cationic polymerization of glycidyl phenyl ether using xanthene based phosphonium salts

3.3.3.1. Polymerization

3.3.3.1.1. Effect of counter anion

The polymerization of GPE was carried out with 1 mol % of initiator (**3.4b**, **3.4c**, **3.4d** and **3.4e**) at 25-200 °C for 1 h (Scheme 3.5, Table 3.7).



Scheme 3.5: Polymerization of GPE with xanthenylphosphonium salts

The phosphonium salts were completely soluble in GPE at ambient temperature but GPE did not polymerize at all under this condition. After polymerization, the percentage conversion was determined by ^1H NMR of crude polymerization mixture and then polymer was precipitated with methanol.

Table 3.7: Polymerization of GPE using xanthenyl phosphonium salts (**3.4**)^a

Initiator	Temperature (°C)	Conversion ^b (%)	M _n ^c	M _w /M _n
3.4b	100	0		
	110	16	2500	1.3
	120	29	2600	1.4
	130	68	3100	1.4
	140	87	3200	1.4
	150	94	3400	1.4
	160	100	3400	1.5
3.4c	120	0		
	130	7	1900	1.2
	140	15	2200	1.2
	160	25	3000	1.3
	180	33	2800	1.4
	200	33	3000	1.4
	3.4d	120	0	
130		3	1800	1.2
140		7	2200	1.2
160		16	2500	1.2
180		28	2400	1.2
200		27	2200	1.2
3.4e		120	0	
	130	2	1300	1.2
	140	5	1500	1.2
	160	19	1800	1.2
	180	25	2000	1.2
	200	25	2000	1.2

^aConditions; initiator 1 mol % vs. GPE for 1 h. ^bDetermined by ¹H NMR. ^cDetermined by GPC based on polystyrene standards.

Figure 3.29 shows the temperature-conversion curve of the polymerization. The polymerization of GPE proceed above 100, 120, 120 and 120 °C temperature with **3.4b**, **3.4c**, **3.4d** and **3.4e**, respectively to afford the polymer with molecular weight (M_n) of 1400-3400.

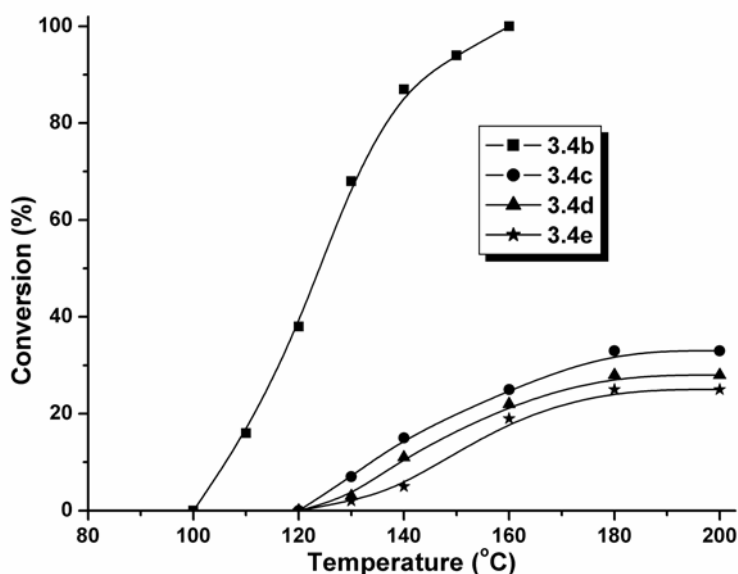


Figure 3.29: Temp-conversion curve in polymerization of GPE with **3.4b-3.4e** for 1 h

This reveals the thermal latency characteristic of these phosphonium salt initiators. Above these temperatures conversion (%) increases with various rates with the increase in polymerization temperature and attains their limiting conversion. Among all the initiators, the maximum conversion (100 %) has been found with **3.4b** at 160 °C with highest rate of conversion. For example, above the threshold temperature, at particular point, **3.4b**, **3.4c**, **3.4d** and **3.4e** have shown 16 % (at 110 °C), 7 % (130 °C), 3 % (130 °C) and 2 % (130 °C) conversion, respectively. Similarly, other than **3.4b**, which attains 100 % conversion at 160 °C, other initiators have shown the limiting conversions at 200 °C, which are 33 % with **3.4c**, 28 % with **3.4d** and 25 % with **3.4e**. The overall order of initiator activity was found as **3.4b** > **3.4c** > **3.4d** > **3.4e**. The difference in activity can be explained by nucleophilicity of the counter anion ($\text{SbF}_6^- < \text{PF}_6^- < \text{AsF}_6^- < \text{BF}_4^-$), which depends on inter-ionic distance

between the oxonium cation and counter anions. The longer inter-ionic distance denotes the lesser nucleophilicity of counter anion, hence more activity of the initiator^[29].

Further to see the activity of initiators in low conversion region (at 135 °C) for longer reaction time (70 h), the polymerization of GPE was performed with 1 mol % of initiator (**3.4b**, **3.4c**, **3.4d** and **3.4e**).

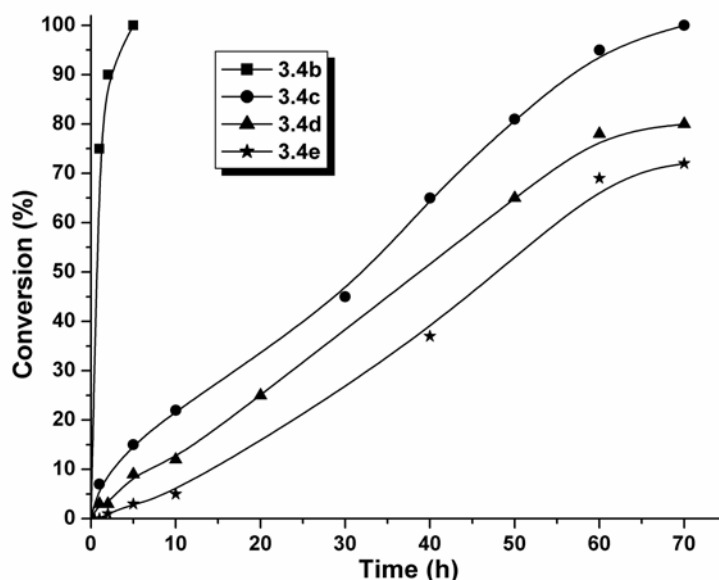


Figure 3.30: Time - conversion curve in polymerization of GPE with **3.4b-3.4e** at 135 °C

Figure 3.30 shows time–conversion curve in the polymerization of GPE. The monomer conversion increases with the increase in reaction time and attains respective limiting conversion. The initiator **3.4b**, which showed 100 % conversion in 4 h, while other initiators have shown the maximum limiting conversions after 70 h, which are 100 % with **3.4c**, 80 % with **3.4d** and 69 % with **3.4e**. The order of initiator activity remains same in longer duration and found as **3.4b** > **3.4c** > **3.4d** > **3.4e**.

3.3.3.1.2. Effect of phosphine moiety

Figure 3.31 shows temperature–conversion curve in polymerization of GPE with Ph_3P (**3.4b**) and Bu_3P (**3.5**) based phosphonium salts (1 mol %) at 25-170 °C temperature for 1 h (Table 3.8).

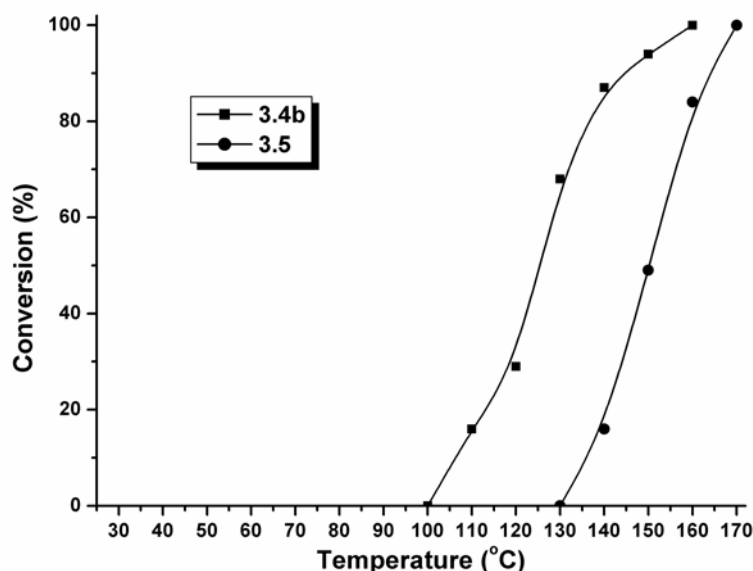
Table 3.8: Polymerization of GPE using xanthenyltri-*n*-butylphosphonium salt (**3.5**)^a

Initiator	Temperature (°C)	Conversion ^b (%)	M _n ^c	M _w /M _n
3.5	130	0		
	140	18	2600	1.4
	150	39	2500	1.4
	160	78	2800	1.4
	170	87	3000	1.4
	180	100	3100	1.5

^aConditions; initiator 1 mol % vs. GPE for 1 h. ^bDetermined by ¹H NMR.

^cDetermined by GPC based on polystyrene standards.

It can be seen that the conversion is started above 100 and 130 °C with **3.4b** and **3.5**, respectively to afford the polymer with molecular weight (M_n) of 2600-3100.

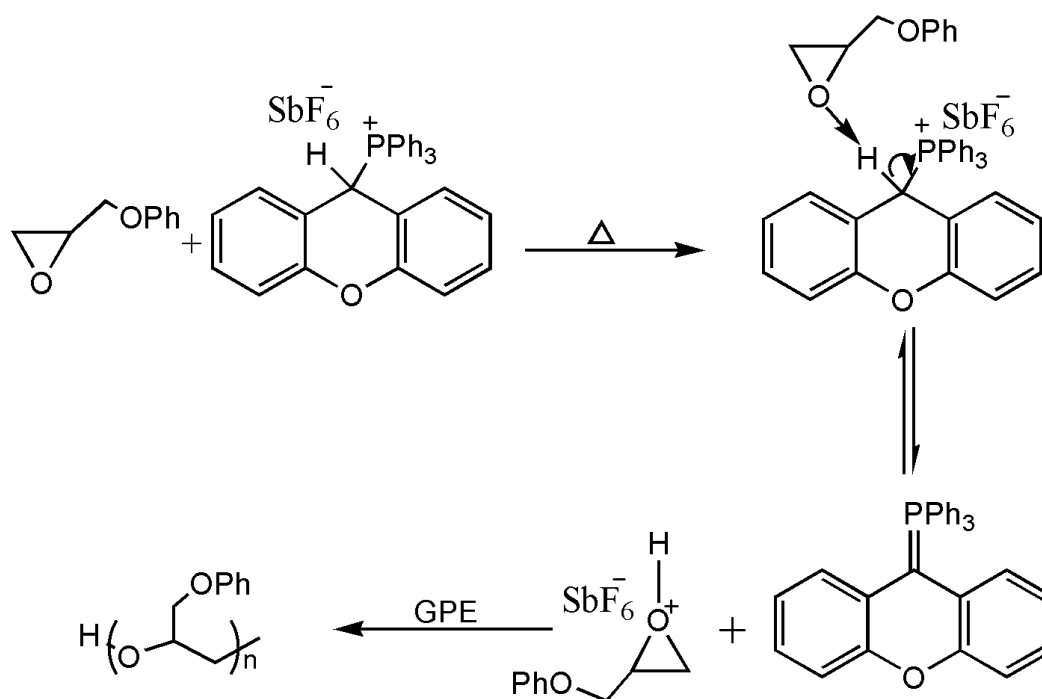
**Figure 3.31:** Effect of temperature on polymerization with **3.4b** and **3.5** for 1 h.

With the increase in polymerization temperature, the conversion (%) increases with different rates. The maximum conversion (100 %) has been found with **3.4b** and **3.5** at 160 °C and 170 °C, respectively. The order of initiator activity was observed as **3.4b** > **3.5**. It can be attributed to the fact that the acidity of methine proton, which is higher for **3.4b** than **3.5**. The increase in acidity of methine proton in **3.4b** can be explained by – I effect of

three phenyl rings of phosphine moiety, whereas + I effect of butyl groups in **3.5** decrease the acidity of methine proton. This phenomenon is supported by chemical shift of methine proton of xanthenyl phosphonium salts **3.4b** and **3.5** at 7.05 and 5.69 ppm in ^1H NMR, respectively. In addition, the higher reactivity of **3.4b** can also be attributed to the formation of more stable ylide on thermal initiation. The stability of ylide can be explained by extended conjugation of three phenyl rings of triphenyl phosphine with xantheno nucleus compare to *n*-butyl groups [37,38].

3.3.3.1.3. Polymerization mechanism

Based on the literature of phosphonium salts [20,26], it is assumed that the initiating species in the present system could be methine protons, beside formation of phosphonium ylide (Scheme 3.6).



Scheme 3.6: Mechanism of GPE polymerization

It suggests that on thermal initiation, phosphonium salt undergo thermal cleavage of methine C-H bond in presence of GPE and generates oxonium cation, which further propagates the chain polymerization. To confirm this mechanism through formation of

ylide, a Wittig reaction of **3.4b** with sodium hydride in tetrahydrofuran (THF) was performed at ambient temperature. The appearance of red color during the reaction indicates formation of ylide, which was found to be unstable under ambient condition. To this reaction mixture benzaldehyde was added and stirred overnight, which gives a yellow color solid, alkene (9-Benzylidene-9H-xanthene), whose structure was confirmed by ^1H NMR spectrum (Figure 3.32).

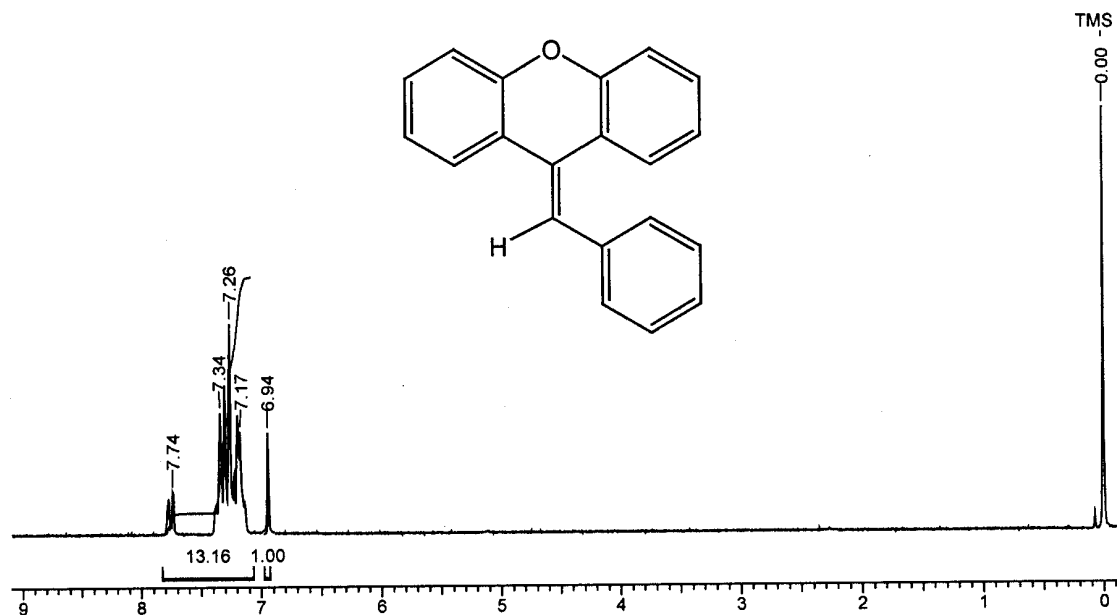


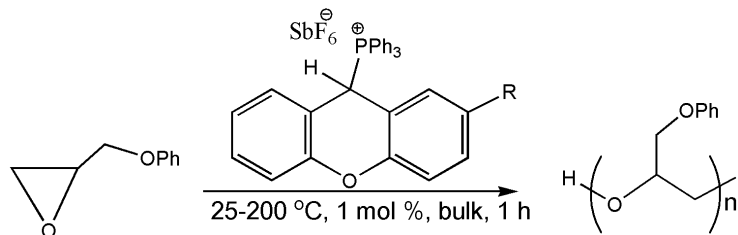
Figure 3.32: ^1H NMR spectrum of 9-benzylidene-9H-xanthene

Therefore, the methine proton can be regarded as the initiation species.

3.3.4. Cationic polymerization of epoxides using substituted xanthenyl phosphonium salts as thermo-latent initiator

3.3.4.1. Polymerization of GPE

The bulk polymerization of GPE was carried out with 1 mol % of initiator (**3.4b**, **3.6d**, **3.7d** and **3.8d**) in 25-200 °C temperature range for 1 h (Scheme 3.7, Table 3.9).



R = Cl, H, Me, OMe

Scheme 3.7: Polymerization of GPE with 2-substituted xanthenyltriphenylphosphonium hexafluoroantimonate

The effect of substituents on initiator activity was rationalized by monitoring monomer conversion as a function of reaction temperature (Figure 3.33).

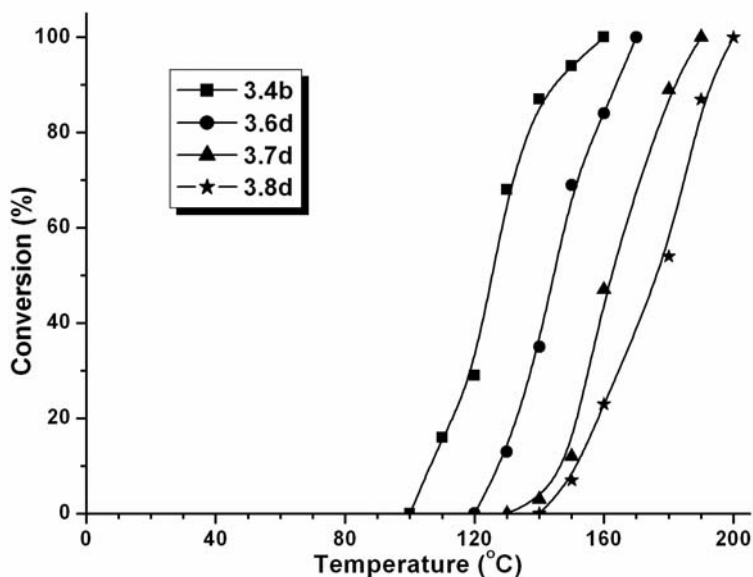


Figure 3.33: Temperature - conversion curve in GPE polymerization

It shows the effect of substituents on initiator activity, which exhibit that the conversion (%) increases with the increase in reaction temperature. GPE undergoes polymerization with **3.4b**, **3.6d**, **3.7d** and **3.8d** above 100, 120, 130 and 140 °C, respectively. For the above-mentioned initiators, the rate of polymerization increases faster after the corresponding threshold temperature of initiation to afford the polymer with M_n of 2100-3400. A quantitative conversion with **3.4b**, **3.6d**, **3.7d** and **3.8d** was observed at 160, 170, 190 and 200 °C, respectively. The order of initiator activity was found as **3.4b** > **3.6d** > **3.7d** > **3.8d**.

Table 3.9: Polymerization of GPE with 2-substitutedxanthenylphosphonium salts ^a

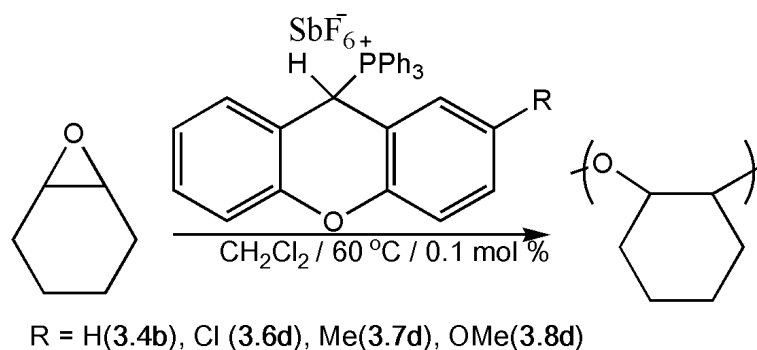
Initiator	Temperature (°C)	Conversion^b (%)	M_{n,SEC}^c	M_w/M_n
3.4b	100	0		
	110	16	2500	1.3
	120	29	2600	1.4
	130	68	3100	1.4
	140	87	3200	1.4
	150	94	3400	1.4
	160	100	3400	1.5
3.6d	120	0		
	130	13	2600	1.4
	140	35	3000	1.4
	150	69	2900	1.4
	160	84	3100	1.5
	170	100	3100	1.6
3.7d	130	0		
	140	3	2100	1.3
	150	12	2300	1.4
	160	47	2700	1.4
	180	89	2900	1.5
	190	100	3000	1.5
3.8d	140	0		
	150	7	2300	1.2
	160	23	2200	1.3
	180	54	2600	1.4
	190	87	2500	1.4
	200	100	2500	1.5

^aConditions; initiator 1 mol % vs. GPE for 1 h. ^bDetermined by ¹H NMR. ^cDetermined by GPC based on polystyrene standards.

This order of activity can be explained by electronic effect of substituents in the xanthenyl ring of phosphonium salts. This trend is similar to the observation by Endo et al. [30]. Additionally, the change in ^1H NMR chemical shift [39] of xanthenyl methine proton and ^{31}P NMR chemical shift [40] of phosphine in phosphonium salts supports the order of initiator activity. According to δ values of methine proton, **3.6d** must be initiator with highest activity but **3.4b** exhibit highest activity. For the reduced activity of **3.6d** compared to **3.4b**, may be ascribed to the combined effect of steric hindrance caused by the monomer and the bulkiness of chloro-substituent on xanthenyl ring [30].

3.3.4.2. Polymerization of CHO

To understand the steric effect of monomer on initiator activity, polymerization of CHO was performed with phosphonium salts (0.1 mol %) in CH_2Cl_2 solvent at 60°C for 1 and 5 h (Scheme 3.8, Table 3.10).



Scheme 3.8: Polymerization of CHO with 2-substituted xanthenyltriphenyl phosphonium hexafluoroantimonate

Table 3.10: Polymerization of CHO with 2-substituted xanthenylphosphonium salts^a

Initiator	Conversion (%)		$M_{n,SEC}$ ^b		M_w/M_n	
	1 h	5 h	1 h	5 h	1 h	5 h
3.4b	25	55	25,600	1,10,000	2.35	2.81
3.6d	37	72	26,500	1,16,000	2.21	2.55
3.7d	11	23	15,900	40,100	1.85	1.87
3.8d	7	19	13,300	31,300	1.70	1.72

^aConditions; initiator 0.1 mol % vs. GPE for 1 h. ^bDetermined by GPC based on polystyrene standards.

The order of reactivity was found as **3.6d** > **3.4b** > **3.7d** > **3.8d**. However CHO attains the substantial percentage conversion after 5 h. The molecular weight of polymer was found comparatively higher than GPE due to higher polymerizability of CHO. This can be explained by stability of resulting cyclohexyl cation during polymerization and more nucleophilicity of the CHO monomer due to its restricted conformation^[41]. The polymerization results with CHO also supports that steric effect of monomer alters the order of initiator activity in GPE polymerization.

3.4. Conclusions

The novel thermo latent phosphonium salts based on dibenzosuberene and xanthen nucleus were synthesized to study the effect of reactivity factor (such as counter anion, phosphine moiety and ring structure) on initiator activity. The order of reactivity with respect counter anion with the dibenzosuberene nucleus was observed as **3.1b** > **3.1e** > **3.1c** > **3.1d** whereas with the xanthen nucleus is observed as **3.4b** > **3.4c** > **3.4d** > **3.4e**. The higher activity of **3.1e** over **3.1c** and **3.1d** may be explained by more acidity of methine proton of C-H bond, which is supported by single crystal X-ray data. The triphenylphosphine based phosphonium salts were found more active compare to tri-*n*-butyl phosphonium salts in the both cases. Dibenzosuberenyli tri-*n*-butylphosphonium salt (**3.2**) and xanthenyl tri-*n*-butylphosphonium salt (**3.5**) exhibit similar activity in polymerization of GPE. The dibenzosuberenyli triphenylphosphonium salt (**3.1b**) having

double bond in ring shows more reactivity compare to dibenzosuberyltriphenyl phosphonium salts (**3.3**) in low conversion region and similar reactivity in high conversion region. The effect of substituents on initiator activity was studied with 2-substituted (Cl, H, Me and OMe) xanthenyltriphenylphosphonium hexafluoroantimonate in polymerization of GPE. The order of activity was observed as **3.4b** > **3.6d** > **3.7d** > **3.8d**. This order of reactivity increases with electron withdrawing substituents on xanthenyl nucleus. To study the effect of steric factor on initiator activity, polymerization of CHO was studied and the order of activity was observed as **3.6d** > **3.4b** > **3.7d** > **3.8d**. All the initiators are latent at ambient temperature and initiate cationic polymerization on thermal initiation. The thermal stability, solubility in various organic solvents and epoxy monomers and the resistance toward air and moisture make these initiators as worthy latent thermal cationic initiator. Therefore, it may be concluded that having different structural parameters in initiator, the activity of initiator can be controlled. This work may contribute in design of more active initiators with varied reactivity.

3.5. References

1. H. Lee, K. Neville, *Handbook of Epoxy Resins*; McGraw-Hill, New York, **1967**.
2. H. F. Mark, N. G. Gaylord, N. M. Bikajes, *Encyclopedia of Polymer Science and Technology*; Eds; Interscience: New York, **1968**, 8, 303.
3. Y. Yagci, I. Reetz, *Prog. Polym. Sci.* **1998**, 23, 1485.
4. Y. Yagci, T. Endo, *Adv. Polym. Sci.* **1997**, 127, 59.
5. Y. C. Kim, S. J. Park, J. R. Lee, *Polym. J.* **1997**, 29, 759.
6. M. K. Gupta, R. P. Singh, *Macromol. Symp.* **2006**, 240, 186.
7. S. Murai, Y. Nakano, S. Hayase, *J. Appl. Polym. Sci.* **2001**, 80, 181.
8. S. J. Park, G. Y. Heo, *Macromol. Chem. Phys.* **2005**, 206, 1134.
9. J. V. Crivello, T. P. Lockhart, J. L. Lee, *J. Polym. Sci. Polym. Chem.* **1983**, 21, 97.
10. K. Morio, H. Murase, T. Tsuchiya, T. Endo, *J. Appl. Polym. Sci.* **1986**, 32, 5727.
11. O. Shimomura, I. Tomita, T. Endo, *J. Polym. Sci Part A: Polym Chem.* **2000**, 38, 18.
12. O. Shimomura, I. Tomita, T. Endo, *J Polym Sci Part A: Polym Chem.* **1999**, 38, 127.
13. O. Shimomura, I. Tomita, T. Endo, *Macromol. Rapid. Commun.* **98**, 19, 493.
14. S. B. Lee, T. Takata, T. Endo, *Macromolecules* **1990**, 23, 431.
15. S. B. Lee, T. Takata, T. Endo, *Macromolecules* **1991**, 24, 2689.
16. S. Nakano, T. Endo, *J. Polym. Sci. Part A Polym. Chem.* **1996**, 34, 475.
17. S. Nakano, T. Endo, *J. Polym. Sci. Polym. Chem.* **1995**, 33, 505.
18. T. Endo, F. Sanda, *Macromol. Symp.* **1996**, 107, 237.
19. M. S. Kim, S. B. Lee, K. W. Lee, T. Endo, *J. Appl. Polym. Sci.* **2005**, 95, 1439.
20. K. Takuma, T. Takata, T. Endo, *Macromolecules* **1993**, 26, 862.

21. H. Kim, F. Sanda, Y. Nakamura, T. Endo, *Macromol. Chem. Phys.* **2000**, 201, 1691.
22. H. Kim, F. Sanda, T. Endo, *Macromolecules* **2000**, 33, 2359
23. H. Kim, F. Sanda, T. Endo, *Macromolecules* **1999**, 32, 8291.
24. S. D. Lee, T. Takata, T. Endo, *Macromolecules* **1996**, 29, 3317.
25. T. Hino, T. Endo, *J. Polym. Sci. Part A: Polym. Chem.* **2004**, 42, 2162.
26. T. Toneri, F. Sanda,; T. Endo, *J Polym Sci Part A: Polym Chem.* **1998**, 36, 1957.
27. M. Kim, F. Sanda, T. Endo, *J. Appl. Polym. Sci.* **2001**, 81, 2347.
28. H. Morikawa, A. Sudo, H. Nishida, T. Endo, *J. Appl. Polym. Sci.* **2005**, 96, 372.
29. T. Toneri, K. Watanabe, F. Sanda, T. Endo, *Macromolecules* **1999**, 32, 1293.
30. T. Toneri, F. Sanda, T. Endo, *Macromolecules* **2001**, 34, 1518.
31. W. L. F. Armarego, D. D. Perrin, *Purification of Organic Chemicals*, 4th ed, Butter Worth-Heinemann, Lineacre House, Jordon Hill, Oxford OX2 8 DP.
32. R. F. Pellon, R. Carrasco, V. Milian, L. Rodes, *Synth. Commun.* **1995**, 25, 1077.
33. M. Pickert, A. W. Frahm, *Arch Pharma, Pharm. Med. Chem.* **1998**, 331, 177.
34. F. Hamanzu, S. Akashi, T. Koizumi, T. Takata, T. Endo, *Macromol. Chem. Rapid. Commun.* **1992**, 13, 203.
35. Brüker (**2003**). SADABS (Version 2.05), SMART (Version 5.631), SAINT (Version 6.45) and SHELXTL (Version 6.14). Brüker AXS Inc., Madison, Wisconsin, USA.
36. G. M. Sheldrick, SHELXL97: University of Göttingen, Germany **1997**.
37. L. Meriwether, M. L. Fiene, *J. Am. Chem. Soc.* **1959**, 81, 4200.
38. A. Jonson, R. B. LaCount, *Tetrahedron*, **1960**, 9, 130.
39. The δ values of xanthenyl methine proton in ^1H NMR spectra were observed with 3.4b, 3.6d, 3.7d and 3.8d at 7.04, 7.05, 6.94 and 6.70 ppm in DMSO- d_6 , respectively.
40. The δ values of phosphine in ^{31}P NMR spectra were observed at 21.42 ppm with 3.4b, at 21.72 and 25.67 ppm with 3.6d, at 21.14 and 25.88 ppm with 3.7d and at 20.99 and 25.67 ppm with 3.8d.
41. B. Ottar, *Acta Chem Scand* **1947**, 1, 283.

Chapter 4: Photo chemically and thermally induced radical promoted cationic polymerization using allylic phosphonium salts as initiators

4.1. Introduction

In last few decades, importance of latent cationic initiators, which show activity by external stimulation such as heat or light, has been recognized in number of different industrial applications such as microelectronics, photolithography, curing and adhesives ^[1]. Many technologically important monomers such as vinyl ether and cyclic oxiranes, are polymerizable in cationic mode, therefore, development of more efficient photo and thermal latent cationic initiators are desirable ^[2-7]. Photo polymerization by direct initiation of a general onium salts can be performed below 290 nm. This limits its potential use in the cationic polymerization mainly, when visible light-emitting sources are used. To overcome this problem, several indirect pathways such as radical sources ^[8-11], photosensitizers ^[12-16] and electron-donating compounds ^[17] in combination with onium salts were proposed and extensively studied. Among these, the use of free radical sources in combination of allylic onium salt is an easy and flexible way to generate active species for cationic polymerization. The attractive features of this technique involve availability of suitable radical sources with wide range of absorption characteristics and temperature, which have been successfully utilized in free radical promoted cationic polymerization. In such system, radical source undergoes fragmentation and generates free radicals (photo or thermally), which add to the double bond of allylic onium salts and produce radical cation as initiating species ^[7]. Yagci et al have employed various allylic onium salts such as sulfonium salts ^[18-19], pyridinium salts ^[20], allyloxy pyridinium salts ^[21-22], anilinium ^[23] salts etc for cationic polymerization. Earlier, Yagci et al have developed acrylates based on allylic phosphonium salts as photo and thermo-latent initiators in the cationic polymerization ^[24]. To the best of our knowledge, the chemistry of amide based phosphonium salt, as an addition fragmentation agent in thermally and photo-chemically initiated cationic polymerization has not been studied. The present chapter describes the

synthesis of novel amide based phosphonium salts and examines their efficiency as an addition fragmentation agent in the combination of radical (photo and thermal) sources in the cationic polymerization.

4.2. Experimental

4.2.1. Materials

N, N-Dimethylacrylamide, acryloylmorpholine, cyclohexene oxide (CHO), isobutyl vinyl ether (IBVE), *n*-butyl vinyl ether (*n*-BVE), glycidyl phenyl ether (GPE) and N-vinyl carbazole (NVC) were purchased from Aldrich chemicals. All other chemicals (> 99 %) were purchased from S.D. Fine Chemicals Ltd, Mumbai, India. Monomers (CHO, IBVE, *n*-BVE and GPE) and solvent (CH₂Cl₂) were distilled over CaH₂ and used just before polymerization. Triphenyl phosphine (Ph₃P) was recrystallized from *n*-hexane. NVC, AIBN, benzoin and benzophenone were recrystallized from ethanol. 2,4,6-trimethylbenzoyl biphenyl phosphine oxide (TMDPO) and benzoyl peroxide (BPO) were recrystallized from diethyl ether.

4.2.2. Phenyl azotriphenylmethane (PAT) ^[25]

In a 100 mL round bottom flask, a solution of triphenylchloromethane (2.84 g, 10 mmol) and phenyl hydrazine (2.17 mL, 22 mmol) in anhydrous diethylether (50 mL) was allowed to reflux for 2 h. The reaction mixture was cooled to ambient temperature and resulting precipitate was filtered and the solution was evaporated under vacuum. The residue was dissolved in benzene to remove the remaining phenyl hydrazine hydrochloride and the solution was filtered. The filtrate was evaporated under vacuum and the resulting slurry was dissolved in 20 mL of diethyl ether. To this solution, a mixture of 20 mL NaHCO₃ and 5 mL of 30 % H₂O₂ was added and this two-phase mixture was stirred at ambient temperature for 3 h. Later, a solution of 0.1 N Cu(II)SO₄ (1 mL) was added to catalyze the reaction and stirred overnight. The ether layer was washed with water, dried over Na₂SO₄ and evaporated under vacuum. The pale orange color compound was crystallized three times with dichloroethane/ethanol.

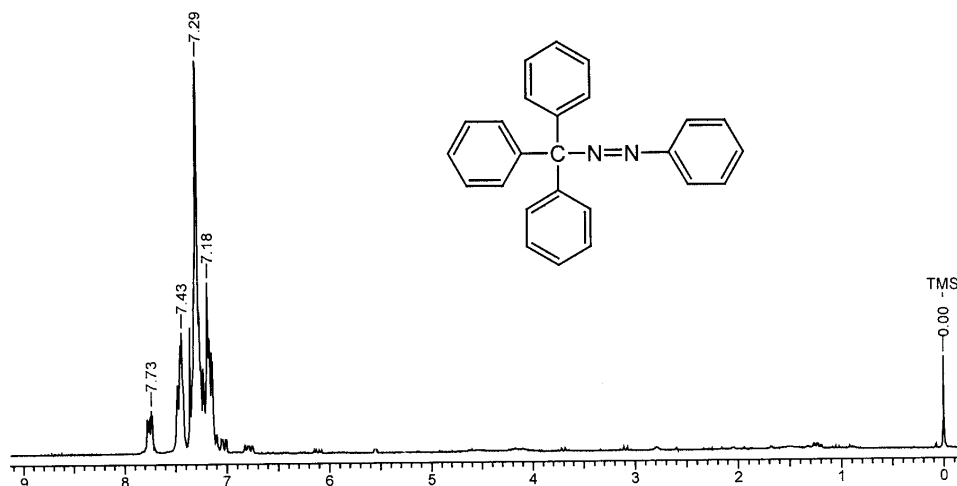


Figure 4.1: ^1H NMR spectrum of phenyl azotriphenyl methane (PAT)

Yield: 1.2 g (35 %), mp. 110-111 °C, Elemental analysis Cal for: $\text{C}_{25}\text{H}_{20}\text{N}_2$ (348.17 g mol $^{-1}$) C, 86.17 %; H, 5.79 %; Found: C, 85.89 %; H, 5.63 %; ^1H NMR (CDCl_3) δ = 6.70-7.80 (Ph) ppm.

4.2.3. 2-(Bromomethyl)-N, N-dimethyl acryl amide (BMDMA) ^[26]

In 250 mL round bottom flask, paraformaldehyde (19.52 g, 650 mmol), DABCO (15.04 g, 130 mmol) and phenol (3.06g, 32.50 mmol) were placed and flask was fitted with a septum and degassed for 15 min. A *t*-BuOH/ H_2O (3:7) solvent mixture (8.10 mL) and N, N-dimethyl acrylamide (13.42 mL, 130 mmol) was added to the flask via syringe. The resulting mixture was stirred for 24 h at 80 °C. The reaction mixture was allowed to cool up to ambient temperature and water from reaction mixture was removed with toluene under vacuum. The reaction mixture was then filtered over celite with CH_2Cl_2 and concentrated under vacuum. The crude compound was purified by column chromatography (AcOEt/EtOH 8:2, R_f = 0.30), which afforded the crude alcohol (22.56 g, 130 mmol, about 100 %). The alcohol was subsequently dissolved in dry diethyl ether (100 mL) in a 500 mL round bottom flask equipped with a magnetic stirring under nitrogen pressure. DMF (100 mL) was added to the reaction flask and cooled to -5 °C. A solution of PBr_3 (6.12 mL, 65 mmol) in dry diethyl ether was added and stirred overnight at ambient temperature. The light orange color reaction mixture was quenched by hydrolysis with 100 mL of H_2O . The

aqueous layer was separated and extracted with ethyl acetate (3 x 100 mL). The organic layers were combined and washed with H₂O (5 x 125 mL) to remove DMF. Then, the combined organic layer was dried over Na₂SO₄ and concentrated in vacuum. The purification by column chromatography afforded as a colorless liquid. Yield: 3.42 g (27 %), IR (CHCl₃): 2933, 1643, 1613, 1500, 1390, 1212, 1144, 1102, 935, ¹H NMR (CDCl₃): δ = 5.57 (s, 1H, =CH₂), 5.21 (s, 1H, =CH₂), 4.23 (s, 2H, Br-CH₂), 3.15 (s, 3H, N-CH₃), 3.04 (s, 3H, N-CH₃) ppm.

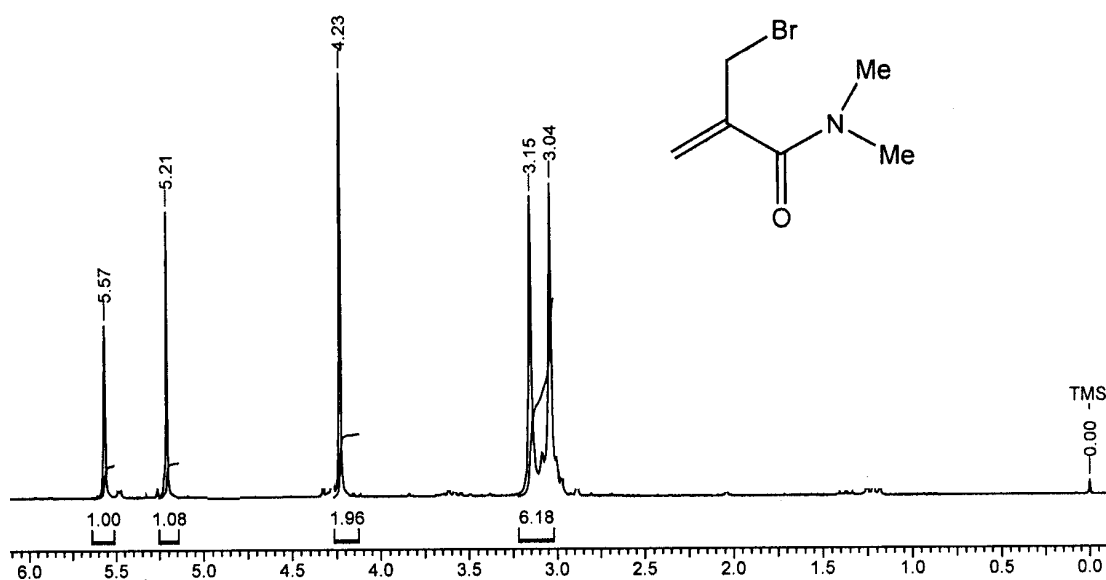


Figure 4.2: ¹H NMR spectrum of 2-(bromomethyl)N,N-dimethyl acrylamide (**BMDMA**)

4.2.4. 2-(Bromomethyl) acryloyl morpholine (**BMAM**)

This compound was synthesized in the similar manner as described for **BMDMA**. Yield: 3.42 g (34 %), IR (CHCl₃): 2933, 1643, 1613, 1500, 1390, 1212, 1144, 1102, 935, ¹H NMR (CDCl₃): δ = 5.55 (s, 1H, =CH₂), 5.15 (s, 1H, =CH₂), 4.23 (s, 2H, Br-CH₂), 3.71 (s, 8H, N-CH₂, O-CH₂) ppm.

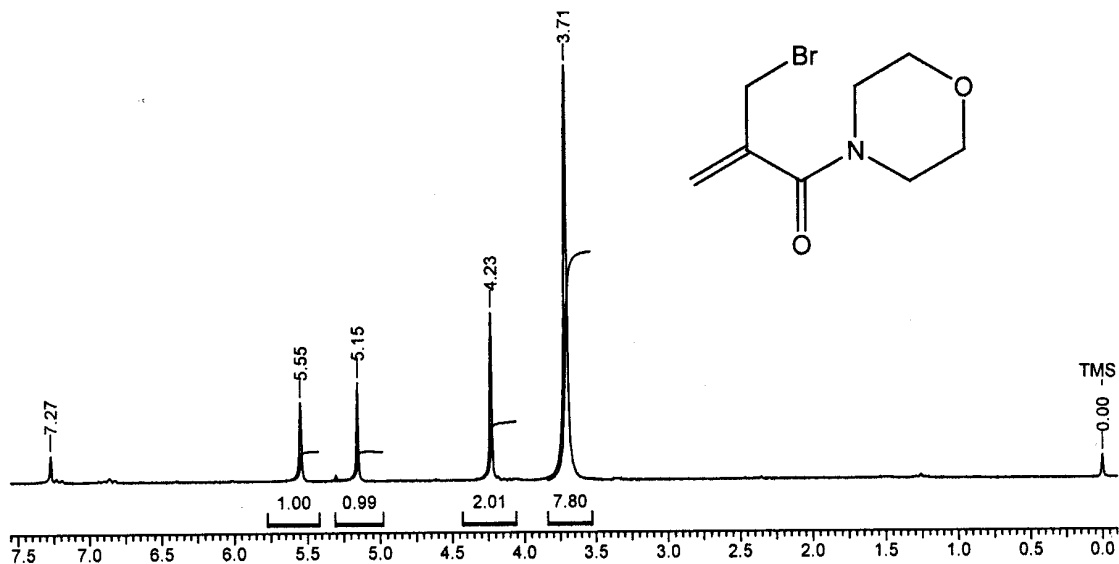


Figure 4.3: ¹H NMR spectrum of 2-(bromomethyl)-acryloyl morpholine (**BMAM**)

4.2.5. 2-(N, N-Dimethylcarboxy-propenyl) triphenylphosponium hexafluoroantimonate (**DMTPH**)

To a solution of Ph₃P (5 mmol, 1.31 g) in toluene (10 mL), 2-(bromomethyl)- N, N-dimethyl acrylamide (**BMDMA**) (5 mmol, 1.04 g) was added and allowed to stir for 1 h. The resulting white precipitate was dissolved in H₂O and washed with petroleum ether. Finally, NaSbF₆ was added to the aqueous part in one portion.

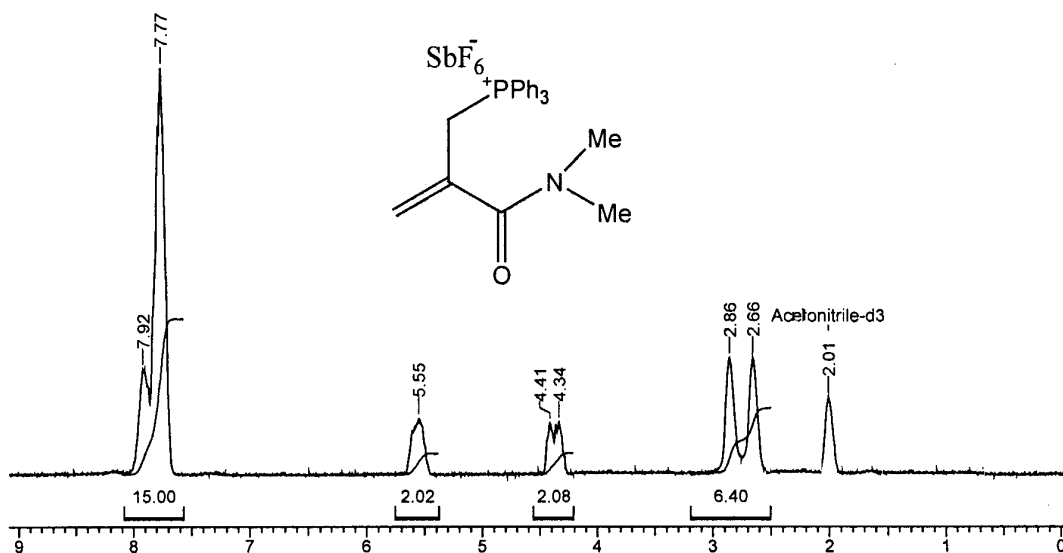


Figure 4.4: ¹H NMR spectrum of 2-(N, N-dimethylcarboxy-propenyl) triphenyl phosphonium hexafluoroantimonate (**DMTPH**)

The resulting white precipitate was filtered, washed with water and dried under vacuum. Yield: 2.2 g (77 %), white crystals, Elemental analysis cal for: $C_{24}H_{25}NOPSbF_6$ (609.06 g mol^{-1}) C, 47.24 %; H, 4.13 %; N, 2.30 % Found: C, 47.15 %; H, 4.16 %; N, 2.27 %, IR (KBr): 3457, 3400, 3085, 3055, 2911, 2972, 1611, 1586, 1489, 1438, 1110, 960 cm^{-1} , 1H NMR (CD_3CN): δ = 7.6-8.1 (m, 15 H, Ph), 5.55 (s, 2 H, CH_2), 4.41, 4.34 (s, 2H, $=CH_2$), 2.86, 2.66 (s, 3H, $-NCH_3$) ppm.

4.2.6. 2-(Morpholinocarboxy-propenyl) triphenylphosponium hexafluoroantimonate (MTPH)

This compound was synthesized in the similar manner as described for **DMTPH**.

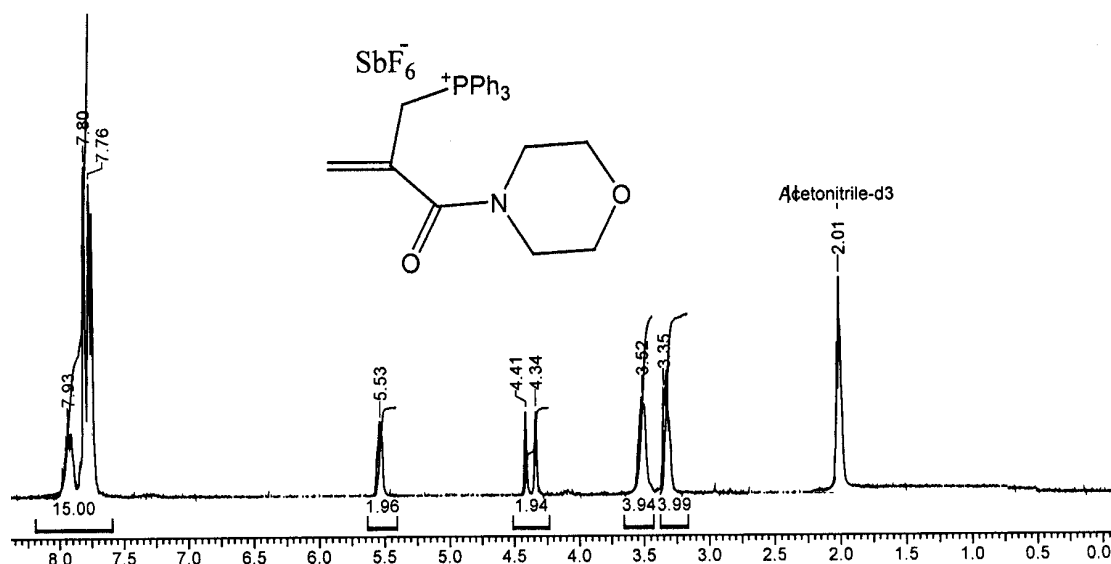


Figure 4.5: 1H NMR spectrum of 2-(morpholinocarboxy-propenyl) triphenylphosponium hexafluoroantimonate (**MTPH**)

Yield: 2.8 g (79 %), white crystals, Elemental analysis Cal for: $C_{26}H_{27}NO_2PSbF_6$ (651.07 g mol^{-1}): C, 47.88 %; H, 4.17 %; N, 2.15 %, Found: C, 47.75 %; H, 4.16 %; N, 2.11 %, IR (KBr): 3408, 3050, 2951, 2863, 1640, 1520, 1480, 1460, 1265, 1208, 1114, 997 cm^{-1} , 1H NMR (CD_3CN): δ = 7.6-8.1 (m, 15 H, Ph), 5.53 (s, 2H, CH_2), 4.41, 4.34 (s, 2H, $=CH_2$), 3.52 (t, 4H, $-NCH_2$), 3.35 (t, 4H, $-OCH_2$) ppm.

4.2.7. Characterization

Molecular weight of polymers was measured by gel permeation chromatography (GPC) in chloroform as eluent (flow rate: 1 mL/min) on a setup consisting of a pump and six Ultra Styragel column (50 to 10^5 Å porosities) and detection was carried out with the aid of UV-100 and RI-150 detectors. Molecular weight (M_n) and polydispersities (M_w/M_n) were determined using a calibration curve obtained by polystyrene standards. NMR spectra were recorded on a Brüker 200 MHz instrument with $CDCl_3$ and acetonitrile (for initiators) as solvent and tetramethylsilane as internal standard. IR spectra were recorded on a Perkin-Elmer model 683 grating IR spectrometer. Elemental analysis was performed on a Thermo Finnigan Flash EA-1112 Microanalyser instrument. The UV spectra were recorded on Perkin-Elmer UV spectrophotometer. Irradiated solution was analyzed by gas chromatography (Varian CP-3800 GC) in conjugation with mass spectroscopy (Varian Saturn 2200 GC/MS).

4.2.8. Polymerization procedure

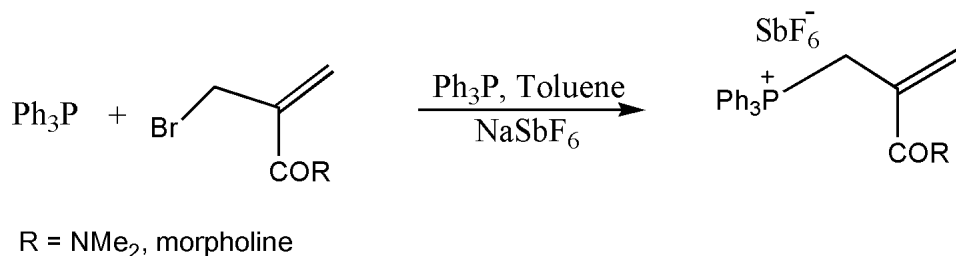
A mixture of monomer and initiator (with or without radical source) was placed in a flame dried ampoule equipped with three way stopcock connected to manifold and degassed for 30 min with three freeze-pump-thaw cycles and sealed off. The ampoule was immersed in an oil bath at constant temperature. Photo polymerization was performed in similar way to thermal polymerization except Pyrex test tubes were employed and reaction mixture was irradiated with 450 W medium pressure mercury lamp with quartz-jacket. After reaction for set time, the polymerization mixture was dissolved in DCM and precipitated with excess methanol then dried under vacuum at ambient temperature. The percentage conversion was determined by gravimetrically.

4.3. Results and discussion

4.3.1. Initiator synthesis

The allylic phosphonium salts (**DMTPH** and **MTPH**) used in this study were synthesized by reaction of corresponding allyl bromide with triphenylphosphine (Ph_3P) followed by anion exchange of bromide (Br^-) with hexafluoroantimonate (SbF_6^-) anion. The structure of

initiators was identified by ^1H NMR, IR and elemental analysis as described in the experimental section (Scheme 4.1).



Scheme 4.1: Synthesis of amide based allylic phosphonium salts

Both the initiators were found to be stable to air and moisture. None of the salt exhibits absorption at wavelength above 300 nm (Figure 4.6).

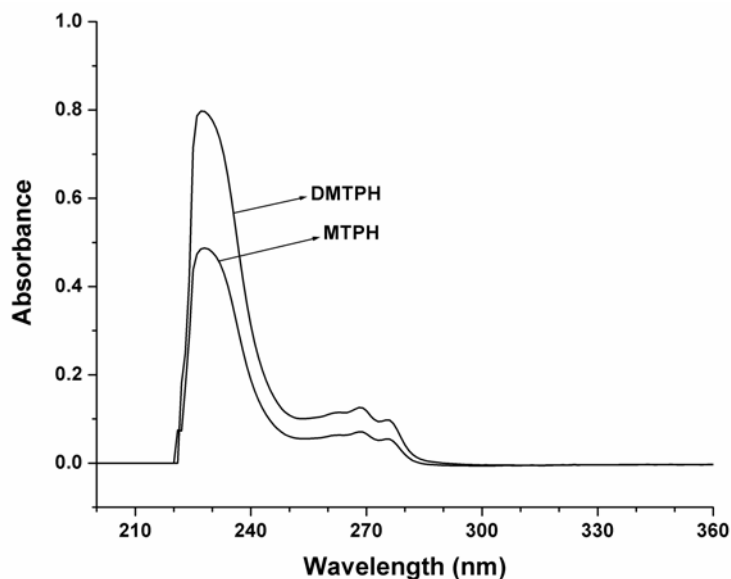


Figure 4.6: UV absorption spectrum of phosphonium salts in CH₂Cl₂ solvent

4.3.2. Polymerization

For the polymerization reactions, CHO was used as model monomer for cationic polymerization with phosphonium salts due to non-polymerizable nature of CHO using free radicals.

4.3.2.1. Thermal polymerization of CHO

4.3.2.1.1. Polymerization in the absence of radical sources

Figure 4.7 shows, temperature-conversion curve for polymerization of CHO in absence of added free radical source. It can be seen that the polymerization with both initiators proceed above 90 °C and reaches to 100 % conversion at 130 °C. It is assumed that in this case, radicals are formed by thermal decomposition of the phosphonium salts. This assumption is supported by fact that no polymerization of CHO is observed with benzyltriphenylphosphonium salt at 120 °C [24].

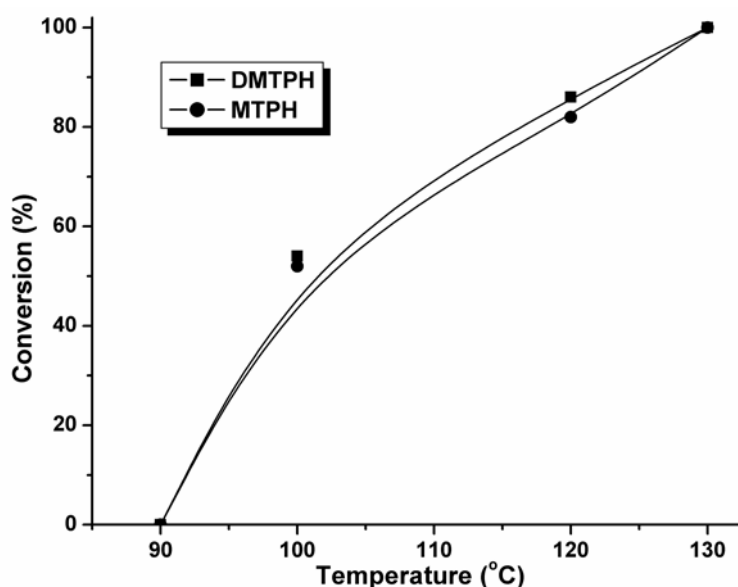


Figure 4.7: Temperature-conversion curve in polymerization of CHO with allylic phosphonium salts in the absence of radical sources.

4.3.2.1.2. Polymerization in the presence of radical sources

The bulk polymerization of CHO was performed with 0.1 mol % of phosphonium salt initiators (**DMTPH** and **MTPH**) in the presence of free radical sources (namely **AIBN**, **BPO** and **PAT**) at 70 °C up to 2 h (Table 4.1). Figure 4.8 shows the time-conversion curve for the polymerization of CHO with **DMTPH** in the presence of thermal radical source (**AIBN**, **BPO** and **PAT**). It can be seen that with increasing in reaction time, polymerization of CHO proceeds with each phosphonium salt/radical source combination and attains respective limiting conversion.

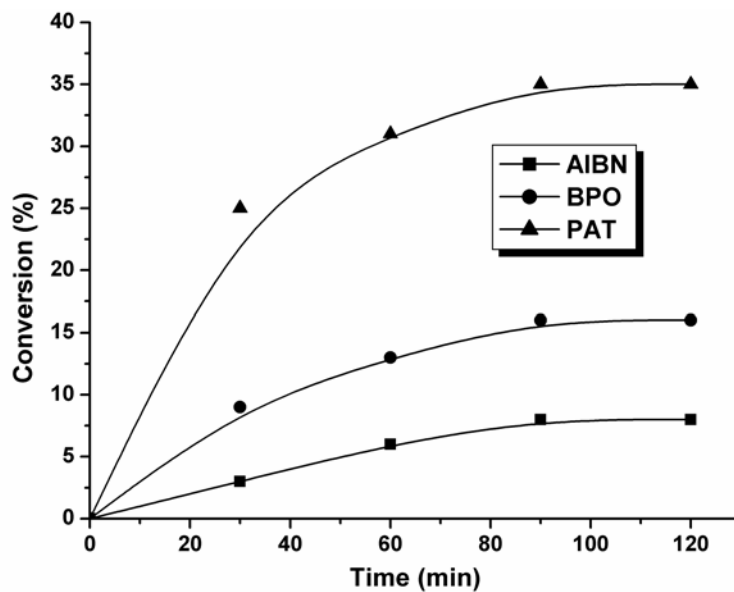


Figure 4.8: Time-conversion curve in polymerization of CHO with **DMTPH** in the presence of radical sources at 70 °C [CHO: initiator: radical source = 5 mol l⁻¹ : 5 x 10⁻³ mol l⁻¹ : 5 x 10⁻³ mol l⁻¹]

Table 4.1: Thermal polymerization of CHO initiated at 70 °C by thermal radical sources ^a

Initiator	Radical source	Time	Conversion ^b	M _n (M _w /M _n) ^c
		(min)	(%)	
DMTPH	PAT	60	30	5600 (1.69)
	BPO	120	16	6766 (1.94)
	AIBN	120	8	6600 (1.84)
MTPH	PAT	60	27	6000 (1.79)
	BPO	120	16	6900 (1.81)
	AIBN	120	7	8200 (1.62)

^aConditions; monomer: initiator: radical source = 5 mol l⁻¹ : 5 x 10⁻³ mol l⁻¹ : 5.0 x 10⁻³ mol l⁻¹, ^bdetermined gravimetrically, ^cdetermined by GPC based on polystyrene standards.

The limiting conversion with **PAT**, **BPO** and **AIBN** was found as 35 (60 min), 16 (120 min) and 8 (120 min), respectively. The order of initiator activity was observed as **PAT** > **BPO** > **AIBN**.

Figure 4.9 shows the time-conversion curve for the polymerization of CHO with **MTPH** in the presence of radical sources (Table 4.1). It also shows an increase in percentage conversion with the increase in reaction time. The limiting conversion with **PAT**, **BPO** and

AIBN was found as 31 (60 min), 16 (120 min) and 7 (120 min), respectively. The order of initiator activity was observed as **PAT** > **BPO** > **AIBN**. This can be explained by the difference in the decomposition rate constant and the reactivity of radical toward the double bond of phosphonium salts ^[27].

The molecular weight (M_n) of polymer was found in the range of 5600-8200. The above results suggest that in presence of radical source, the polymerization rate of CHO can be enhanced, whereas no polymerization was observed in the absence of radical sources even at 90 °C.

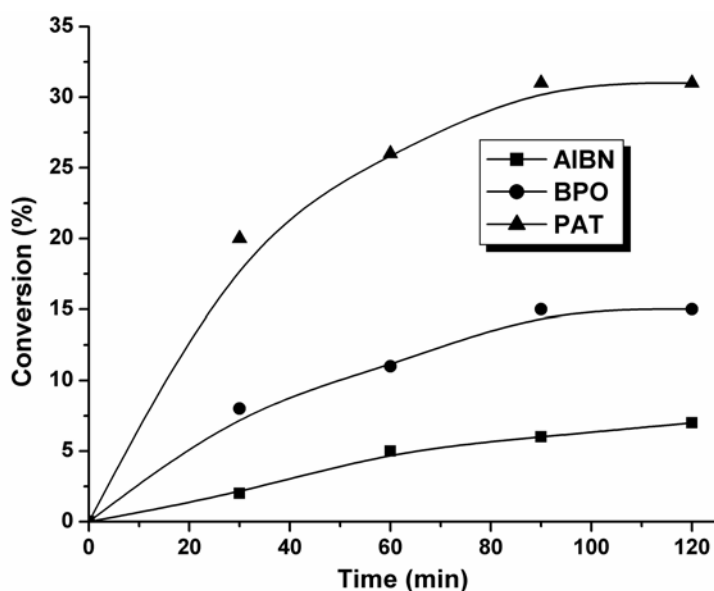


Figure 4.9: Time-conversion curve in polymerization of CHO with **MTPH** in presence of radical sources at 70 °C [CHO: initiator: radical source = 5 mol l⁻¹: 5 x 10⁻³ mol l⁻¹: 5 x 10⁻³ mol l⁻¹]

4.3.2.2. Photo polymerization of CHO

4.3.2.2.1. Polymerization in the absence of radical source

In the absence of radical sources, the photolysis of a solution containing CHO and **DMTPH** at $\lambda < 290$ nm failed to produce any polymer.

4.3.2.2.2. Polymerization in the presence of radical source

The polymerization of CHO was performed with 0.1 mol % of phosphonium salts in presence of added photo free radical sources namely **benzophenone**, **TMDPO** and **benzoin** at $\lambda > 290$ nm whereas phosphonium salts do not absorb. Table 4.2 shows the

results of polymerization of CHO with free radical sources (**benzophenone**, **TMDPO** and **benzoin**).

Table 4.2: Photopolymerization of CHO with allylic phosphonium salts in presence of various radical sources at $\lambda > 290 \text{ nm}^a$

Initiator	Radical source	Time (min)	Conversion ^b (%)	$M_n (M_w/M_n)^c$
DMTPH	Benzophenone	120	12	7,030 (2.29)
	TMDPO	120	1	4,436 (1.94)
	Benzoin	10	30	8,236 (1.56)
MTPH	Benzophenone	120	8	6,800 (1.79)
	TMDPO	120	1	4,900 (1.81)
	Benzoin	10	28	9,158 (1.77)

^aConditions; monomer: initiator: radical source = $5 \text{ mol l}^{-1} : 5 \times 10^{-3} \text{ mol l}^{-1} : 5 \times 10^{-3} \text{ mol l}^{-1}$ ^bdetermined gravimetrically, ^cdetermined by GPC based on polystyrene standards.

In comparison of **TMDPO** and **benzophenone**, **benzoin** was found more efficient radical source to enhance the rate of polymerization. The order of initiator activity with respect to radical source was observed as **benzoin** > **benzophenone** > **TMDPO**. The higher activity with **benzoin** can be explained by its high quantum efficiency to generate radicals and the easy oxidation of these radicals ^[18]. **Benzoin** absorbs light in the near UV region and shows faster polymerization compared to other radical source-phosphonium salt combinations. It was selected as radical source to study the effect of radical concentration on initiator activity. The concentration of **benzoin** was increased up to four times. With both the initiators, CHO attain 85 % conversion in 10 min with phosphonium salt : radical source (1:4). Figure 4.10 shows the kinetics of CHO polymerization with **DMTPH** in presence of two different concentration of **benzoin**. The CHO attains 30 % and 85 % conversion with the concentration of **benzoin** 5×10^{-3} and: $2 \times 10^{-2} \text{ mol l}^{-1}$, respectively without change in the CHO and **DMTPH** concentration. The four times increase in concentration of **benzoin** increases the rate of polymerization approximately three times.

The high efficiency in this case again understood to be proof of the efficiency of addition-fragmentation.

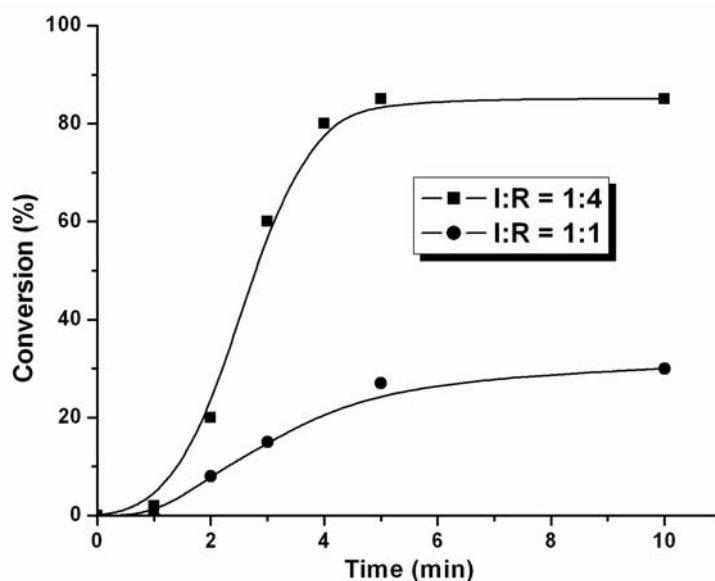


Figure 4.10: Photopolymerization of CHO with **DMTPH** in presence of different concentration of **benzoin** [5×10^{-3} and 2×10^{-2} mol l⁻¹]

Further, photopolymerization of other cationically polymerizable monomers (*n*-BVE, IBVE, NVC and GPE) was performed with **DMTPH** and **benzoin** at $\lambda > 290$ nm for 10 min (Table 4.3). The monomers, such as *n*-BVE, IBVE and NVC undergo efficiently polymerization, whereas GPE failed to produce polymer on photo-irradiation up to 120 min.

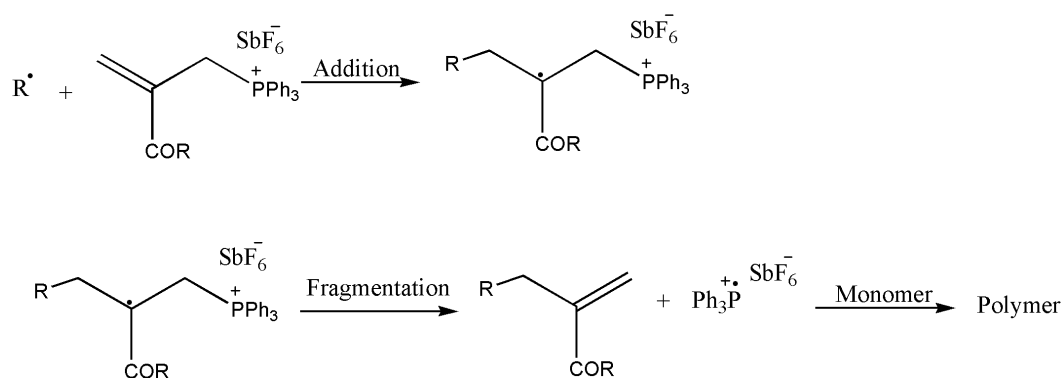
Table 4.3: Photopolymerization of other cationic monomers with **DMTPH** and **benzoin**^a

Monomer	Solvent	Conversion ^c (%)	M _n ^d (g mol ⁻¹)	M _w /M _n
CHO	Bulk	85	7,030	2.29
BVE	CH ₂ Cl ₂	95	19,700	2.36
IBVE	CH ₂ Cl ₂	100 (explosive)	24,200	1.29
NVC	CH ₂ Cl ₂	100	41,500	1.69
GPE ^b	Bulk	-	-	-

^aConditions; monomer: initiator: radical source 5 mol l⁻¹ : 5×10^{-3} mol l⁻¹ : 2.0×10^{-2} mol l⁻¹, time = 10 min, at $\lambda > 290$ nm ^btime = 120 min, ^c determined gravimetrically, ^ddetermined by GPC based on polystyrene standards.

4.3.3. Polymerization mechanism

Based on literature reports [7, 24], and our experimental results, it is assumed that in present system, on external stimulation (thermal and photo), radical sources undergo fragmentation. The generated radicals add to the double bond of allylic phosphonium salts and produce triphenylphosphine radical cations as initiating species, which react with the monomer and propagates the chain polymerization (Scheme 4.2).



Scheme 4.2: Polymerization mechanism *via* addition fragmentation pathway

4.4. Conclusions

The amide based allylic phosphonium salts were synthesized and successfully used as photo and thermo-latent initiator in the presence of free radical source as addition fragmentation agent in the cationic polymerization. In thermal polymerization, without use of radical source, conversion starts above 90 °C. The rate of polymerization can be accelerated with the use of free radical source at 70 °C and was observed as **PAT** > **BPO** > **AIBN**. No photo polymerization was observed without use of radical source while; it proceeds in the presence of radical source. The rate of polymerization with photo radical source was observed as **benzoin** > **benzophenone** > **TMDPO**. Thus, the addition of radical source to phosphonium salt initiators does not only improve the time-conversion behavior but also enables to use light of longer wavelength to initiate polymerization. The experimental results reveal that the activity of initiator is not affected by presence of different amide group in phosphonium salts and remains approximately same with the both thermal and photo chemical sources. It indicates that double bond of initiators have a role

with radical sources to initiate polymerizations on external stimulation. This proves the initiation through addition fragmentation mechanism. It can be concluded that a wide range of thermal and photo radical source can be employed to tune the conditions (temperature and wavelength) to enhance the rate of polymerization.

4.5. References

- 1 S. P. Pappas *UV Curing Science and Technology*; Technology marketing corporation, Norwalk CT, **1978**.
- 2 J. V. Crivello, *Adv. Polym. Sci.* **1984**, 1, 62.
- 3 Y. Yagci, I. Reetz, *Prog. Polym. Sci.* **1998**, 23, 1485.
- 4 J. V. Crivello, *J. Polym. Sci., Polym Chem Ed.* **1999**, 37, 4241.
- 5 Y. Yagci, Y. Yuksel, D. B. Aydogan, *The Chemical Record* **2007**, 7, 78.
- 6 Y. Yagci, I. Reetz, *Reactive and Functional Polymers* **1999**, 42, 255.
- 7 Y. Yagci, A. Onen, I. Reetz, *Macromol Symposia* **2001**, 174, 255.
- 8 A. Ledwith, *Polymer* **1978**, 19, 1217.
- 9 F. A. M. Abdul Rasoul, A. Ledwith, Y. Yagci, *Polymer* **1978**, 19, 1219.
- 10 Y. Yagci, W. Schnabel, *Macromol Chem., Macromol Symp.* **1992**, 60, 133.
- 11 A. Ledwith, Y. Yagci, *J Polym Sci Polym Chem. Ed.*, **1988**, 26, 1911.
- 12 Y. Yagci, I. Lukac, W. Schnabel, *Polymer* **1993**, 34, 1130.
- 13 D. Dossow, Q. Zhu, G. Hizal, Y. Yagci, W. Schnabel, *Polymer* **1996**, 37, 2821.
- 14 J. V. Crivello, J. L. Lee, *Macromolecules* **1981**, 14, 1141.
- 15 Y. Chen, T. Yamamura, K. Igarashi, *J Polym Sci Polym Chem* **2000**, 38, 90.
- 16 E. W. Neison, T. P. Cater, A. B. Scraton, *J Polym Sci Polym Chem. Ed* **1995**, 33, 247.
- 17 G. Hizal, Y. Yagci, W. Schnabel, *Polymer* **1994**, 35, 2428.
- 18 S. Denizligil, Y. Yagci, C. MacArdle, *Polymer* **1995**, 36, 3093.
- 19 S. Denizligil, Y. Yagci, C. MacArdle, J. P. Fouassier, *Macromol. Chem. Phys.* **1996**, 197, 1233.
- 20 M. Onciu, A. Onen, Y. Yagci, *Polym. Int.* **2001**, 50, 144.
- 21 I. Reetz, V. Bacak, Y. Yagci, *Macromol. Chem. Phys.* **1997**, 198, 19.
- 22 I. Reetz, V. Bacak, Y. Yagci, *Polym. Int.* **1997**, 43, 27.
- 23 A. Onen, Y. Yagci, *Macromolecules*, **2001**, 34, 7608.
- 24 L. Atmaca, I. Kayihan, Y. Yagci, *Polymer* **2000**, 41, 6035.
- 25 R. G. Kyager J. P. Lorand, N. R. Stevenes, N. R. Herron. *J. Am Chem Soc* **1977**, 99, 7589.
- 26 M. Davoust, J-F. Briere, P. Metzner, *Org. Biomol. Chem.* **2006**, 4, 3048.
- 27 Y. Yagci, A. Onen, *J. Polym. Sci., Polym. Chem.* **1996**, 34, 3621.

Chapter 5: Photo cationic polymerization using benzophenone based allyl ammonium salts as initiators

5.1. Introduction

In recent years, externally stimulated polymerization has attracted considerable attention due to control over initiation and curing process of epoxy and thermosetting resins ^[1, 2]. A large number of new latent initiators have been developed because of their ability to initiate polymerization by certain stimulation such as heat or light, which has been industrially used in coating, adhesive, printing ink, microelectronics and photolithography ^[3, 4]. Among them photo cationic polymerization became well known to be very useful technology for UV-curable system ^[5]. Onium salts such as iodonium, sulfonium, alkoxy pyridinium and phosphonium salts are the commercially important and well studied as photo cationic initiators ^[6]. However, the poor absorption of these initiators above 290 nm limits their practical utilization. In recent years, to shift the spectral sensitivity towards higher wavelength region, several indirect systems have been proposed and extensively studied ^[7]. Such systems involve radical initiators, photosensitizers and electron donor compounds in combination with onium salts. Among these systems, radical initiator in combination with allylic onium salt appears to be an elegant and flexible way to initiate cationic polymerization ^[8-17]. The initiation can be stimulated by heat or light with the selection of appropriate radical initiator. However, for photo induced industrial applications, the use of one component system having long wavelength absorption characteristics has an advantage over other two component systems due to additional problem associated with co-initiator such as solubility in monomer, compatibility, migration and cost ^[18, 19]. Yagci et al have employed ethylacrylate based ammonium salts having benzophenone moiety as one component addition fragmentation agent ^[20]. In present chapter, N, N-dimethylacrylamide and acryloylmorpholine based allyl ammonium salts containing benzophenone moiety with hexafluoroantimonate counter anion was synthesized and used as one component addition fragmentation agent in photo

polymerization of cyclohexene oxide, butyl vinyl ether, isobutyl vinyl ether and N-vinylcarbazole at $\lambda > 290$ nm.

5.2. Experimental

5.2.1. Materials

N, N-Dimethylacrylamide, acryloylmorpholine, 4-(dimethylamino) benzophenone (DMABP), cyclohexene oxide (CHO), isobutyl vinyl ether (IBVE), *n*-butyl vinyl ether (*n*-BVE), N-vinyl carbazole (NVC), and sodium hexafluoroantimonate (NaSbF_6) were purchased from Aldrich chemicals. All other chemicals were purchased from S.D. Fine Chemicals Ltd, Mumbai, India and used after purification^[21]. 2-(bromomethyl)- N, N-dimethyl acryl amide and 2-(bromomethyl)-acryloyl morpholine were synthesized as reported^[22]. Monomers (CHO, IBVE and *n*-BVE) and solvent (CH_2Cl_2) were distilled over CaH_2 and used just before polymerization. N-vinyl carbazole was recrystallized twice from ethanol and used immediately.

5.2.2. 2-(N, N-Dimethylcarboxy-3-propenyl) (phenylcarbonyl-4-phenylene) dimethylammonium hexafluoroantimonate (DMPDA)

In a 50 mL round bottom flask, a mixture of 2-(bromomethyl)- N, N-dimethyl acrylamide (BMDMA) (0.5 mL, 2 mmol) and 4-(dimethylamino) benzophenone (0.44 g, 2 mmol) in acetonitrile (15 mL) was stirred overnight at ambient temperature. The solvent was evaporated under vacuum and the residue was washed with diethyl ether. This bromo salt was dissolved in acetone-methanol (6:4) mixture and stirred with NaSbF_6 (0.516 g, 2 mmol) overnight. The solvent was evaporated and the residue was washed with water and recrystallized with dichloromethane. Yield: 0.60 g (63 %), Elemental analysis: $\text{C}_{21}\text{H}_{25}\text{N}_2\text{O}_2\text{SbF}_6$ (572.09 g mol⁻¹), Calcd. C, 44.00; H, 4.40; N, 4.89 Found: C, 44.13; H, 4.43; N, 4.89, ¹H NMR (acetonitrile-*d*₃) = 8.1-7.5 (m, 9H, Ph), 5.98, 5.81 (d, 2H, =CH₂), 4.80 (s, 2H, N-CH₂), 3.66 (s, 6H, CON(CH₃)₂), 2.64-2.77 (s, 6H, N(CH₃)₂) ppm, IR (KBr): 3400, 3377, 3028, 3056, 2932, 1702, 1667, 1637, 1610, 1491, 1446, 1415, 1324, 1202, 1137, 970, 897, 792 cm⁻¹.

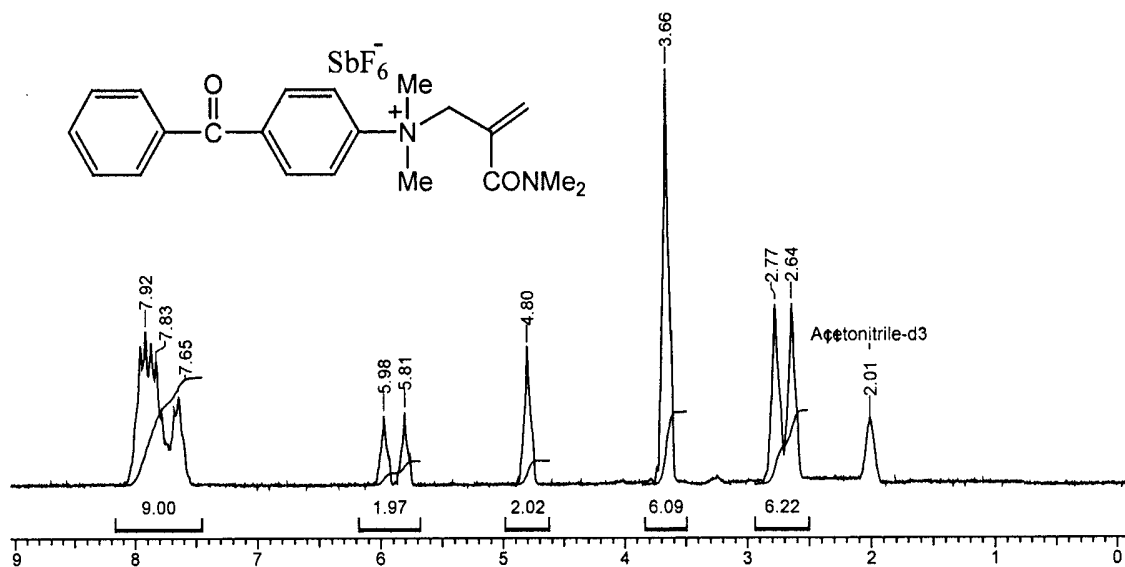


Figure 5.1: ¹H NMR spectrum of 2-(N, N-dimethylcarboxy-3-propenyl)(phenylcarbonyl-4-phenylene) dimethylammonium hexafluoroantimonate (DMPDA)

5.2.3. 2-(Morpholinocarboxy-3-propenyl) (phenylcarbonyl-4-phenylene) dimethylammonium hexafluoroantimonate (MPDA)

This compound was synthesized in similar manner as described for **DMPDA**.

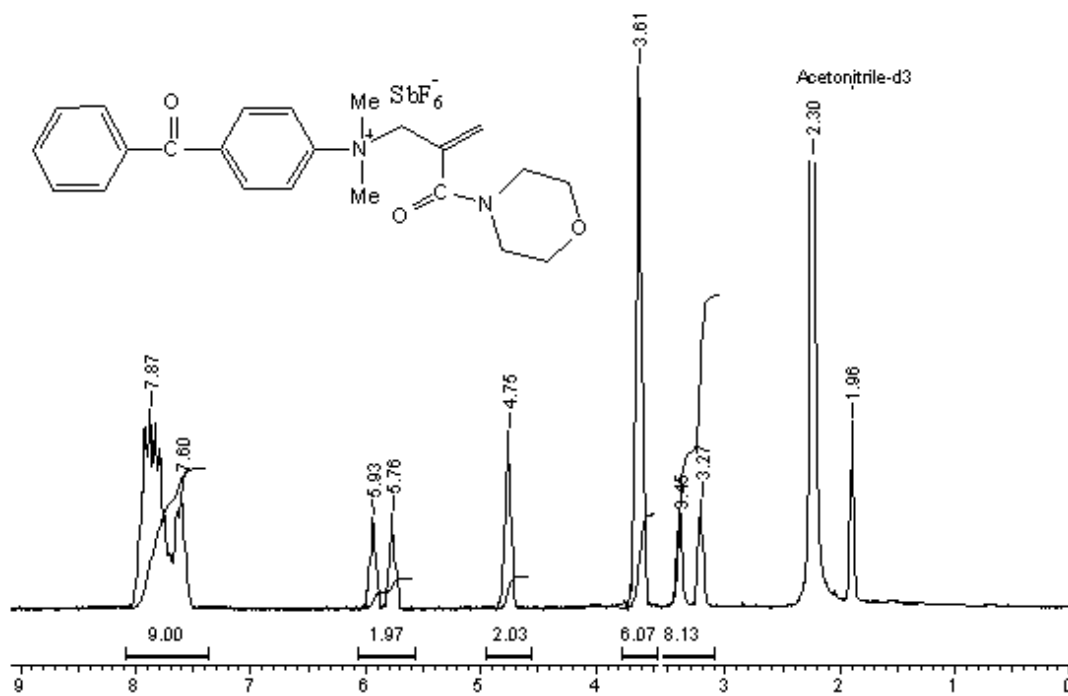
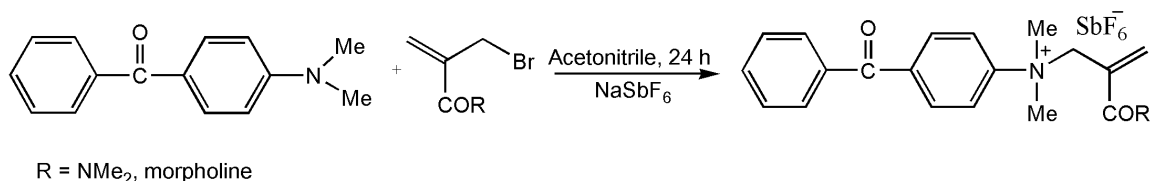


Figure 5.2: ¹H NMR spectrum of 2-(morpholinocarboxy-3-propenyl) (phenylcarbonyl-4-phenylene) dimethylammonium hexafluoroantimonate (MPDA)

Yield: 0.45 g (47 %), white crystals, Elemental analysis: $C_{23}H_{27}N_2O_3SbF_6$ (614.10 g mol⁻¹), Calcd. C, 44.90; H, 4.42; N, 4.55 Found: C, 44.82; H, 4.43; N, 4.55, ¹H NMR (acetonitrile- d₃) = 8.1-7.5 (m, 9H, Ph), 5.93, 5.76 (d, 2H, =CH₂), 4.75 (s, 2H, N-CH₂), 3.61 (s, 6H, CON(CH₃)₂), 3.45 (t, 4H, O-CH₂), 3.27 (t, 4H, N-CH₂) ppm.

5.2.4. Typical polymerization procedure

An appropriate solution of monomer and initiator was placed in a flame dried Pyrex ampoule equipped with three way stopcock connected to manifold and degassed for 30 min with three freeze-pump-thaw cycles before irradiation. After reaction for set time, the mixture was dissolved in CH₂Cl₂ and precipitated with methanol then dried under vacuum at room temperature. The 450-Watt Hanovia medium pressure mercury vapor lamp was used in this study. The conversion (%) was determined by gravimetrically. The molecular weight of polymer was determined by gel permeation chromatography (GPC).



Scheme 5.1: Synthesis of benzophenone based allylic ammonium salts

5.2.5. Measurements

The methods of characterization are described in chapter 4

5.3. Results and discussion

5.3.1. Initiator synthesis

The allylic ammonium salts namely **DMPDA** and **MPDA** were synthesized by the alkylation of the amino group of 4-(dimethyl-amino)benzophenone (DMABP) with the 2-(bromomethyl)-N, N-dimethyl acryl amide and 2-(bromomethyl)-acryloylmorpholine, respectively. The bromo counter anion was exchanged with least nucleophilic SbF₆ anion (Scheme 5.1). Both the initiators were characterized by ¹H NMR, IR and elemental

analysis as described in the experimental section. Figure 5.3 depicts the UV absorption spectra of ammonium salt and DMABP in which **DMPDA** has absorption near 300 nm.

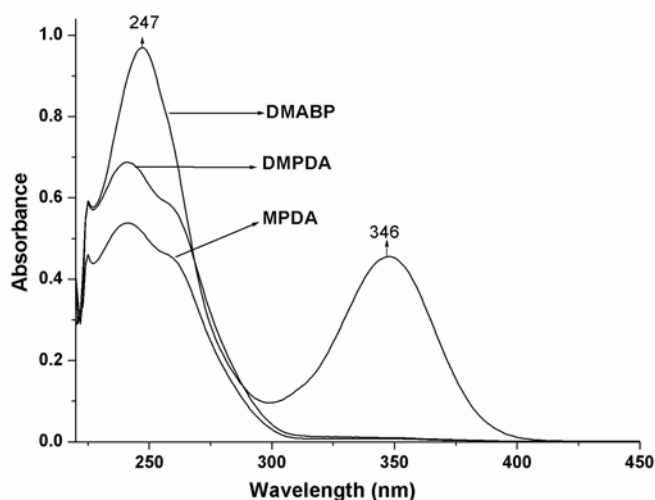


Figure 5.3: UV absorption spectra of DMABP, DMPDA and MPDA in CH_2Cl_2 solvent

5.3.2. Photopolymerization

The polymerization of CHO, IBVE and *n*-BVE was performed with different concentrations of **DMPDA** and **MPDA** at $\lambda > 290$ nm. Both the initiators show similar activity under experimental conditions (Table 5.1, 5.2 and 5.3). Therefore, the kinetics of polymerizations is discussed with **DMPDA**.

Figure 5.4 shows time-conversion curve in the polymerization of CHO with different concentrations (10^{-5} , 10^{-4} and 10^{-3}) of benzophenone based allylic ammonium salt (**DMPDA**) at $\lambda > 290$ nm (Table 5.1).

Table 5.1: Photopolymerization of CHO using various concentrations of allylic ammonium salt in CH₂Cl₂ solvent^a

Initiator	Concentration	Conversion ^b	M _n (g mol ⁻¹) ^c	M _w /M _n
DMPDA	5 x 10 ⁻⁵	36	6,600	2.59
	5 x 10 ⁻⁴	65	9,400	2.51
	5 x 10 ⁻³	75	8,300	1.56
MPDA	5 x 10 ⁻⁵	32	6,300	2.29
	5 x 10 ⁻⁴	63	11,859	2.34
	5 x 10 ⁻³	72	10,845	2.04

^a conditions $\lambda > 290$ nm, ambient temperature for 10 min ^bdetermined gravimetrically, ^cdetermined by GPC based on polystyrene standards.

It can be seen that conversion to poly(CHO) increases with time and reaches to limiting values in 30 min. In Figure 5.4 (A), conversion reaches to limiting value of 75 % within 2 min and remains the same while in Figure 5.4 (B) and 5.4 (C), it attains limiting value of 70 % and 55 % conversion in 15 min, respectively.

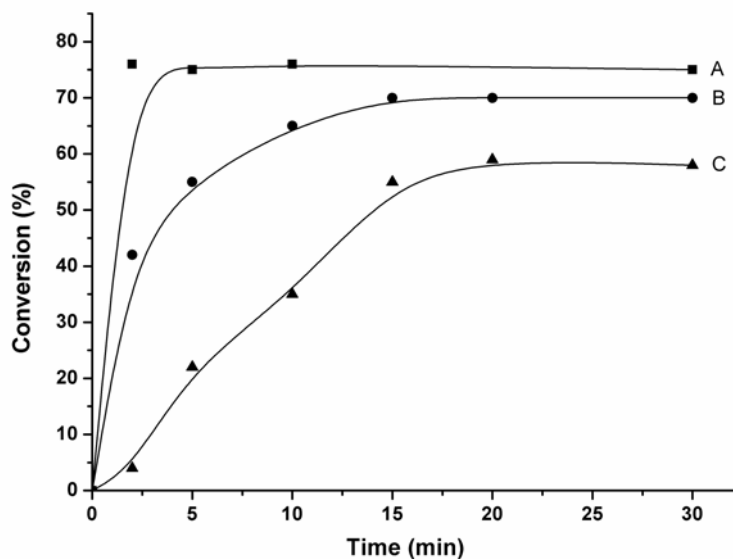


Figure 5.4: Photopolymerization of CHO in presence of **DMPDA** [CHO] = 5 mol l⁻¹, $\lambda > 290$ nm, 25 °C, (A) **DMPDA** = 5 x 10⁻³ mol l⁻¹, (B) **DMPDA** = 5 x 10⁻⁴ mol l⁻¹ and (C) **DMPDA** = 5 x 10⁻⁵ mol l⁻¹.

The Figure 5.5 shows the polymerization of IBVE with **DMPDA** in CH₂Cl₂ solvent above 290 nm (Table 5.2).

Table 5.2: Photopolymerization of IBVE using various concentrations of allylic ammonium salt in CH₂Cl₂ solvent^a

Initiator	Concentration	Conversion ^b	M _n (g mol ⁻¹) ^c	M _w /M _n
DMPDA	5 x 10 ⁻⁵	28	28,500	2.51
	5 x 10 ⁻⁴	90	25,600	2.36
	5 x 10 ⁻³	100	19,655	2.35
MPDA	5 x 10 ⁻⁵	23	29,600	1.86
	5 x 10 ⁻⁴	90	26,415	1.29
	5 x 10 ⁻³	100	15,937	1.85

^a conditions $\lambda > 290$ nm, ambient temperature for 10 min ^bdetermined gravimetrically, ^cdetermined by GPC based on polystyrene standards.

As can be seen from Figure 5.5, IBVE can be polymerized effectively in presence of **DMPDA**. In the present case, conversion (%) increases with time and attains limiting value. In Figure 5.5(A), conversion reaches to 90 and 100 % in 2 and 5 min, respectively. The Figure 5.5 (B) shows 90 % conversion in 5 min while Figure 5.5 (C) 22 % conversion in 10 min and remains the same with further increase in the reaction time.

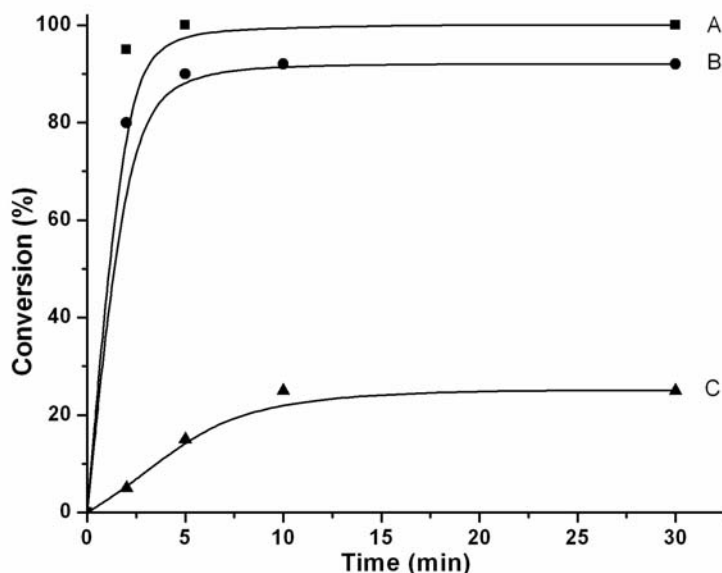


Figure 5.5: Photopolymerization of IBVE in presence of **DMPDA** [CHO] = 5 mol l⁻¹, $\lambda > 290$ nm, 25 °C, (A) **DMPDA** = 5 x 10⁻³ mol l⁻¹, (B) **DMPDA** = 5 x 10⁻⁴ mol l⁻¹ and (C) **DMPDA** = 5 x 10⁻⁵ mol l⁻¹.

The photo polymerization of *n*-BVE was performed under similar conditions as in the case of CHO polymerization (Table 5.3).

Table 5.3: Photopolymerization of *n*-BVE using various concentrations of allylic ammonium salt in CH₂Cl₂ solvent^a

Initiator	Concentration	Conversion ^b	M _n (g mol ⁻¹) ^c	M _w /M _n
DMPDA	5 x 10 ⁻⁵	15	18,600	2.29
	5 x 10 ⁻⁴	80	17,300	2.05
	5 x 10 ⁻³	100	11,700	2.35
MPDA	5 x 10 ⁻⁵	12	21,200	2.50
	5 x 10 ⁻⁴	80	19,400	2.36
	5 x 10 ⁻³	100	10,500	2.42

^a conditions λ > 290 nm, ambient temperature for 10 min ^bdetermined gravimetrically, ^cdetermined by GPC based on polystyrene standards.

Figure 5.6 shows that conversion (%) increases with the increase in reaction time and reaches to limiting values. In Figure 5.6(A), conversion reaches to 38 and 80 and 100 % in 2, 5 and 10 min, respectively. In Figure 5.6(B) and 5.6 (C), 90 and 22 % conversion reaches in 15 and 20 min, respectively.

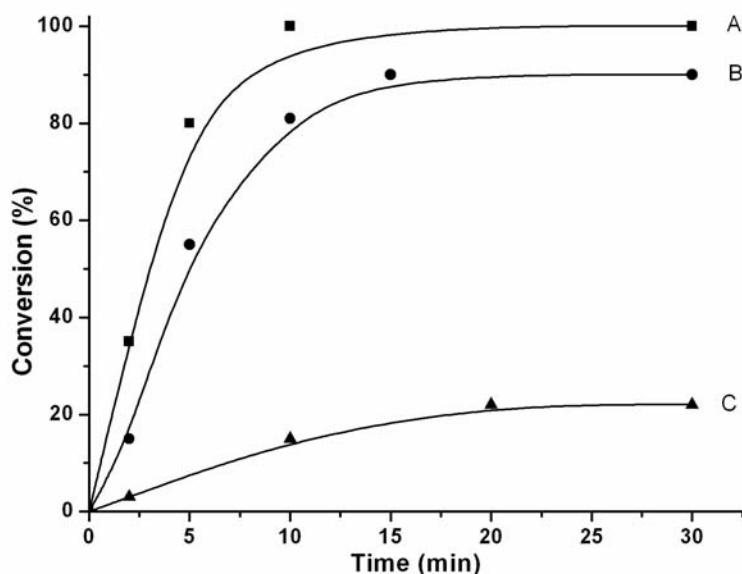


Figure 5.6: Photopolymerization of *n*-BVE in presence of **DMPDA** [CHO] = 5 mol l⁻¹, λ > 290 nm, 25 °C, (A) **DMPDA** = 5 x 10⁻³ mol l⁻¹, (B) **DMPDA** = 5 x 10⁻⁴ mol l⁻¹ and (C) **DMPDA** = 5 x 10⁻⁵ mol l⁻¹.

In general, conversion (%) increases with the increases in initiator concentration.

The Table 5.4 shows polymerization results of various cationic monomers in presence of **DMPDA** at $\lambda > 290$ nm. CHO, NVC and IBVE undergo efficiently polymerization upon irradiation while GPE failed to produce any polymer even up to 60 minutes.

Table 5.4: Photopolymerization of various monomers in the presence of **DMPDA**^a

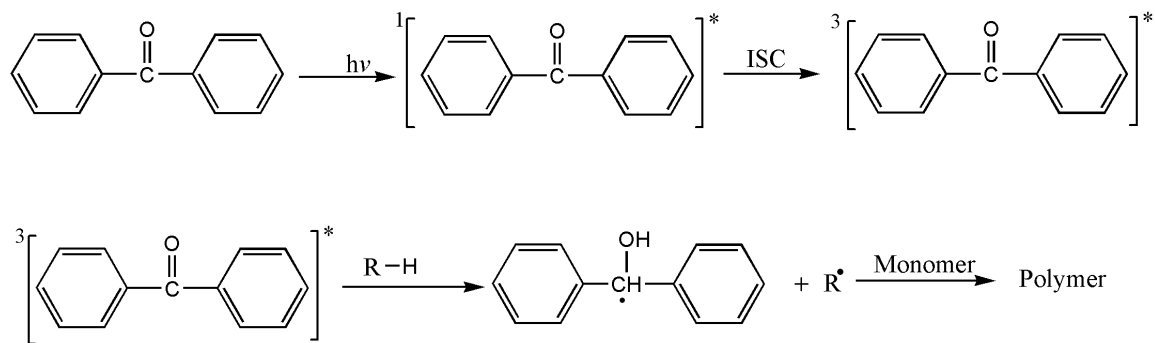
Monomer	Time (min)	Conversion ^b		M_n^c	M_w/M_n
		(%)			
CHO	10	65		9,400	2.51
NVC	10	92		1,12,000	2.85
IBVE	2 (explosive)	90		25,600	2.36
BVE	10	80		17,300	2.05
GPE	60	-		-	-

^a Monomer: Initiator = 5 mol l⁻¹: 5 x 10⁻⁴ mol l⁻¹ in CH₂Cl₂ solvent at room temperature ($\lambda > 290$ nm)

^bdetermined gravimetrically, ^cdetermined by GPC based on polystyrene standards.

5.3.3. Mechanism of photopolymerization

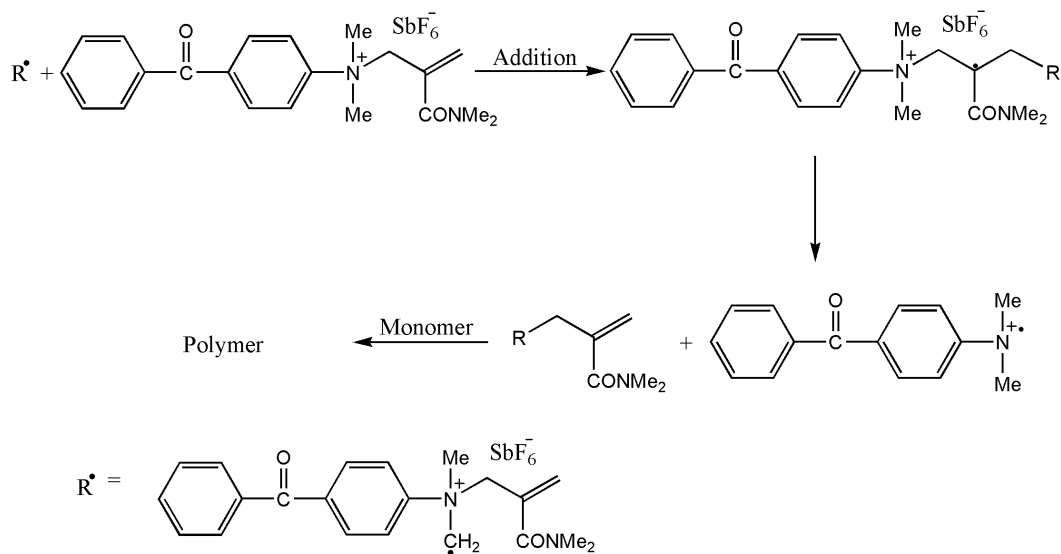
Benzophenone and its derivatives are good radical initiator to initiate radical polymerization through hydrogen abstraction mechanism as shown in Scheme 5.2.



Scheme 5.2: Radical polymerization via hydrogen abstraction mechanism

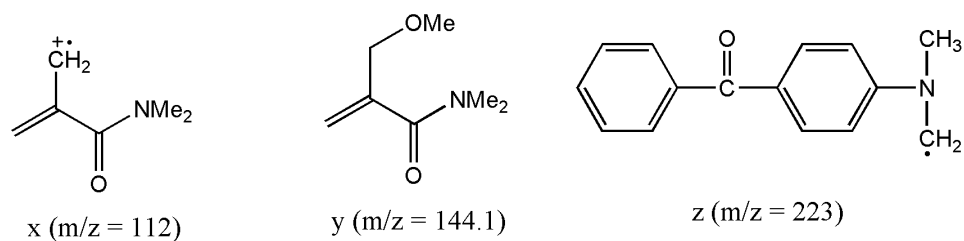
In present study, upon irradiation of benzophenone based allylic ammonium salt (**DMPDA**), the benzophenone moiety produces radical species by hydrogen abstraction

from ground state **DMPDA** in a mechanism similar to that described in Scheme 5.2. These radicals add to the allylic double bond and subsequently generate ammonium radical cations, which initiate polymerization (Scheme 5.3).



Scheme 5.3: Polymerization via radical addition fragmentation mechanism

The additional support for mechanism through addition fragmentation process is obtained by irradiation of 5×10^{-3} M solution of **DMPDA** in methanol. On analysis of GC-MS fragmentation products, the peaks at m/z value of 112, 144.1 ($m+1$) and 223 ($m-1$) indicates for product (x), (y) and (z), respectively (Scheme 5.4, Figure 5.7 & 5.8). The fragmentation product y results from reaction of x with methanol whereas the product z results from hydrogen abstraction according to Scheme 5.2.



Scheme 5.4: Photo fragmentation of **DMPDA** in GC-MS analysis

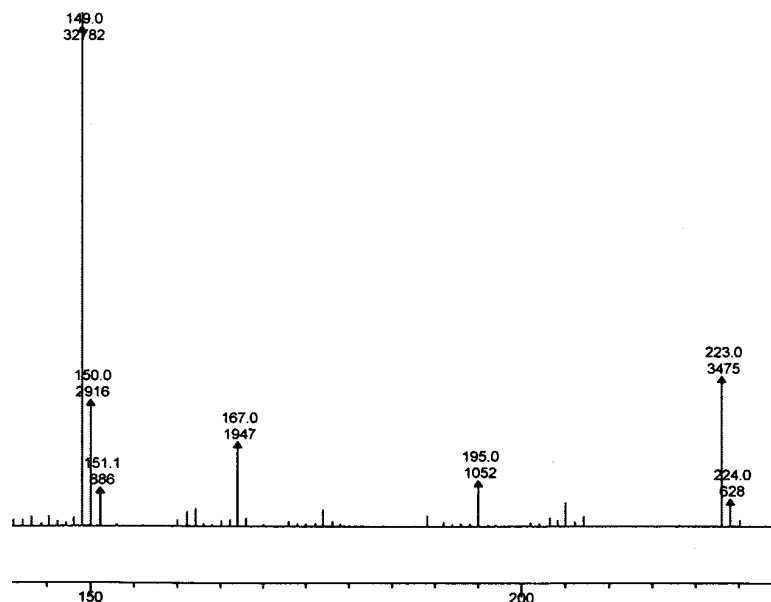


Figure 5.7: Photo fragmentation spectrum of **DMPDA** in GC-MS analysis

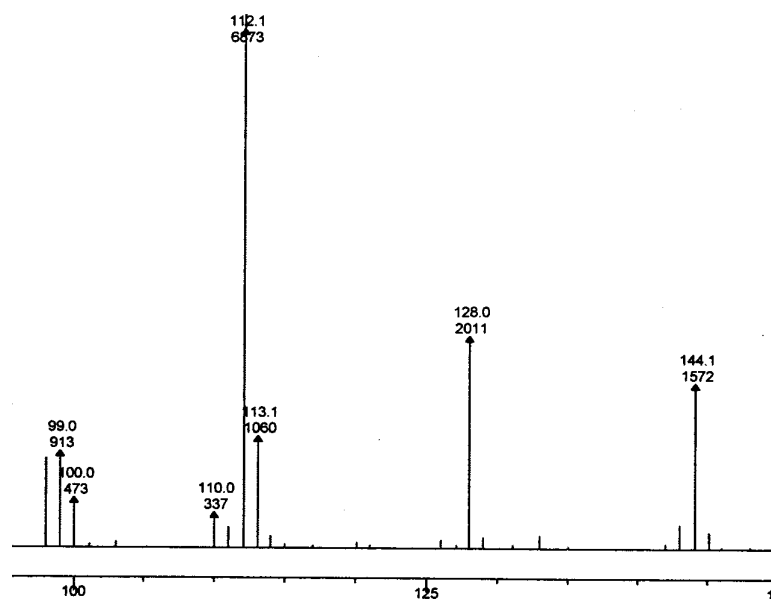


Figure 5.8: Photo fragmentation spectrum of **DMPDA** in GC-MS analysis

These photolysis products and increase in conversion (%) with the increase in initiator concentration supports the proposed mechanism in present system. Moreover, the mechanism of initiation was confirmed by polymerization of CHO with **DMPDA** in presence of 2,6-di-*t*-butyl-4-methyl pyridine (DTBP) as a proton scavenger. CHO did not polymerize in the presence of DTBP, which supports the proposed mechanism via hydrogen abstraction and further addition fragmentation process.

5.4. Conclusions

The benzophenone based allylic ammonium salts were found to be efficient photoinitiator in cationic polymerization. The activity of the initiator increases with the increase in initiator concentration and reaction time. The initiator possesses an intrinsic chromophoric group for the radical generation and an allylic ammonium salt structure for addition fragmentation agent. Thus, photo initiation can be induced in the absence of additional radical sources above 290 nm.

5.5. References

1. H. Lee, Neville, K. *Handbook of Epoxy Resins*; McGraw-Hill, New York, **1967**.
2. H. F. Mark, N. G. Gaylord, N. M. Bikajes, *Encyclopedia of Polymer Science and Technology*; Interscience: New York, **1968**, 8, 303.
3. J. V. Crivello, *Adv. Polym. Sci.* **1984**, 1, 62.
4. J. V. Crivello, *J. Polym. Sci., Polym Chem Ed.* **1999**, 37, 4241.
5. S. P. Pappas, *UV Curing Science and Technology; Technology marketing corporation*, Norwalk CT, **1978**.
6. Y. Yagci, I. Reetz, *Prog. Polym. Sci.* **1998**, 23, 1485.
7. Y. Yagci, W. Schnabel, *Macromol Chem Macromol Symp.* **1994**, 85, 115.
8. S. Denizligil, Y. Yagci, C. MacArdle, *Polymer* **1995**, 36, 3093.
9. S. Denizligil, Y. Yagci, C. MacArdle, J. P. Fouassier, *Macromol. Chem. Phys.* **1996**, 197, 1233.
10. Y. Yagci, A. Onen, *J. Polym. Sci., Polym. Chem.* **1996**, 34, 3621.
11. I. Reetz, V. Bacak, Y. Yagci, *Macromol. Chem. Phys.* **1997**, 198, 19.
12. I. Reetz, V. Bacak, Yagci, Y. *Polym. Int.* **1997**, 43, 27.
13. L. Atmaca, A. Onen, Y. Yagci, *Eur. Polym. J.* **2001**, 37, 677.
14. M. A. Onciu, Onen, Y. Yagci, *Polym. Int.* **2001**, 50, 144.
15. Y. Yagci, S. Yildirim. A. Onen, *Macromol. Chem. Phys.* **2001**, 202, 527.
16. A. Onen, Y. Yagci, *Macromol. Chem.* **2001**, 202, 1950.
17. A. Bottcher, K. Hasebe, G. Hizal, P. Stelberg, Y. Yagci, *Polymer* **1991**, 32, 2289.
18. A. Onen, Y. Yagci, *Polymer* **2001**, 42, 6681.
19. Y. Yagci, S. Yildirim, A. Onen, *Macromol. Chem. Phys.* **2001**, 202, 527.
20. S. Yurteri, A. Onen, Y. Yagci, *Eur. Polym. J.* **2002**, 38, 1845.
21. W. L. F. Armarego, D. D. Perrin, *Purification of Organic Chemicals*, 4th ed, Butterworth-Heinemann, Linecre House, Jordon Hill, Oxford OX2 8 DP.
22. M. Davoust, J-F Briere, P. Metzner, *Org. Biomol. Chem.* **2006**, 4, 3048.

Chapter 6: Diselenides as novel non-salt photo initiator for photosensitized cationic polymerization Of N-vinyl carbazole

6.1. Introduction

Enhanced research activity for cationic polymerization has been centered towards the design and synthesis of novel photo polymerization system due to increasing commercial and technical applications^[1-3]. Onium salt initiated cationic polymerization is performed below 300 nm that limits its practical applications^[4-7], therefore, it is required to extend the spectral sensitivity to high wavelength (> 300 nm) region where medium and high-pressure mercury lamp emits most spectrum of their radiation. This problem can be solved either by chemical attachment of chromophoric groups to the initiator or by using photosensitization process. The latter process is convenient and more applicable as compared to incorporation of chromophore. A photosensitization includes photoelectron transfer (PET) either with photo-excited sensitizer^[8-11], free radical^[12-13] or with electron donor compounds in the excited charge transfers complexes^[14]. Single electron transfer (SET) induced generation of radical ions and their synthetic potential is an emerging concept in organic synthesis^[15]. Diselenides with aromatic nitriles are well-known photosensitization system for *insitu* generation of electrophilic selenium species in the selenenylation reactions^[16]. However, the same methodology^[16] was used to study the photo polymerization of N-vinyl carbazole (NVC). The present chapter describes the use of diselenide (**DPDS** and **DBDS**) as non-salt initiator for photosensitized cationic polymerization of NVC. To the best of our knowledge with existing literature, the present system is a novel photosensitization system for the cationic polymerization.

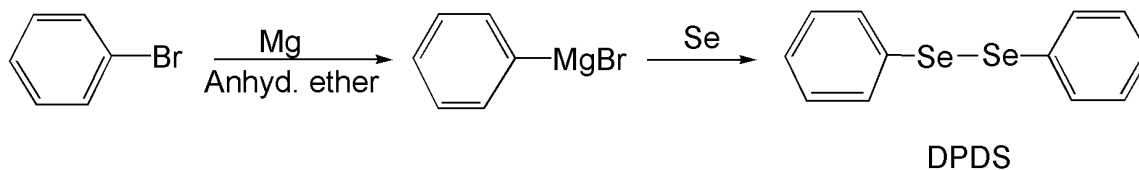
6.2. Experimental

6.2.1. Materials

N-vinylcarbazole (NVC) (Aldrich) was recrystallized twice from ethanol, thoroughly dried under vacuum and used just before polymerization. Dichloromethane (CH₂Cl₂) purified by usual methods^[17] and doubly distilled over CaH₂ before use. Anthracene, naphthalene,

bromine, cuprous cyanide (CuCN), N, N-dimethyl formamide (DMF), copper sulphate (CuSO₄), dioxane, acetonitrile and diethyl ether were purchased from Merck (India).

6.2.2. Synthesis of Diphenyl diselenide (DPDS) ^[18]



Scheme 6.1: Synthesis of DPDS

To a flame dried three-necked 50 mL round-bottom flask, equipped with a reflux condenser, mechanical stirrer, addition funnel and nitrogen inlet, 0.56 g (24.3 mmol) of Mg turnings and a crystal of iodine, were placed. A solution of bromobenzene (3.80 g, 24.3 mmol) in 20 mL of anhydrous ether was placed in the addition funnel. To the Mg turnings in anhydrous ether, bromobenzene were added to initiate the reaction. Once initiated, the reaction mixture was stirred vigorously and the halide was added slowly to maintain a gentle reflux. Stirring of the brown solution was continued for 30 minutes and the dropping funnel was replaced with a glass stopper. Powdered black selenium (1.92 g, 22.3 mmol) was added slowly to the vigorously stirred solution, over a 3 h period; the resulting green color suspension was stirred for 30 minutes. The reaction mixture was poured into a 50 mL erlenmeyer flask containing crushed ice, then concentrated hydrochloric acid (4 mL) was slowly added with swirling until all of the ice had been melted. The contents of the flask were poured into a 100 mL separating funnel, the aqueous layer was removed and extracted with 20 mL of ether and the combined organic layers were passed through a celite pad into a 50 mL filtration flask. To stirring the dark orange solution, in the same flask, 15 mL of 95 % ethanol, one pellets of KOH were added. The flask was stoppered with a one-hole cork and a glass tube inserted, until it just reached the surface of the liquid. Air was drawn rapidly over the vigorously stirred solution until a thick yellow precipitate was formed and the odor of selenophenol had disappeared. The yellow slurry was filtered on a Buchner funnel, washed several times with cold ethanol (95

%) and dried under vacuum, which was recrystallized by *n*-hexane. Yield: (75 %, 2.86 g), bright yellow crystals, mp: 62-64 °C, Elemental analysis: calcd. for C₁₂H₁₀Se₂: C, 46.13; H, 3.2. Found: C, 46.12; H, 3.2, IR (Nujol): 3020 (Ar C-H Str.), 1600, 1500, 1461, 1400 (Ar C-H bending), 823, 757 cm⁻¹, ¹H NMR (200 MHz, CDCl₃): δ: 7.59 (m, 2H, Ph), 7.23 (m, 3H, Ph) ppm.

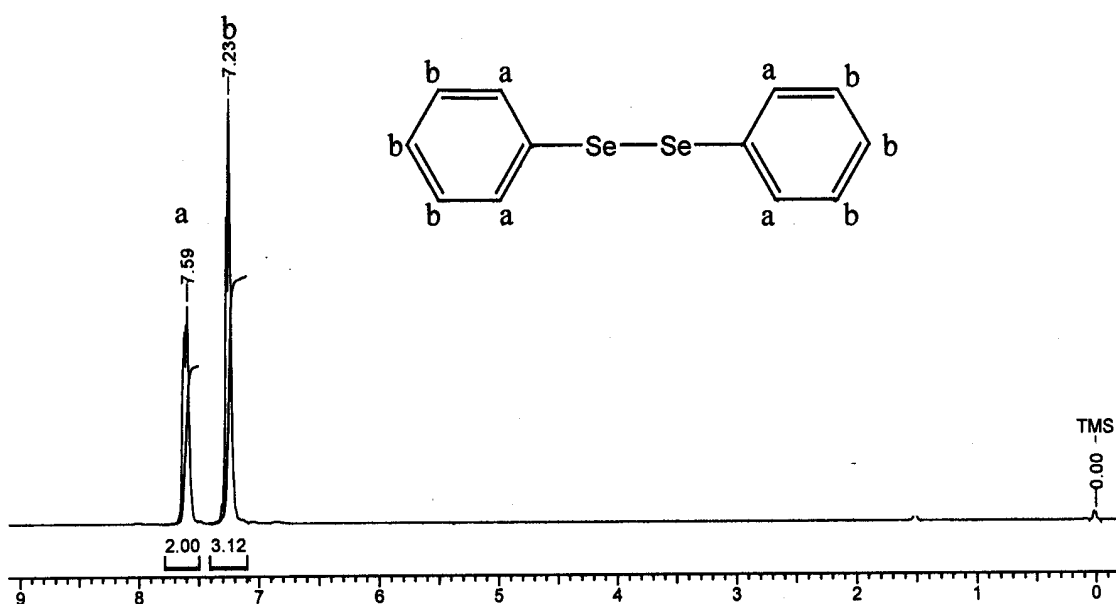
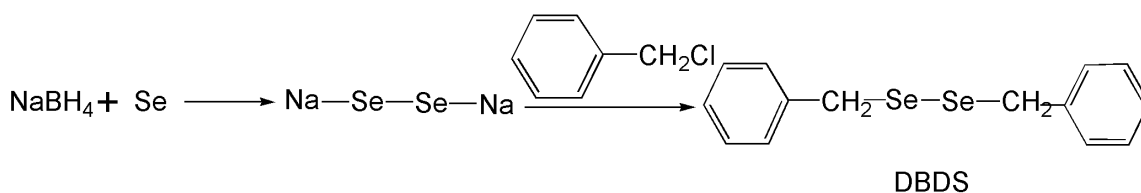


Figure 6.1: ¹H NMR spectrum of diphenyl diselenide (DPDS)

6.2.3. Synthesis of Dibenzyl diselenide (DBDS) ^[19]



Scheme 6.2: Synthesis of DBDS

Selenium powder (2.3 g, 29 mmol) was added to stirring solution of sodium borohydride (2.3 g, 61 mmol) in water (25 mL) at ambient temperature. To this prepared NaHSe solution, benzyl chloride (7.3 g, 58 mmol) was added and the mixture was stirred at ambient temperature for 18 h. The solid product was collected, washed with water and recrystallized from *n*-hexane. Yield: (86 %, 6.5 g), Pale yellow rods, mp 44-45 °C. Elemental analysis: calcd for C₁₄H₁₄Se₂: C, 49.38; H, 2.93 Found: C, 49.34; H, 2.96, IR

(Nujol): 3020 (Ar C-H Str.), 1570, 1465, 1438 (Ar C-H bending), 823, 757 cm^{-1} , ^1H NMR (200 MHz, CDCl_3): δ : 7.23 (m, 5H, Ph), 3.82 (s, 2H, Ph) ppm.

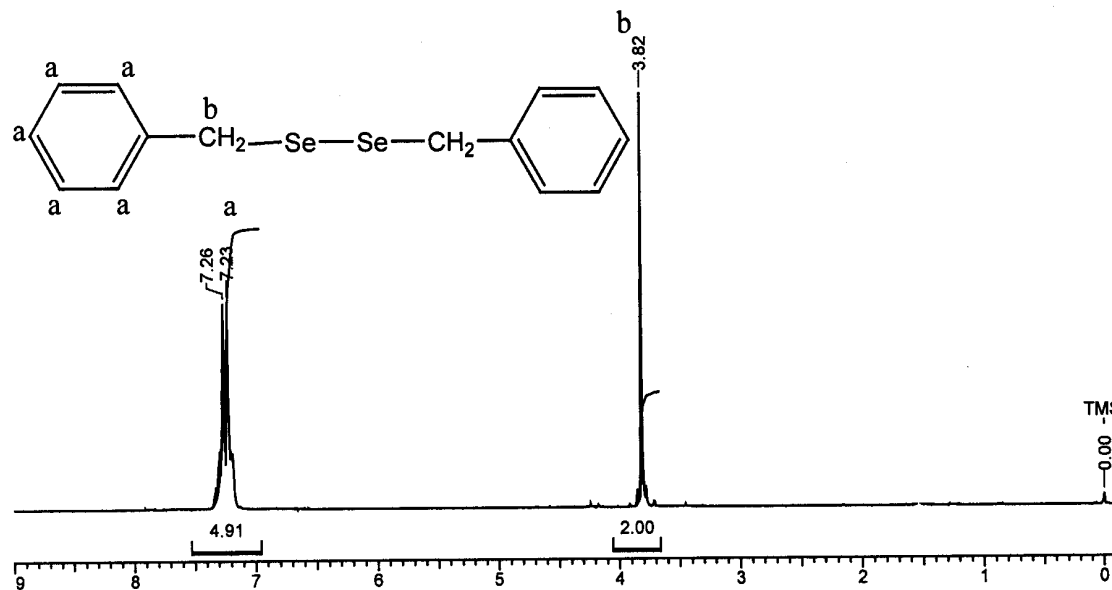
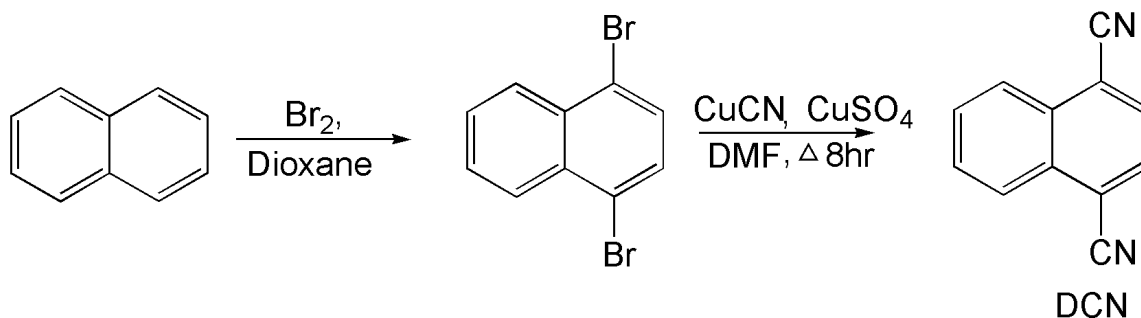


Figure 6.2: ^1H NMR spectrum of dibenzyl diselenide (DBDS)

6.2.4. Synthesis of 1, 4-Dicyanonaphthalene (DCN): It was synthesized in two steps as shown in Scheme 6.3.



Scheme 6.3: Synthesis of DCN

6.2.4.1. Synthesis of 1, 4-Dibromonaphthalene (DBN) ^[20]

In 250 mL two-necked round bottom flask, bromine (5.13 mL, 100 mmol) was added slowly to stirring dioxane (8.5 mL, 50 mmol) at ambient temperature. Naphthalene (6.4 g, 50 mmol) was added in portion to the above-formed bright red complex. The reaction mixture was allowed to stir for 1 h and then liquid mixture was heated to 45 $^{\circ}\text{C}$ for 6 h and

allowed to stand overnight at ambient temperature. Reaction mixture was neutralized with 10 % aqueous NaOH solution. Solid was filtered and washed with ice-cold ethanol. Crude solid was dried and recrystallized twice with 95 % ethanol, which gave slight orange needle crystals. Yield: 19.05 g (67 %), slight orange needle crystals, mp: 82-83 °C, Elemental analysis: calcd for C₁₀H₆Br₂: C, 41.95; H, 2.1; Br, 55.94. Found: C, 41.82; H, 2.2; Br, 55.89, IR (Nujol): 3030 (Ar C-H Str.), 1600, 1500, 1463 (Ar C-H bending), 850 cm⁻¹, ¹H NMR (200 MHz, CDCl₃): δ: 8.20 (m, 2H, Ph), 7.56 (m, 4H, Ph) ppm.

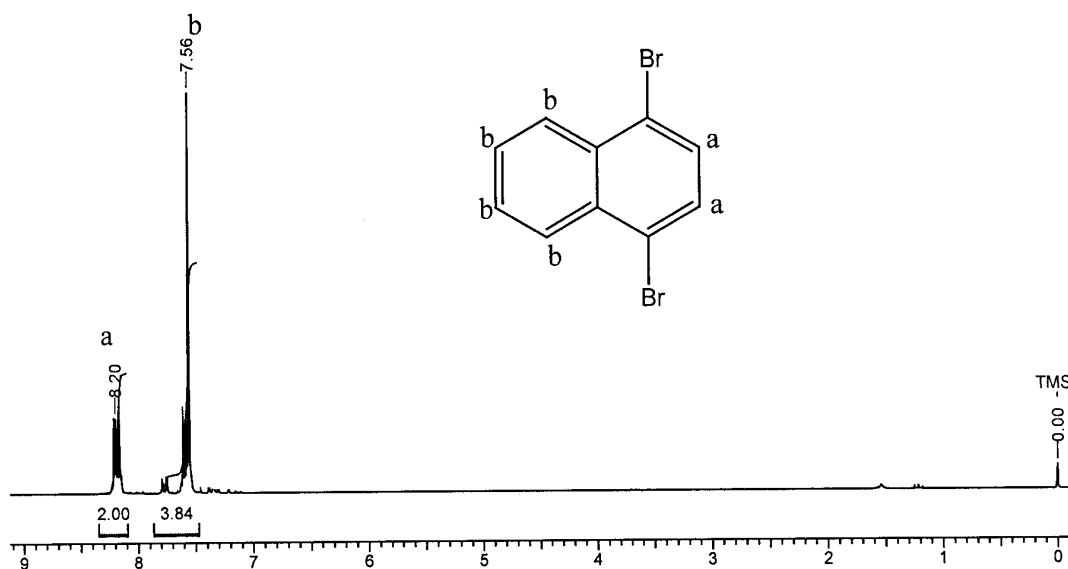


Figure 6.3: ¹H NMR spectrum of 1, 4-dibromonaphthalene (DBN)

6.2.4.2. Synthesis of 1, 4-Dicyanonaphthalene (DCN) ^[21]

Dibromonaphthalene (10 g, 35 mmol), cuprous cyanide (6.89 g, 77 mmol) and CuSO₄ (0.1 g catalytic) were refluxed in DMF (150 mL) solvent for 8 h under argon environment. Reaction mixture was cooled to ambient temperature and poured into 100 mL saturated FeCl₃ solution, precipitate appeared that was filtered and successively washed with 10 M HCl, water and finally with ice cold ethanol. Crude product was dried, decolorized with animal charcoal and recrystallized twice with 95 % ethanol, which gives white crystalline needles. Yield: 32 %, white crystalline needles, mp: 208-210 °C, Elemental analysis: calcd for C₁₂H₆N₂: C, 80.89; H, 3.1; N, 15.73 Found: C, 80.93; H, 3.2; N, 15.73, IR (Nujol): 3030 (Ar C-H Str.), 2225 (C≡N Str.), 1600, 1500, 1463 (Ar C-H bending), 850 cm⁻¹, ¹H NMR (200 MHz, CDCl₃): δ: 8.34 (m, 2H, Ph), 7.98 (m, 4H, Ph) ppm.

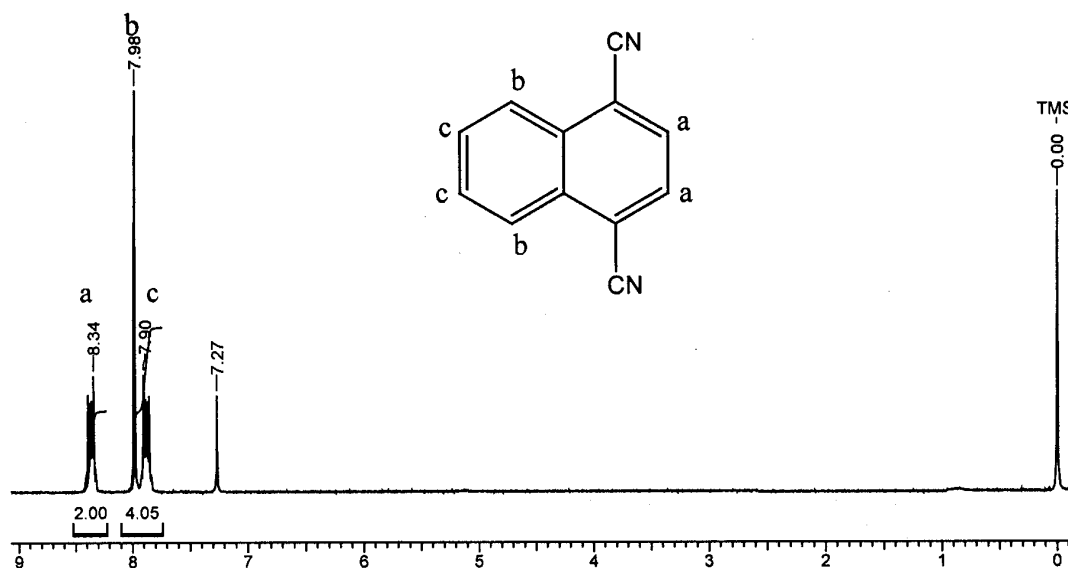
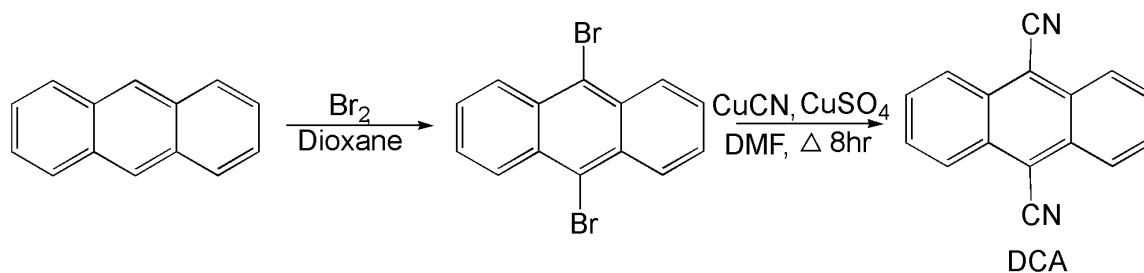


Figure 6.4: ¹H NMR spectrum of 1,4-dicyanonaphthalene (DCN)

6.2.5. Synthesis of Dicyanoanthracene (DCA): It was synthesized in two steps as shown in Scheme 6.4.



Scheme 6.4: Synthesis of DCA

6.2.5.1. Synthesis of 9,10-Dibromoanthracene (DBA)

The method was exactly the same as that employed for DBN in Scheme 6.3. Yield (69 %), mp: 222-223 °C, Elemental analysis: Calcd for C₁₄H₈Br₂: C, 50.00; H, 2.3; Br, 7.61 Found: C, 49.53; H, 2.4; Br, 7.57, IR (Nujol): 3030 (Ar C-H Str.), 1600, 1580 1461 (Ar C-H bending), 840 cm⁻¹, ¹H NMR (200 MHz, CDCl₃): δ: 8.58 (s, 4H, Ph), 7.63 (s, 4H, Ph) ppm.

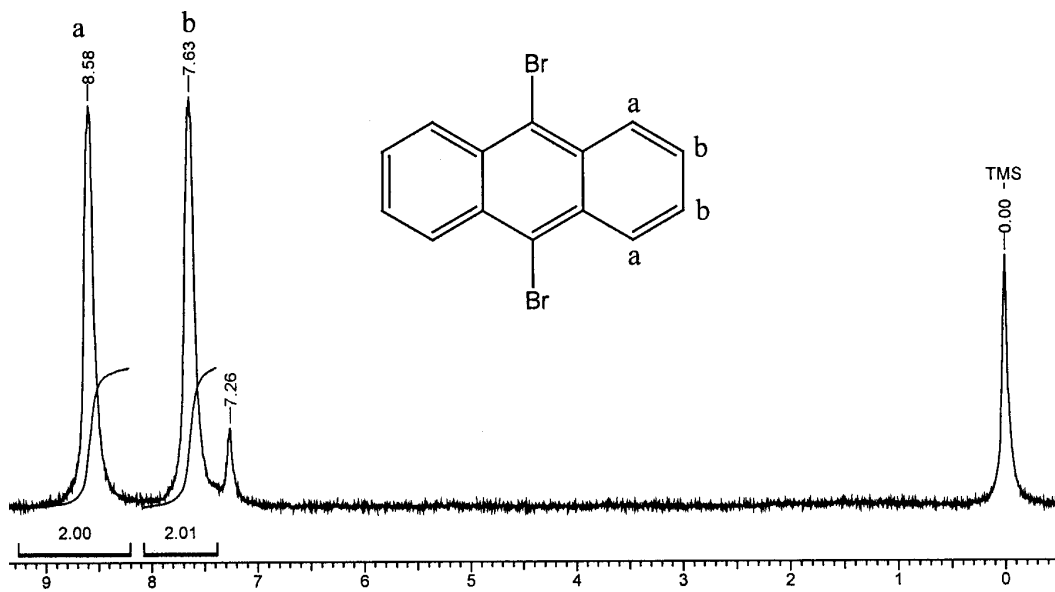


Figure 6.5: ^1H NMR spectrum of 9, 10-dibromoanthracene (DBA)

6.2.5.2. Synthesis of 9, 10-Dicyanoanthracene (DCA)

It was synthesized by using the above precursor molecule (DBA). It was synthesized similar manner to DCN.

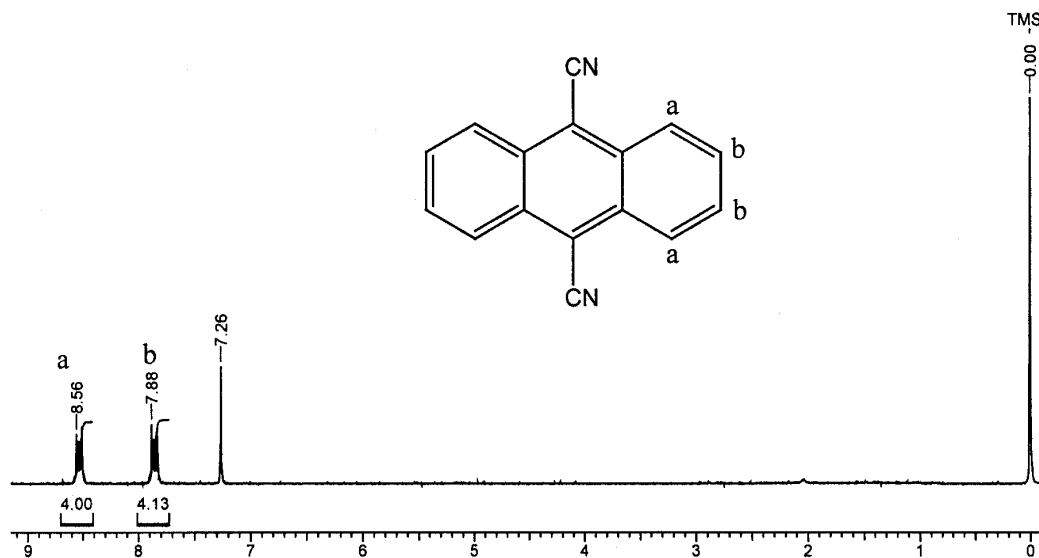


Figure 6.6: ^1H NMR spectrum of 9, 10-dicyanoanthracene (DCA)

Yield: 37 %, mp: 338 °C, Elemental analysis: calcd for $\text{C}_{16}\text{H}_8\text{N}_2$: C, 84.30; H, 3.5; N, 12.20. Found: C, 84.20; H, 3.6; N, 12.23, IR (Nujol): 3030 (Ar C-H Str.), 2362, 2212

(C≡N Str.), 1622, 1500, 1463 (Ar C-H bending), 763 cm^{-1} , ^1H NMR (200 MHz, CDCl_3): δ : 8.56 (m, 4H, Ph), 7.88 (m, 4H, Ph) ppm.

6.2.6. General Procedure for Photo polymerization of NVC

A mixture of monomer (NVC, 390 mg, 2 mmol), initiator (**DPDS/DBDS**, 6.0/6.7 mg, 0.02 mmol) and sensitizer (**DCN/DCA**: 3.6/4.6 mg, 0.02 mmol) were placed in flame dried Pyrex ampoule equipped with a three-way stopcock connected to manifold. The flask was degassed for 30 minutes followed by the addition of freshly dried dichloromethane. Three freeze-pump-thaw cycles were performed in order to make the reaction contents free of dissolved gases. Finally, the reaction mixture was irradiated in a Pyrex vessel at a distance of 8 cm from the 450 W Hanovia (medium pressure) lamp having quartz-jacketed immersion well in combination with a Pyrex filter at ambient temperature. After running the reaction certain period of time, the polymer was precipitated with 10-fold excess of methanol, washed and dried at ambient temperature under vacuum. Polymer molecular weight and structure were determined by size exclusion chromatography (SEC) and ^1H NMR spectroscopy, respectively.

6.2.7. Measurements

The methods of characterization are described in chapter 4.

6.3. Results and Discussion

6.3.1. Synthesis of initiator and sensitizer

The sensitizer (**DCN** and **DCA**) and initiator (**DPDS** and **DBDS**) were synthesized and well characterized by ^1H NMR & IR spectroscopy besides elemental analysis; both initiator and sensitizers are stable in air and moisture. Figure 6.7 depicts UV absorption spectra of **DCN**, **DCA** and **NVC**. Fluorescence quenching of sensitizer, i.e., **DCN** ($\lambda_{\text{max}} = 320$ nm, $\lambda_{\text{em}} = 391$ nm) and **DCA** ($\lambda_{\text{max}} = 430$ nm, $\lambda_{\text{em}} = 461$ nm) by initiator, **DPDS**, follows the Stern-Volmer relation.

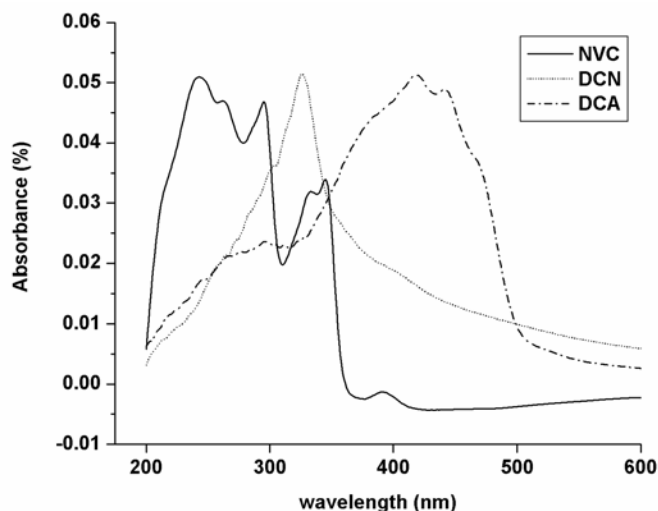


Figure 6.7: UV absorption spectrum of sensitizer (**DCN**, **DCA**) and monomer (**NVC**)

Fluorescence quenching in these cases occurs *via* the single electron transfer (SET) mechanism involving the charge transfer (CT) stabilized exciplex. The Weller equation^[22] that describes the thermodynamics of the interaction (i.e., free energy change (ΔG_{ET})) between the photosensitizer and the initiator during single electron transfer photosensitization is given by equation 1 as,

$$\Delta G_{ET} = E_{1/2}^{ox}[D] - E_{1/2}^{red}[A] - E_{o,o} \quad (1)$$

Here $E_{1/2}^{ox}[D]$ is the oxidation potential of the **DPDS** (donor), $E_{1/2}^{red}[A]$ the reduction potential of the acceptor (**DCN** & **DCA**) and $E_{o,o}$ the singlet excited state energy of sensitizer species. Putting the literature values of the oxidation potential of **DPDS**,^[23] reduction potential, and excitation energy^[24] of **DCN** and **DCA** involved in equation 1 gives the free energy value of the photosensitization system utilized in the study. The negative value of free energy was obtained in the both cases, which suggests that photosensitization is possible with the **DPDS/DCA** and **DPDS/DCN** system, respectively (Table 6.1).

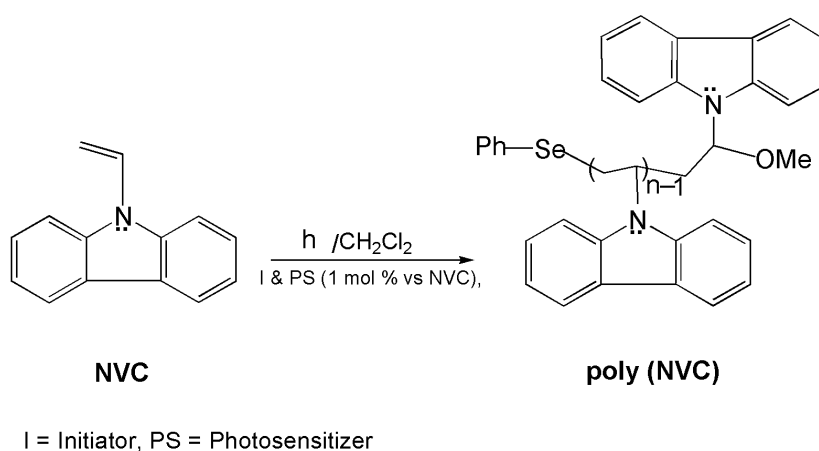
Table 6.1: Free energy estimation of photosensitization process

Sensitizer	$E_{0,0}$ ^{a)} (eV)	$E_{1/2}^{\text{red}}$ ^{b)} (eV)	ΔG_{ET} ^{c)} (Kcal. /mol)	Photosensitization possible
DCN	3.45	-1.28	-18.90	Yes
DCA	2.88	-0.89	-14.75	Yes

^{a)} singlet state energy of sensitizers; ^{b)} half wave reduction potential (vs standard calomel electrode); ^{c)} Free energy change of sensitizers

6.3.2. Polymerization

The objective of the present study was to develop a novel photosensitization system based on non-salt initiator for the cationic polymerization in the near UV and Visible region of light. It is well known fact that both **DCN** and **DCA** absorb at longer wavelength region (> 290 nm) and initiates **DPDS** to generate selenium cation radical ^[16]. Moreover, desired reactions products resulted when the various α -olefins add to this formed selenium radical cation ^[16, 25]. We have employed this concept of the photochemical generation of selenium radical cation in the photopolymerization of NVC at ambient temperature in CH_2Cl_2 as shown in Scheme 6.5.

**Scheme 6.5:** Photo polymerization of NVC

The mole ratios of various components involved are given as [NVC]: [Initiator]: [Sensitizer] = 100: 1: 1. In all the cases, the reaction was quenched at regular time intervals

(3, 6, 10 and 15 h) in 10-fold excess of methanol as precipitating solvent and percentage conversion was determined gravimetrically.

6.3.2.1. Photo polymerization of NVC using DPDS as initiator

Table 6.2 shows the results of the photopolymerization of NVC with **DPDS** as initiator and **DCN** and **DCA** as photosensitizer. The molecular weight reached after running the reaction for 15 h with **DCN/DPDS** and **DCA/DPDS** was 21,200 and 11,800. However, the monomer conversion (run number 4) was higher in case of **DCN/DPDS** as compared to **DCA/DPDS** with relatively lower polydispersity (2.1). The higher activity of **DCN/DPDS** system as compared to **DCA/DPDS** system could be ascribed due to the formation of better exciplex (CT complex) between initiator and sensitizer upon photo-irradiation (Scheme 6.6).

Table 6.2: Photosensitized cationic polymerization of NVC ^{a)} with **DPDS**

Run	Sensitizer	Time (h)	Conv ^{b)} (%)	M _{n,SEC} ^{c)} (x10 ⁻³)	PDI ^{d)}
1	DCN	3	55	8.4	1.6
2		6	62	15.0	1.8
3		10	68	17.0	1.9
4		15	80	21.2	2.1
5	DCA	3	47	3.6	1.7
6		6	51	7.6	2.2
7		10	59	11.5	2.6
8		15	62	11.8	2.7

^{a)} [NVC] = 2 M in CH₂Cl₂; ^{b)} gravimetric; ^{c)} obtained from SEC, ^{d)} Calibrated using PS standards with CHCl₃ as eluent.

6.3.2.2. Photo polymerization of NVC using DBDS as initiator

Table 6.3 shows polymerization results of NVC with **DBDS** as initiator and **DCN** and **DCA** as photosensitizer. Monomer undergoes polymerization with **DBDS/DCN** combination and rate of polymerization increases with increase in time, which reaches to limiting conversion. With **DBDS/DCA** system, NVC undergo less than 1 % conversion up to 6 h. This may be ascribed by incompatibility to form CT complex between **DBDS** and **DCA** upon photo-irradiation.

Table 6.3: Photosensitized cationic polymerization of NVC ^{a)} with **DBDS**

Run	Sensitizer	Time (h)	Conv ^{b)} (%)	M _{n,SEC} ^{c)} (x10 ⁻³)	PDI ^{d)}
1	DCN	3	25	8.4	1.6
2		6	37	15.0	1.8
3		10	42	17	1.9
4		15	47	21.2	2.1
5	DCA	6	< 1	3.6	1.7

^{a)} [NVC] = 2 M in CH₂Cl₂; ^{b)} gravimetric; ^{c)} obtained from SEC, ^{d)} Calibrated using PS standards with CHCl₃ as eluent.

The **DPDS** found good initiator with both the sensitizers while **DBDS** shows activity only with **DCN**. Moreover, **DPDS** form more effective CT complex with **DCN** as compared to **DCA**. The overall order of activity was observed as **DCN/DPDS** > **DCA/DPDS** > **DCN / DBDS** > **DCA / DBDS**.

Figure 6.8 and 6.9 show GPC eluograms of 3 h and 15 h for **DCN/DPDS** and **DCA/DPDS** systems respectively. The GPC eluograms show that there is a low molecular weight hump, which is observed after 15 h in **DCA/DPDS** system. However, a low molecular weight hump that was present in **DCN/DPDS** system at 3 h has disappeared at 15 h of reaction. The hump during the reaction could be due to the two different active species

prevailing at the time of initiation out of which one got dead and other continued to grow with time, whereas initial hump might be because of an impurity within the system. The nature and type of such reaction is a speculation to the observation seen from our experimental results.

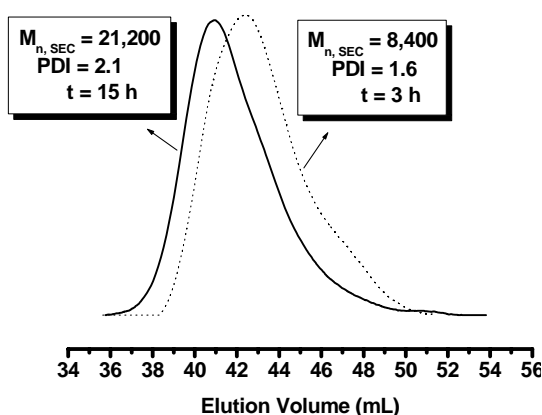


Figure 6.8: GPC eluograms of pNVC where, [NVC] = 2M in CH₂Cl₂. [NVC]: [DPDS]: [DCN] = 100:1:1

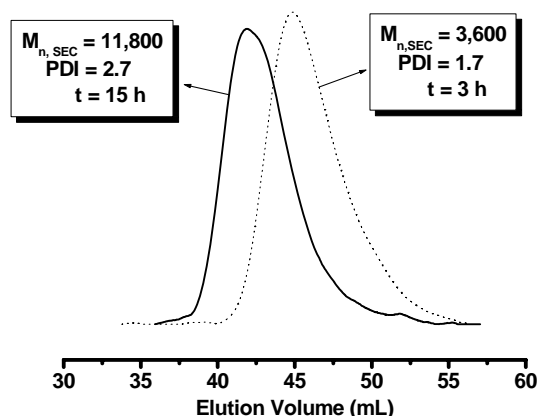
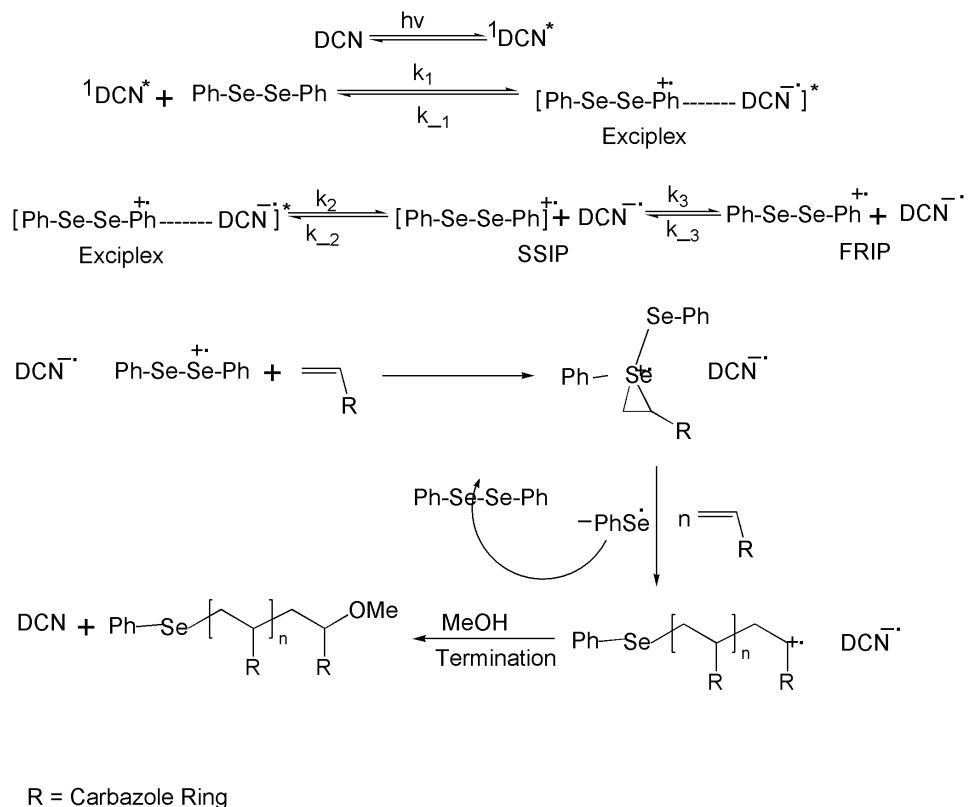


Figure 6.9: GPC eluograms of pNVC where, [NVC] = 2M in CH₂Cl₂. [NVC]: [DPDS]: [DCA] = 100:1:1

However, few controlled experiments were performed for 3 h in order to examine the activity by **DPDS/DCN** system, viz., (a) The polymerization of NVC in dichloromethane at ambient temperature was performed with **DPDS** but without sensitizer (**DCN**), (b) the polymerization of NVC in dichloromethane and (c) the polymerization of NVC in dichloromethane with sensitizer and without **DPDS**. White turbidity appeared in first two cases whereas clear solution was seen in case 'c' during precipitation of the reaction mixture in cold methanol. The mother liquor with the white turbidity was evacuated under vacuum and sample submitted for ¹H NMR analysis. The ¹H NMR spectrum resembles the peaks due to monomer (NVC) and not the polymer. In addition, no polymer peak was seen in RI detector during GPC analysis, therefore, no polymer in controlled experiments. Thus, the aforementioned observation with the obtained experimental data plus favorable free energy of photosensitization supports our strategy for cationic polymerization of NVC at ambient temperature.

6.3.3. Mechanism of polymerization

A plausible mechanism for the photosensitized cationic polymerization of NVC with **DPDS** and **DCN** as a representative example is illustrated in Scheme 6.6. The mechanism of photosensitization using **DCN** or **DCA** with **DPDS** system was reported by Pandey *et al.* [25] It was shown that the reactivity of PhSe[•] radical towards π bond is low because of faster rate of radical recombination reactions [26] that is reversible in nature. [27] This clearly indicates that electrophilic selenium radical cation acts as true species in initiating the cationic polymerization of NVC. The mechanism involves selenium radical cation [16] which is the actual initiating species that is formed by single electron transfer from ground state initiator to excited state sensitizer upon photo-irradiation and reacts with NVC to give corresponding radical cation, which further propagates the chain by reacting subsequent NVC molecules.



Scheme 6.6: Mechanism of photocationic polymerization of NVC

6.4. Conclusions

The present study proposed a combination of novel non-salt initiator (**DPDS** and **DBDS**) along with different (**DCN** or **DCA**) sensitizer for the photocationic polymerization of NVC. The sensitizers and initiators were synthesized and well characterized. The polymer, pNVC, was formed with both sensitization systems but with relatively broader molecular weight distribution. However, it was found that molecular weight increases with time in both the cases. Finally, a mechanism of photopolymerization occurring with selenium radical cation was proposed and found to fit our experimental results. Thus, our study proves that the present photosensitization system effectively initiates the cationic polymerization of NVC at ambient temperature.

6.5. References

1. J. V. Crivello, *Adv. Polym. Sci.* **1984**, 1, 62.
2. Y. Yagci, I. Reetz, *Prog. Polym. Sci.* **1998**, 23, 1485.
3. J. V. Crivello, R. Narayan, *Macromolecules* **1996**, 29, 433.
4. J. V. Crivello, J. H. W. Lam, *J. Polym. Sci., Polym. Chem. Ed* **1980**, 18, 2677.
5. J. V. Crivello, J. H. W. Lam, *Macromolecules* **1979**, 10, 1307.
6. T. Takaka, K. Takuma, T. Endo, *Macromol. Chem. Rapid Commun.* **1993**, 14, 203.
7. Y. Yagci, A. Kornowaski, W. Schnabel, *J. Polym. Sci., Polym. Chem. Ed.* **1992**, 30, 1987.
8. Y. Yagci, I. Lukac, W. Schnabel, *Polymer* **1993**, 34, 1130.
9. E. W. Neison, T. P. Carter, A. B. Scranton, *J. Polym. Sci. Chem. Ed.*, **1995**, 33, 247.
10. J. V. Crivello, J. L. Lee, *Macromolecules* **1983**, 16, 684.
11. J. V. Crivello, Y. Hua, *J. Polym. Sci., Polym. Chem. Ed.* **2000**, 38, 3696.
12. A. Ledwith, *Polymer* **1978**, 19, 1217.
13. Y. Yagci, A. Ledwith, *J. Polym. Sci., Polym. Chem. Ed.* **1988**, 26, 1911.
14. G. Hizal, Y. Yagci, W. Schnabel, *Polymer* **1994**, 35, 2428.
15. M. A. Fox, M. Chanon, “*Photo Induced Electron Transfer Reactions: Organic Substrate Part C*, Elsevier Publication, New York, **1988**.
16. G. Pandey, B. B. V. Soma Sekhar, *J. Org. Chem.* **1992**, 57, 4019.
17. W. L. F. Armarego, D. D. Perrin, *Purification of Organic Chemicals*, 4th ed, ButterWorth-Heinemann, Linecre House, Jordon Hill, Oxford OX2 8 DP.
18. K. B. Sarpless, W. M. Young, *J. Org. Chem.* **1975**, 40, 7.
19. D. L. Klayman, T. Scott Griffin, *J. Am. Chem. Soc.* **1973**, 95, 197.
20. R. W. Bayer, Edward J. O'Reilly, Jr. *J. Org. Chem.* **1958**, 23, 311.
21. M. S. Newman, *Organic Synthesis Collect. Vol. 3*, p. 631. Horning, E.C. Ed.; John-Wiley & Sons; London.
22. D. Rehm, A. Weller, *Isr. J. Chem.* **1970**, 8, 259.
23. G. Pandey, B. B. V. Soma Sekhar, *J. Org. Chem.* **1994**, 59, 7367.
24. S. L. Mattes, S. Farid, *Organic Photochemistry*; Padwa, A. Ed ; Marcel Dekker:

- New York, **1983**; Vol 6, p 233.
25. G. Pandey, B. B. V. Soma Sekhar, *J. Chem. Soc., Chem. Commun.*, **1993**, 780.
 26. T. G. Back, M. V. Krisna, *J. Org. Chem.* **1988**, 53, 2533.
 27. O. Ito, *J. Am. Chem. Soc.* **1983**, 105, 850.

Chapter 7: Summary and Conclusions

7.1. Summary and Conclusions

The present study deals with the synthesis of new thermal as well as photo latent cationic initiators, which stimulates cationic polymerization on external stimulation such as heat or light. The prepared initiators show good latency under ambient conditions and effectively initiate polymerization of cationic monomers. The silent highlights and conclusions of present work are summarized below.

- ❖ A detailed investigation on (xanthenyl, dibenzosuberonyl) phosphonium salts as novel thermo-latent initiators for cationic polymerization of epoxy monomers is discussed. The initiator activity was found to depend upon the counter anions, phosphine moiety, ring structure and ring substituents. These initiators are thermally stable, well soluble in monomer (GPE), easy to handle and initiates cationic polymerization of epoxides on thermal initiation. Therefore, changing structural parameters can control the rate of initiation.
- ❖ The amide based allylic phosphonium salts are used as new *addition-fragmentation-agent* in conjugation with photo- and thermal radical initiators in cationic polymerization at $\lambda > 300$ nm. They exhibit enhanced initiation efficiency as photo and thermo-latent initiator, which depends on, added radical initiators (photo or thermal).
- ❖ Novel benzophenone based allylic ammonium salts as one component *addition-fragmentation-agent* in photopolymerization ($\lambda > 300$ nm) of cyclohexene oxide, vinyl ethers and *n*-vinyl carbazole is investigated. This proved to be an efficient latent cationic initiator without use of radical initiators.
- ❖ The non-salt based diselenides-aromatic nitriles as novel photosensitization system for cationic polymerization of NVC is investigated at $\lambda > 300$ nm and found to be efficient at ambient temperature.

7.2. Future prospectus of research

The present research on photo and thermo-latent initiators has opened up many new prospective for future research in cationic polymerization. As these initiators are latent under ambient conditions but initiates polymerization on external stimulation (heat or light). The following sections deals with the future scope for further study.

- ❖ For preparation of thermosetting resin, the phosphonium salts can be used to prepare the epoxy blends from commercial diglycidyl ether of bisphenol A (DGEBA) with other epoxy monomers, such as bio-based epoxidized castor oil (ECO), epoxidized soyabean oil, 3,4-epoxycyclohexylmethyl-3, 4-epoxycyclohexyl carboxylate (EPC), phenol novolac resin and trimethyl propane triglycidyl ether. The prepared epoxy blends are widely has been used as adhesive, high performance coatings and laminating material because these resins have excellent properties, low shrinkage, good adhesion to many metals, resistance to moisture and thermal and mechanical shock.
- ❖ Benzophenone based allylic ammonium salts as component addition fragmentation agent can be used for photo curing of multifunctional epoxy and vinyl ether monomers.
- ❖ The photo and thermal curing of multifunctional epoxides and vinyl ether monomers with allylic phosphonium salts can be triggered, which depends upon selection of radical initiator (photo or thermal).

Publications

- ❖ “Cationic Polymerization of Epoxides using Novel Xanthenyl Phosphonium Salts as Thermo-latent Initiator” **M. K. Gupta** and R. P. Singh (Polymer Bulletin 2008 <http://dx.doi.org/10.1007/s00289-008-0910-1>).
- ❖ “Diphenyldiselenide As Novel Non-salt Photoinitiator for Photosensitized Cationic Polymerization of N-Vinyl Carbazole” **M. K. Gupta** and R. P. Singh. (*Macromolecular Symposia 2006, 240, 186–193*).
- ❖ “Dibenzosuberene based Phosphonium Salts as Novel Thermally Latent Initiator for Cationic Polymerization” **M. K. Gupta** and R. P. Singh (*Under communication*).
- ❖ “Xanthenyl Phosphonium salts as Thermo Latent Initiator for Cationic Polymerization of GPE” **M. K. Gupta** and R. P. Singh (*Under communication*).
- ❖ “Benzophenone based Allylic Anilinium Salts as Novel Addition Fragmentation Agent for Photo Initiated Cationic Polymerization” **M. K. Gupta** and R. P. Singh (*Under Preparation*)
- ❖ Initiation of Cationic Polymerization using Allyl Phosphonium Salts in Presence of Free Radical Initiators **M. K. Gupta** and R. P. Singh (*Under Preparation*)

Symposia/ Seminar / Workshop

- ❖ “Dibenzosuberanyl phosphonium salts as thermally latent initiators for cationic polymerization of glycidyl phenyl ether” **M. K. Gupta** and R. P. Singh, poster presented in “Macro-2006” an international conference on polymers for advanced technologies, December 2006, held at National Chemical Laboratory, Pune-India.
- ❖ “Diselenides as novel non salt initiator for photosensitized cationic polymerization of N-vinylcarbazole” **M. K. Gupta** and R. P. Singh, poster presented in “IP-2005” an international symposium on Ionic Polymerization (Under the auspices of

International Union of Pure and Applied Chemistry-IUPAC), October 2005, held at Goa, India.

- ❖ Junior NOST symposium in organic chemistry November 2003, held at National Chemical Laboratory, Pune-India.

Awards\ Fellowships\Certificates

- ❖ Junior Research Fellowship (June 2002) awarded by Council of Scientific and Industrial Research (CSIR), New Delhi.
- ❖ Holding life membership of Society of Polymer Science (SPS) of India, Pune Chapter ([http:// www.spsindia.org/index.html](http://www.spsindia.org/index.html)), Pune.
- ❖ Best poster award for “Cationic Polymerization of Epoxides using Novel Xanthenyl Phosphonium Salts as Thermo-latent Initiator” **M. K. Gupta** and R. P. Singh on Science Day-2008 organized at National Chemical Laboratory, Pune